

ABSTRACT

Title of Dissertation: AIR EXPRESS NETWORK DESIGN WITH HUB SORTING

Somnuk Ngamchai
Doctor of Philosophy, 2007

Directed By: Dr. Paul M. Schonfeld, Professor
Department of Civil and Environmental
Engineering

This dissertation examines an innovative strategic operation for next day air package delivery. The proposed system, in which some packages are sorted twice at two distinct hubs before arriving at their destinations, is investigated for its potential savings. A *two-stage sorting* operation is proposed and compared to the currently operated *single-stage sorting* operation. By considering the endogenous optimization of hub sorting and storage capacities, cost minimization models are developed for both operations and used for performance comparison.

Two solution approaches are presented in this study, namely the Column Generation (CG) approach and the Genetic Algorithm (GA) approach. The first method is implemented to optimize the problem by means of linear programming (LP) relaxation, in which the resulting model is then embedded into a branch-and-bound approach to generate an integer solution. However, for solving realistic problem sizes, the model is intractable with the conventional time-space formulation. Therefore, a Genetic Algorithm is developed for solving a large-scale problem. The GA solution representation is classified into two parts, a grouping representation for

hub assignment and an aircraft route representation for aircraft route cycles. Several genetic operators are specifically developed based on the problem characteristics to facilitate the search.

After optimizing the solution, we compare not only the potential cost saving from the proposed system, but also the system's reliability based on its slack. To provide some insights on the effects of two-stage operation, several factors are explored such as the location of regional hubs, single and multiple two-stage routings and aircraft mix. Sensitivity analyses are conducted under different inputs, including different demand levels, aircraft operating costs and hub operating costs. Additional statistics on aircraft utilization, hub capacity utilization, circuitry factor, average transfers per package, and system slack gain/loss by commodity, are analyzed to elucidate the changes in system characteristics.

AIR EXPRESS NETWORK DESIGN WITH HUB SORTING

By

Somnuk Ngamchai

Dissertation submitted to the Faculty of the Graduate School of the
University of Maryland, College Park, in partial fulfillment
of the requirement for the degree of
Doctor of Philosophy
2007

Advisory Committee:
Professor Paul M. Schonfeld, Chair
Professor Ali Haghani
Professor Bruce L. Golden
Professor Hani S. Mahmassani
Professor Robert J. Windle

©Copyright by
Somnuk Ngamchai
2007

Dedication
To my dear parents

Acknowledgements

I would like to express my sincerest thank to my advisor, Professor Paul M. Schonfeld, for providing me freedom to let me follow my own research interests and continuously giving me guidance and encouragement throughout my entire research. I am very grateful for his availability whenever I need to talk and for discussions that were helpful and inspiring. It has been my great experience working with him.

I would like to thank my advisory committee members, Professor Ali Haghani, Professor Bruce L. Golden, Professor Hani S. Mahmassani, and Professor Robert J. Windle for their valuable comments and suggestions on this research.

Unforgettable thanks are due to my colleagues in Amtrak, Department of Pricing and Revenue Management, for their support and understanding during my studies. My appreciation also extends to all my friends in College Park who have made this place home. Special thanks are to Woradee Jongadsayakul for her unconditional support throughout my studies.

I thank my dear sisters for their support, and for sharing my responsibilities of taking care of my parents while I am in College Park for all these years. Finally, without them, I am just nobody. I would like to dedicate this dissertation to my parents. Without their continuous encouragement and supports, I would not have made it through. To my dear Mom and Dad, without your love, support, unforeseen vision and encouragement, I would not even have pursued higher education.

Table of Contents

List of Tables	vii
List of Figures.....	ix
Chapter 1 Introduction.....	1
1.1 Background on Express Package Shipment Services	3
1.2 Problem Statement	6
1.3 Research Objectives and Scope	8
1.4 Dissertation Overview	10
Chapter 2 Literature Review	11
2.1 Network Design Problems	11
2.2 Transportation Service Network Design Problems.....	13
2.3 Express Package Delivery Problems	14
2.4 Hub Network Structure and Characteristics	19
2.5 Solution Approaches	25
2.6 Summary.....	26
Chapter 3 Problem Definitions	30
3.1 Problem Characteristics	31
3.1.1 Overview of Current Next-day Air Shipment Operation.....	31
3.1.2 Integration of Hub Operation and Air Routing: Concepts and Contributions.....	32
3.2 Hub Sorting Subproblem	39
Chapter 4 Network Representations	48
4.1 Hub Sorting Network (HSN)	49
4.2 Aircraft Route Network (ARN)	53
4.2.1 Single-Stage Sorting ARN.....	53
4.2.2 Two-Stage Sorting ARN.....	56
4.3 Package Movement Network (PMN).....	58

Chapter 5 NH Models	61
5.1 NH Operational Constraints.....	62
5.1.1 Fleet Balance at Service Center	62
5.1.2 Fleet Balance at Hub	63
5.1.3 Fleet Size.....	64
5.1.4 Hub Landing Capacity	65
5.1.5 Hub Take-off Capacity	65
5.1.6 Hub Sorting Capacity.....	66
5.1.7 Hub Storage Capacity	67
5.1.8 FIFO Package Movement in HSN	67
5.2 Cost Components	69
5.3 NH Model Formulations	69
Chapter 6 NH Solution Approach – Column Generation	73
6.1 Solution Procedures	74
6.2 Package Movement Connectivity (PMC)	76
6.3 Initial Aircraft Route Generation Procedure.....	77
6.4 Column Generation (CG) Approach.....	79
6.4.1 CG Approach for Aircraft Routes.....	81
6.4.2 CG Approach for Package Flow Paths	82
6.5 Computational Analyses	84
6.5.1 Case Study 1: 2 Hubs, 8 Service Centers, 1 Aircraft Type.....	84
6.5.2 Case Study 2: 2 Hubs, 8 Service Centers, 2 Aircraft Types	93
6.6 Summary	95
Chapter 7 NH Solution Approach – Genetic Algorithm	96
7.1 GA Solution Framework.....	99
7.2 Solution Representation	101
7.2.1 Grouping Representation – 1 st GA Layer	101
7.2.2 Aircraft Route Representation – 2 nd GA Layer.....	104
7.2.3 Labeling and Encoding Scheme.....	106
7.3 Initialization Process	107
7.4 Genetic Operators	111

7.4.1	Grouping Operators	112
7.4.2	Aircraft Route Operators.....	117
7.5	Network Evaluation Process.....	126
7.5.1	CG Approach for Package Flow Paths	128
7.5.2	Analytical Model for Hub Design Characteristics.....	128
7.5.3	Other Operational Requirements	131
7.6	Slack Analysis.....	131
7.6.1	Pickup Route.....	132
7.6.2	Delivery Route	134
7.6.3	Interhub Route	135
7.7	GA Performance Validation	136
7.8	Computational Analyses	138
7.8.1	Case Study 3: 2 Hubs at Louisville, KY and Dallas, TX.....	139
7.8.2	Case Study 4: 2 Hubs at Louisville, KY and Columbia, SC.....	150
7.9	Summary	153
Chapter 8 Large System Computational Analyses		154
8.1	Outline of Computational Analyses and Inputs	159
8.2	Computational Performance	162
8.3	Case Study 5: Single Location Two-stage Operation.....	163
8.4	Case Study 6: Multiple Location Two-stage Operation	177
8.5	Case Study 7: Effects of Aircraft Mix and Demand Levels	183
8.6	Case Study 8: Economies of Scale in Aircraft.....	187
8.7	Summary	188
Chapter 9 Conclusions and Future Research.....		190
9.1	Conclusions.....	191
9.2	Future Research	196
Appendix A Abbreviations.....		197
Appendix B Notation		199
References		206

List of Tables

Table 2.1: Summary reviews for express package delivery studies	18
Table 2.2: Summary reviews for hub network structures and characteristics	22
Table 2.3: Summarized solution approach applied to express shipment service network design	28
Table 6.1: O/D demand matrix for Case Studies 1 and 2	85
Table 6.2: Service center characteristics.....	86
Table 6.3: Hub characteristics.....	86
Table 6.4: Aircraft characteristics.....	86
Table 6.5: Computational results for Case Study 1	87
Table 6.6: Comparison of operating characteristics for Case Study 1.....	88
Table 6.7: Comparison of cost distributions for Case Study 1	88
Table 6.8: Changes in total operating cost for Case Studies 1 and 2.....	94
Table 6.9: Effect of demand level on sorting stages.....	95
Table 7.1: GA parameters for performance validation	137
Table 7.2: GA performance evaluation.....	137
Table 7.3: Selected service centers for Case Study 3	140
Table 7.4: Selected hubs for Case Study 3	140
Table 7.5: O/D demand matrix for Case Study 3.....	140
Table 7.6: Hub characteristics for Case Study 3.....	140
Table 7.7: Aircraft characteristics for Case Study 3.....	141
Table 7.8: GA parameters for Case Study 3	141
Table 7.9: Selected service centers for Case Study 4	151
Table 7.10: Selected hubs for Case Study 4	151
Table 7.11: O/D demand matrix for Case Study 4.....	151
Table 8.1: Top 150 metropolitan areas in the United States.....	156
Table 8.2: UPS hub locations for Case Study 5.....	161
Table 8.3: Hub characteristics for Case Study 5.....	161
Table 8.4: EPT and LDT for Case Study 5.....	161

Table 8.5: Aircraft characteristics for Case Study 5	161
Table 8.6: GA parameters for Case Study 5	162
Table 8.7: Scenario analysis: UPS network with 100 SCs, $Q = 0.8M$ packages, and two-stage KY-PA routing	166
Table 8.8: Scenario analysis: UPS network with 100 SCs, $Q = 0.8M$ packages, and two-stage KY-SC routing	167
Table 8.9: Scenario analysis: UPS network with 100 SCs, $Q = 0.8M$ packages, and two-stage KY-TX routing	168
Table 8.10: Scenario analysis: UPS network with 100 SCs, $Q = 0.8M$ packages, and two-stage KY-CA routing	169
Table 8.11: Detailed slack analysis for two-stage operation (KY-PA, $Q = 0.8M$, $u_l =$ $150,000$)	170
Table 8.12: Detailed slack analysis for two-stage operation (KY-SC, $Q = 0.8M$, $u_l =$ $150,000$)	170
Table 8.13: Detailed slack analysis for two-stage operation (KY-TX, $Q = 0.8M$, $u_l =$ $150,000$)	170
Table 8.14: Detailed slack analysis for two-stage operation (KY-CA, $Q = 0.8M$, $u_l =$ $150,000$)	170
Table 8.15: Scenario analysis: UPS network with 100 SCs and multiple two-stage routings	179
Table 8.16: Two-stage total cost comparison when varying aircraft mix.....	185

List of Figures

Figure 1.1: Comparison of UPS and FedEx yearly domestic next day air revenues	2
Figure 1.2: Comparison of UPS and FedEx yearly operating margin	3
Figure 1.3: Integrating single hub sorting operation and aircraft route design.....	7
Figure 1.4: Integrating hub sorting operation and air service network design for package distribution	7
Figure 3.1: Existing next day air operation.....	32
Figure 3.2: Worst-case scenario for the current number of flight legs (without integrated hub sorting operation)	35
Figure 3.3: Worst-case scenario for the proposed number of flight legs (with integrated hub sorting operation)	35
Figure 3.4: Worst-case scenario for the current number of aircraft required (without integrated hub sorting operation)	36
Figure 3.5: Worst-case scenario for the proposed number of aircraft required (with integrated hub sorting operation)	36
Figure 3.6: Arrival/sorting and sorted packages in FIFO sorting process at hub location.....	40
Figure 3.7: Inventory sorting model for hub sorting process.....	41
Figure 3.8: One arrival aircraft waits until the next grid time to unload packages.....	43
Figure 3.9: All aircraft unload packages immediately after arriving.....	43
Figure 3.10: Using knowledge of sorted package ODs to identify an aircraft dispatch time	44
Figure 3.11: Coordination between hub sorting operations and air route design	46
Figure 3.12: Expected sorting end time	47
Figure 4.1: HSN representation for hub h	50
Figure 4.2: Package flow in FIFO HSN.....	51
Figure 4.3: Network representation of R_p^f	55
Figure 4.4: Network representation of R_H^f	58

Figure 4.5: Example of single-stage-sorting PMN	60
Figure 4.6: Example of two-stage-sorting PMN.....	60
Figure 5.1: Example of fleet balancing in HSN.....	64
Figure 6.1: Solution procedure	75
Figure 6.2: PMC for single-stage operation.....	77
Figure 6.3: PMC for two-stage operation	77
Figure 6.4: Example of dummy pickup aircraft routes	79
Figure 6.5: Column generation approach.....	80
Figure 6.6: Modified arc costs associated to each type of arc	83
Figure 6.7: Network physical locations for Case Study 1	85
Figure 6.8: Network configuration for Case Study 1 - single-stage operation	89
Figure 6.9: Network configuration for Case Study 1 - two-stage operation.....	89
Figure 6.10: Effect of sorting cost on each operation for Case Study 1	90
Figure 6.11: Effect of aircraft cost per mile on each operation for Case Study 1	90
Figure 6.12: Total operating cost for each operation vs. demand for Case Study 1 ...	91
Figure 6.13: Total operating cost for each model vs. demand for Case Study 2	93
Figure 7.1: General GA solution approach.....	98
Figure 7.2: Genetic Algorithm procedure for the NH problem	98
Figure 7.3: GA solution procedure for NH problem.....	100
Figure 7.4: Example of GA grouping representation.....	103
Figure 7.5: Grouping representation for Figure 7.4.....	104
Figure 7.6: Equivalence of path-based and cycle-base aircraft routes.....	105
Figure 7.7: Example of aircraft route representation with cycle-based variables.....	106
Figure 7.8: Illustration of randomly selected hub assignment.....	109
Figure 7.9: Initialization process.....	110
Figure 7.10: Set of GA operators applicable to different sorting policies	112
Figure 7.11: Total change in transferred demand at hubs.....	114
Figure 7.12: Example of single-point grouping crossover operator	115
Figure 7.13: Maximum possible demand in hub territory	116
Figure 7.14: Example of path-swapping operator.....	119
Figure 7.15: Capacity decrease operator.....	121

Figure 7.16: Interhub usage operator	126
Figure 7.17: Determination of hub sorting capacity for single-stage operation	129
Figure 7.18: Determination of hub sorting capacity for two-stage operation.....	129
Figure 7.19: Determining the latest hub arrival time, $LAH(r, h)$	133
Figure 7.20: Slack analysis on pickup route	133
Figure 7.21: Determining the earliest delivery time, $EDH(r, h)$	134
Figure 7.22: Slack analysis on delivery route.....	134
Figure 7.23: Slack analysis on interhub route.....	135
Figure 7.24: Cost saving from two-stage operation at 100% demand.....	143
Figure 7.25: Percentage of hub sorting cost at 100% demand.....	143
Figure 7.26: Cost saving from two-stage operation at 150% demand.....	144
Figure 7.27: Percentage of hub sorting cost at 150% demand.....	144
Figure 7.28: Cost saving from two-stage operation at 200% demand.....	145
Figure 7.29: Percentage of hub sorting cost at 200% demand.....	145
Figure 7.30: Change in two-stage network configuration when unit hub sorting cost increases	146
Figure 7.31: Change in two-stage network configuration when unit aircraft operating cost increases	146
Figure 7.32: Cost saving from two-stage operation as demand increases	147
Figure 7.33: Detailed slack gain/loss analysis by commodity.....	147
Figure 7.34: Utilization of hub sorting capacity	149
Figure 7.35: Cost saving from two-stage operation for Case Study 4.....	152
Figure 7.36: Detailed slack gain/loss analysis by commodity, Case Study 4.....	152
Figure 8.1: Computational performance vs. network size	163
Figure 8.2: Optimized network configuration for single-stage operation, $Q = 0.8M$ packages.....	171
Figure 8.3: Optimized network configuration for two-stage operation (KY-PA, $Q =$ $0.8M, u_i = 150,000$).....	171
Figure 8.4: Optimized network configuration for two-stage operation (KY-SC, $Q =$ $0.8M, u_i = 150,000$).....	172

Figure 8.5: Optimized network configuration for two-stage operation (KY-TX, $Q = 0.8M$, $u_i = 150,000$).....	172
Figure 8.6: Optimized network configuration for two-stage operation (KY-CA, $Q = 0.8M$, $u_i = 150,000$).....	173
Figure 8.7: Multiple-location two-stage operation, KY-SC & KY-TX, $Q = 0.8M$.	182
Figure 8.8: Multiple-location two-stage operation, Triangular KY-SC-TX, $Q = 0.8M$	182
Figure 8.9: Total cost comparisons when varying aircraft mix and demand levels .	184
Figure 8.10: Circuitry factor at various aircraft mixes and demand levels	186
Figure 8.11: Average transfers per package at various aircraft mixes and demand levels	187
Figure 8.12: Economies of scale on interhub flight.....	188

Chapter 1

Introduction

The package delivery industry has recently grown by providing consistent and reliable delivery services. With billions of dollars in revenue at stake, this translates into a highly competitive environment. Most carriers offer a wide range of delivery services, such as same day service, next day service, deferred service, and ground service, to increase their market shares.

During the period 1998 - 2004, the domestic next day air revenues of United Parcel Service (UPS) and Federal Express (FedEx), the two dominant players in this industry, have mostly grown, as shown in Figure 1.1 (United Parcel Service, 2000 – 2004; FedEx Corporation, 2000 – 2004). Comparing the changes in domestic next day air revenue between 1998 and 2004, however, we see that the revenue of FedEx

had increased by only 6% compared to more than 28% for UPS. For that reason, UPS' operating margin, defined by operating profit as a percentage of revenue, had outperformed that of FedEx by approximately a factor of two over those seven years, as shown in Figure 1.2. Having higher operational efficiency, UPS can aggressively price its services and gain market share – a key to the success of UPS' revenue growth.

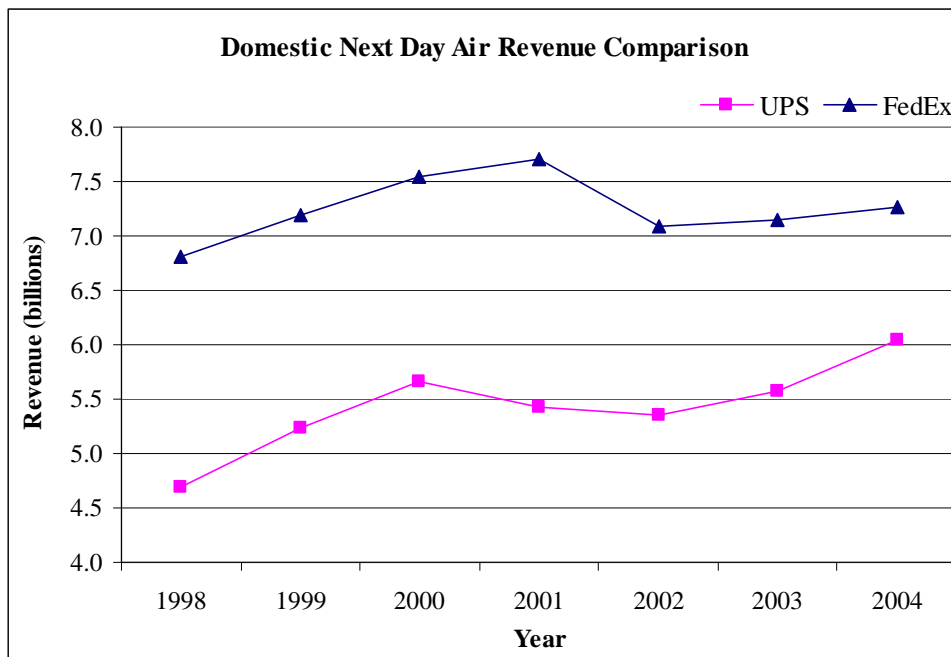


Figure 1.1: Comparison of UPS and FedEx yearly domestic next day air revenues

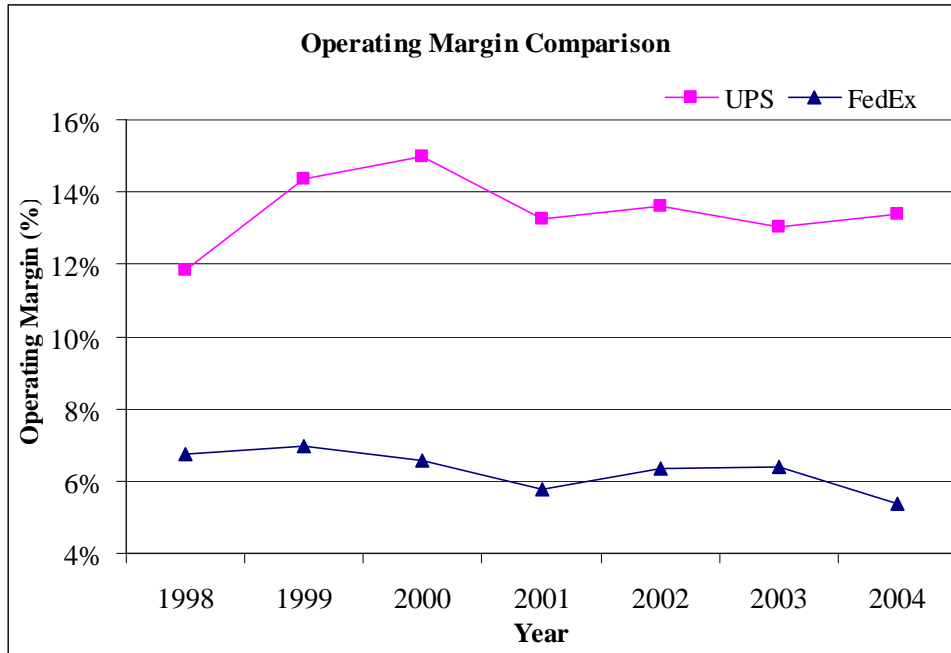


Figure 1.2: Comparison of UPS and FedEx yearly operating margin

While expecting other package delivery firms to strive for the same objective, *new strategic operations* should play an important role in future competitive advantage. In 2003, UPS announced plans for significant improvements in its package sorting and delivery system. It expected to invest \$600 million over the next several years to simplify and optimize package sorting and delivery. Upon expected completion in 2007, the company expects to save \$600 million annually, through productivity improvements and by driving approximately 100 million fewer miles per year (Standard & Poor's Stock Report: UPS, 2006).

1.1 Background on Express Package Shipment Services

Package shipment carriers offer different levels of service, which are mainly characterized by the time duration between pickup and delivery, and charge higher

premiums for higher levels of service. For UPS next-day service provided, a package is guaranteed to be delivered by the early morning, typically before 10 AM, while guaranteed delivery time for second-day service is by the end of the second day. For both services, customers will get a refund if the delivery service cannot be met (UPS Express Critical Term and Condition, 2007).

Brief introductions to air express service networks can be found in Kim et al. (1999), Armacost et al. (2002), and Barnhart and Shen (2004). Typically, packages are transported by ground vehicles to ground centers, where they are sorted to determine the routing of each package based on its destination and level of service. Packages are then transported to an airport, called gateway, either by a ground vehicles or a small aircraft. At gateways, packages are loaded onto jet aircraft and transported to a hub. Upon arrival at hub, which completes the pickup route, packages are unloaded, sorted and consolidated by their destinations. They are then transported by the delivery routes, which are the reversed operation but might be on different routings.

Barnhart and Shen (2004) describe the sequential operation among the next-day and second-day service. The operations for both services are similar, using the same equipments and facilities, but different times. Typically, the same aircraft deliver next-day shipments during the night and second-day shipments during the day. In the current practice, due to problem complexity in solving both services simultaneously, tactical plannings for next-day and second-day are designed sequentially. The fleet positions resulting from next-day planning are used for second-day planning.

Kim (1997) describes two types of planning activities for most express package service operations. Strategic long range planning, which looks several years into the future, focuses on problems such as aircraft acquisition, hub capacity expansion, and new facility location. The decisions can be made without existing resource constraints to determine the required resources under the future operating conditions. The data used in this planning level are often imprecise, relying heavily on forecasts. The second type of planning is near-term operation planning, in which the planning time horizon ranges from one to several months in the future. Its activity includes generating a plan to be executed in the operation. Some planning activities, such as flight crew planning and maintenance planning, are relying on this near-term planning. There are very limited degrees of freedom in terms of changing existing resources. However, this model is used to analyze various scenarios, such as determining the incremental operating costs for a set of demand changes. The results are used to direct market efforts over the next one to two years. This type of analysis is called market planning.

Package volumes normally increase from Monday through mid-week, peaking on Wednesday or Thursday, and decrease through the weekend. Therefore, a seven day planning horizon is desirable for capturing the characteristic daily variations in express package operations. A seven day horizon has the added advantage that all service types, e.g., next day, second day and deferred, can be integrated. However, a week-long planning horizon considering all service types would make the model intractable. Kim (1997) finally focuses on solving the next day operation with a single-day planning horizon.

1.2 Problem Statement

Several studies have proposed different solution approaches to designing an existing next day air service network operation, where packages are sorted and redistributed among flights only once at a hub. In contrast, with a limited time window as a critical factor in next day service, we investigate how shipments can be effectively consolidated into fewer flights by having some packages sorted successively at two distinct hubs before arriving at their destinations. A *two-stage sorting* operation is proposed and its potential cost savings are examined and compared to the currently used *single-stage sorting* operation. The proposed system would not be useful unless efficient integration of hub sorting operations into air service network design is considered. Hub characteristics, including hub sorting capacity and hub storage size, are considered in this study as optimizable design variables, as shown in Figures 1.3 – 1.4.

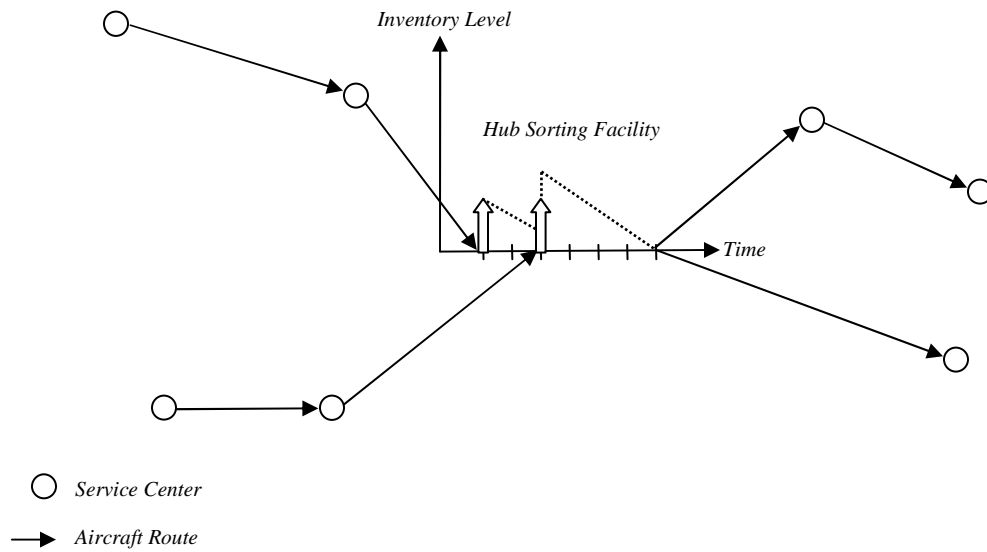


Figure 1.3: Integrating single hub sorting operation and aircraft route design

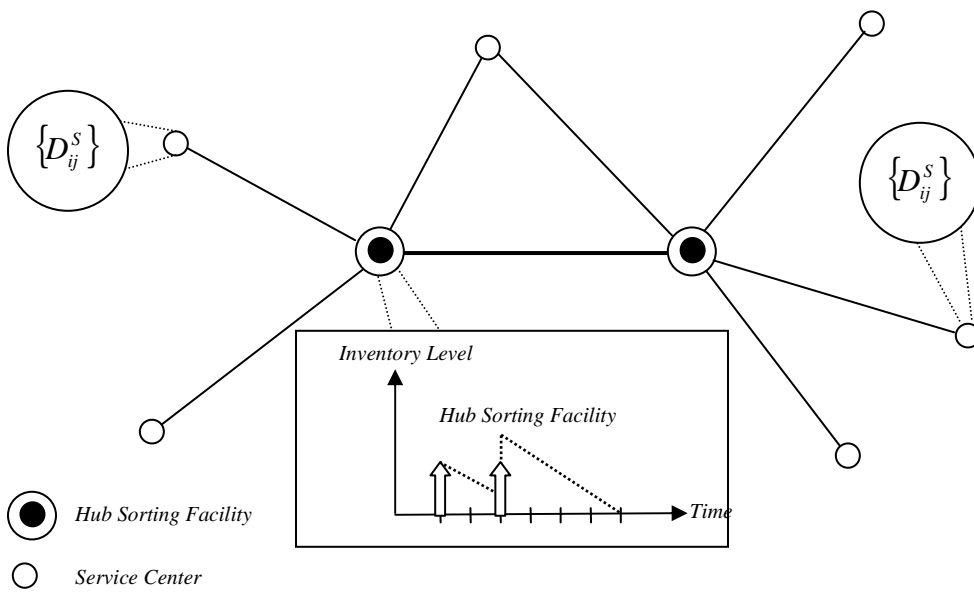


Figure 1.4: Integrating hub sorting operation and air service network design for package distribution

1.3 Research Objectives and Scope

The primary objective in this study is to simultaneously optimize aircraft routing, package flow routing, and aircraft scheduling for both single and two-stage operations. The results are then compared for their costs and operational characteristics. In addition, several impacts of the proposed system should be measured, including hub sorting capacity, hub and aircraft utilization, and system slack gain or loss. The developed models must be able to capture the above characteristics under the common operational constraints.

The principal objectives are as follows:

1. Develop optimization models for next-day air express network design. The models should be able to solve both single-stage and two-stage sorting operations, while satisfying the usual operational constraints, including aircraft balancing, aircraft availability, designing hub sorting/storage capacity, and hub landing/take-off capacity.
2. Develop the conventional time-space network formulation to capture the system's complexities. With the expected large number of variables in the model, a decomposition algorithm, such as the Column Generation approach, should be considered to identify the promising aircraft route and package flow path variables. To limit the expected large number of variable on two-stage operation, each service center is assigned a priori to its closest hub.
3. Develop a heuristic solution approach for solving large problem instances. Given the nature of the problem that includes the hub assignment and network design problems, a Genetic Algorithm is considered. Its solution

representations should reflect those two problem elements. Several genetic operators should be developed based on the problem characteristics to facilitate the search. In some cases where a mixed-stage sorting operation (with both single-stage and two-stage operations for various flows) is better, the model should be able to optimize such an operation. The model must consider all the operational constraints, while, a priori hub assignment for two-stage sorting operations is relaxed.

4. Consider hub characteristics as optimizable designed variables in both the exact and the heuristic optimization models. The hub sorting model is developed and integrated into an air network design problem. For the conventional time-space formulation using the Column Generation approach, hub characteristics, including hub sorting capacity and hub storage size, are simultaneously optimized with other designing elements, while they are separately determined using an analytical model in the Genetic Algorithm approach.
5. Conduct several sensitivity analyses to demonstrate the potential cost savings of two-stage operation over different input parameters. In addition, two-stage routing strategies, which consider the aircraft routing between the main and regional hubs, are analyzed and compared to the single-stage operation.
6. Analyze the possible drawbacks of the proposed system, such as aircraft utilization, hub sorting/storage capacity, hub utilization, and system slack. Since the demand is deterministic in this study, post-solution analysis should be conducted to measure the system slack.

To capture the weekly demand variation (the package volumes increase from Monday through mid-week, peaking on Wednesday or Thursday, and decrease through the weekend), a seven day planning horizon is desirable (Kim, 1999). However, to optimize a system under several operational constraints, hub sorting characteristics, and especially the added complexity of two-stage operation, a week-long planning horizon results in an intractable model. Hence, we only consider a single day planning horizon in this study.

1.4 Dissertation Overview

Chapter 2 provides a comprehensive review and discussion on several topics that are relevant to air network design problem. In chapter 3, the problem definitions are stated and the concepts behinds the proposed two-stage operation are discussed. Chapter 4 presents the conventional time-space network representations, including hub sorting network, aircraft route and package flow path representations. The problems are then formulated by incorporating all the network design and operational characteristics in Chapter 5. Two solution methodologies are presented in this study. The exact solution approach, namely the Column Generation, is introduced in Chapter 6, while the heuristic approach, which uses the Genetic Algorithm, is presented in Chapter 7. In both chapters, sensitivity analyses are conducted on small problems. We demonstrate the model applicability of Genetic Algorithm approach to large problem instances in Chapter 8. Finally, Chapter 9 presents a summary of major findings, contributions and suggested future research directions.

Chapter 2

Literature Review

In this chapter, we review the recent work related to the air express network design (AESD) problem. Because the AESD is one special problem among service network design problems (SNDPs), which fall under the broader network design problem (NDP), we focus on underlying problem characteristics and solution methodologies.

2.1 Network Design Problems

Magnanti and Wong (1984), Minoux (1989) and Ahuja et al. (1993) provide the comprehensive document of network design problem (NDP) surveys. The NDP can generally be classified into two classes, namely capacitated and uncapacitated NDP. Assad (1978) and Kennington (1978) review one special class of NDP, the

multicommodity flow problem, where several physical commodities interact in the same network, or share common arc capacities.

Given a directed graph, $G = (N, A)$, where N is the node set and A is the arc set. Let K denote the set of commodities, $k \in K$, and F be the set of facility types, $f \in F$. Let d^k represent the quantity of commodity k need to be transported over G from its origin node, $O(k)$, to its destination node, $D(k)$. The problem contains two types of decision variables, one modeling integer design decisions and the other modeling continuous flow decisions. Let y_{ij}^f be an integer variable indicating the number of facilities of type f installed over arc (i, j) , u_{ij}^f denote the associated capacity per unit of facility f over the arc (i, j) . Let x_{ij}^k be the flow of commodity k on arc (i, j) . Let c_{ij}^k be the unit cost flow of commodity k on arc (i, j) and c_{ij}^f denote the cost of installing each unit of facility f over arc (i, j) . The network design problem (NDP) is:

$$\min \sum_{k \in K} \sum_{(i,j) \in A} c_{ij}^k x_{ij}^k + \sum_{f \in F} \sum_{(i,j) \in A} c_{ij}^f y_{ij}^f \quad (2.1.1)$$

Subject to

$$\sum_{k \in K} x_{ij}^k \leq \sum_{f \in F} u_{ij}^f y_{ij}^f \quad \forall (i, j) \in A \quad (2.1.2)$$

$$\sum_{j:(i,j) \in A} x_{ij}^k - \sum_{j:(j,i) \in A} x_{ji}^k = \begin{cases} d^k & \text{if } i = O(k) \\ -d^k & \text{if } i = D(k) \\ 0 & \text{otherwise} \end{cases} \quad \forall i \in N, \forall k \in K \quad (2.1.3)$$

$$x_{ij}^k \geq 0 \quad \forall (i, j) \in A, \forall k \in K \quad (2.1.4)$$

$$y_{ij}^f \in \mathbb{Z}_+ \quad \forall (i, j) \in A, \forall f \in F \quad (2.1.5)$$

The objective (2.1.1) is to minimize the total cost, which comprises the variable operating costs and fixed design costs. Constraints (2.1.2) are the “forcing” or “bundle” constraints ensuring that the total flow of all commodities on any arc cannot exceed that arc’s capacity. Constraints (2.1.3) are the general network flow conservation equations.

2.2 Transportation Service Network Design Problems

Crainic (2000) provides a state-of-the-art review of service network design models in freight transportation industry. The author distinguishes between *frequency* and *dynamic* service network design models. The former is typically used to determine how often each selected service is offered during the planning period. Crainic and Rousseau (1986) constitute a prototype of such formulation. The application of frequency service network design can be found in Roy and Delorme (1989). They apply such a formulation to assist less-than-truckload (LTL) motor carriers in their decision-making process for designing their service networks, the routing of freight and empty vehicles balancing, where service frequencies as well as volume of freight moving on each route in the network are the main decision variables. On the other hand, the dynamic formulation targets the planning of schedules and supports decisions related to time of services over a certain number of time periods. Haghani (1989) presents a dynamic service network design combining the empty car distribution with train make-up and routing problems. Farvolden and Powell (1994) present the combined service network design and shipment routing problem in the LTL motor carrier industry using a dynamic formulation.

Kim and Barnhart (1999) focus on the large scale transportation service network design and present three different but equivalent service network design models: node-arc formulation, path formulation, and tree formulations. The route based decision variables are used to capture complex cost structure and reduce the number of constraints in the models.

Because the service network design problem is one special class in the conventional NDP, there are some additional side constraints including to the original network design problem, such as facility balancing constraints, facility availability constraints. Constraints (2.1.6) are the facility balancing constraints included in NDP (2.1).

$$\sum_{j \in N} y_{ij}^f - \sum_{j \in N} y_{ji}^f = 0 \quad \forall i \in N, \forall f \in F \quad (2.1.6)$$

2.3 Express Package Delivery Problems

Grünert and Sebastian (2000) identify important tactical planning tasks facing by postal and express shipment companies and define corresponding optimization models and the relationship among them. Their planning stage is decomposed into air and ground transportation planning. The authors classify the air transportation planning into three problems: direct flight problem, hub flight problem, and mixed air network problem. For ground transportation planning, the feeding problem and pickup-and-delivery problem are stated.

Barnhart and Schneur (1996) develop a model for an express shipment service network design problem with a single hub network. In their study, packages are prohibited from transferring among aircraft at service centers, and only one type of

aircraft is allowed to serve each service center. The authors introduce a two-phase solution process with a preprocessing phase and an optimization phase. The former is used to reduce the size of the problem. For example, shipments assigned to commercial air service are not considered, or shipments that exceed aircraft capacity will be served by commercial air. In their model, package routings are not considered. Therefore, they are completely determined by aircraft routes and there are no interactions between package flow variables and aircraft route variables. As a result, bundle constraints (2.1.2) are not considered. Additional practical considerations are also included in their model:

- Spacing of arrivals and departures of aircraft at the hub. The total packages arriving at the hub should be spread out over the hub sorting time due to limited sorting capacity, while limited crew resources and runway capacity require the number of aircraft departures be distributed after the sort end time.
- Aircraft and airstop restrictions. Some aircraft are not allowed to land at certain service centers due to restrictions on noise, aircraft size/weight, etc.

Kim et al. (1999) develop a model for large-scale transportation service network design for a multihub express shipment problem. Their work is developed from Barnhart and Schneur (1996). They exploit the problem structure using specialized network representation, called a *derived schedule network*, to avoid the massive explosion in the number of nodes and links of a conventional time-space network. Later, a *node consolidation* method is applied to further reduce the problem

size. Given a service network, the authors introduce the package multicommodity flow formulation, in which the objective is to find minimum cost flow of packages from their origins to their destinations satisfying service commitments and network capacity. With a derived schedule network and a package flow model, packages can be transferred between the airstop or multiple aircraft can visit a single service center if found efficient to the system. These consider a more realistic operation than that of Barnhart and Schneur (1996.) To reflect the operational constraints in express package delivery, the model includes fleet balance, fleet size, hub sorting capacity, hub landing capacity, and *connectivity* constraints. With package delivery network containing a major hub and one or more regional hubs, there should be at least one route from any origin location to a major hub, and there should be at least one route from a major hub to any destination location. The concept of the *connectivity* is used to provide the service during service disruption without loss in level-of-service.

Armacost et al. (2002) introduce a *composite variable* formulation for large-scale express package delivery distribution. The new formulation can reduce fractional solution resulted from LP relaxation; it enable their model to solve realistic instances of current network design problem. To obtain stronger bounds than conventional approaches, package flow variables are no longer represented as separate decision variables as in Kim et al. (1999), and each package commodity is assigned *a priori* to a hub, called *fixed hub assignment* in Shen (2004). Therefore, the model is cast purely in terms of the design elements. The sorting capacity at hubs is not considered in their study. Armacost et al. (2004) develop and implement the *Volume, Location and Aircraft Network Optimizer (VOLCANO)* to support next-day-

air network planning within UPS airlines. The underlying idea is taken from Armacost et al. (2002).

Due to the variation in demand for air service which likely increases the opportunity of excess aircraft capacity, Smilowitz et al. (2003) integrate a model of long-haul operation for multimode and multi-service transportation. By shifting deferred items to underutilized aircraft, such integration can increase the operational efficiency of package delivery networks serving multiple services.

Shen (2004) and Barnhart and Shen (2004) study the integration of next day and second day express shipment delivery. The composite variable formulation, as presented in Armacost et al. (2002), is considered, but fixed hub assignment is relaxed.

Table 2.1: Summary reviews for express package delivery studies

Author(s)	Problem Description
Barnhart and Schneur (1996)	Air network in single hub network is considered. Packages are not transferable among aircraft. Only one aircraft is allowed to serve each service center.
Kim et al. (1999)	Multiple modes in multihub network are considered. Package ramp transfers are allowed and multiple aircraft can visit any single service center if that is found to be efficient.
Grünert and Sebastian (2000)	Identify planning tasks faced by postal and express shipment companies and define corresponding optimization models.
Armacost et al. (2002)	Develop new solution approach to the problem in Kim et al. (1999). Each package commodity is a priori assigned to a hub for the designed purpose. Only air network is considered. Hub sorting capacity constraints are relaxed.
Smilowitz et al. (2003)	Shift deferred shipments to underutilized aircraft to increase operational efficiency.
Armacost et al. (2004)	Apply the work from Armacost et al. (2002) to UPS network.

2.4 Hub Network Structure and Characteristics

Hall (1989) examines the impact of overnight restrictions and time zones on the configuration of an air freight network. The location of hub terminal impacts the aircraft arrival pattern to a hub and the sorting rate needed to meet within a specified time window. With growth in overnight package delivery, single-hub operation should be expanded. Multiple-hub network becomes more attractive by reducing the average travel distance. Three basic concepts of routing strategy are used: one-terminal closest routing, two-terminal closest routing, and one-terminal shortest routing. The author investigates five possible routing strategies in the two-hub network, as shown in Hall's Table 2.2. To ship a package from the far west to the far east in the United States, the added sorting time and circuitry make two-hub routing infeasible. However, this does not preclude the movement of packages from east to west using hybrid strategies, as shown in strategies E and D. Due to scale economies, it is better to concentrate packages on fewer routes. In each routing strategy, the number of routes, which provides an indication of savings, is presented. Having far more cities on the east, operating single-terminal routing with master terminal on the east (strategy C) or operating the hybrid strategy with all airports connecting to the master terminal on the east (strategy E) seem to provide nearly the same number of routes. However, because strategy E requires the added expense of sorting some packages at two hubs, strategy C is favored.

In the network used by FedEx, most flights to/from the hub make one or more stopovers, and small cities are served by feeder aircraft which connect to the nonhub cities. Kuby and Gray (1993) explore the possible tradeoffs and savings by comparing

the direct flights to hub to flights with stopovers and feeders in hub-and-spoke network. The results show substantial improvement in cost, miles flown, load factor and number of aircraft used.

Aykin (1995a) considers the hub location and routing problem in which the hub locations and the service types between demand points are determined jointly. For each commodity, one-hub-stop, two-hub-stop and, when permitted, direct services are considered. In addition, flows of each commodity are not aggregated and considered independently. Hub locations are determined from the interaction of two-hub-stop service routes.

Aykin (1995b) presents a framework for a hub-and-spoke distribution system with networking policies and the associated models. The author considers two cases of policies: *nonstrict hubbing*, and *strict and restrictive hubbing*. The first policy allows flows to move via direct transportation or through hub if that is found more efficient, while the second restricts all flows through hubs, in which flows to/from a node are channeled through the same hub. The author discusses various effects of network policies on hub locations and route structure for air passenger and cargo transportation.

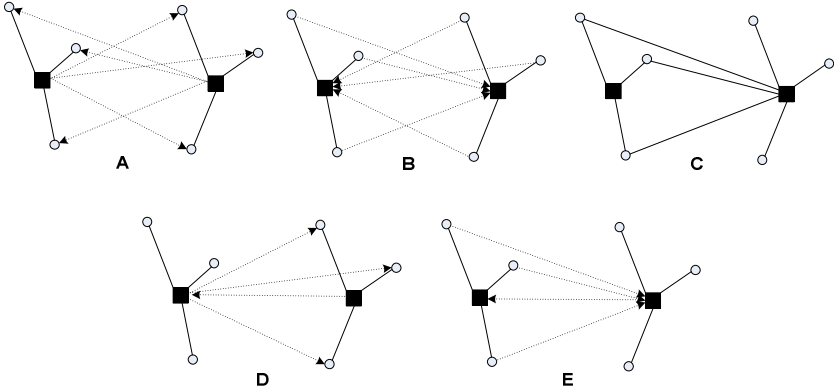
O'Kelly et al. (1996) examine two alternative levels of spoke connectivity for hub location models and discuss the sensitivity of the solutions to the *interhub discount factor*. This discount factor, which ranges between 0 and 1, represents the possibility of cost reduction per unit of flow on high-capacity interhub links. The first alternative allows nodes to be connected to only a single hub, while in the second, a

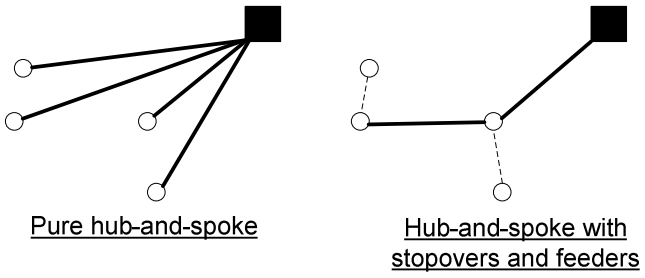
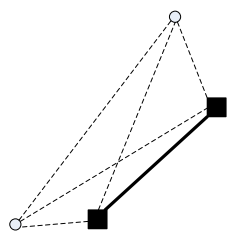
node can interact with multiple hubs. In both cases, the hubs are completely connected and all flows are restricted through the hubs.

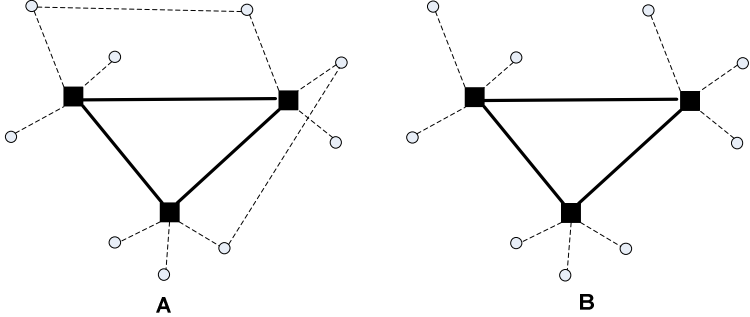
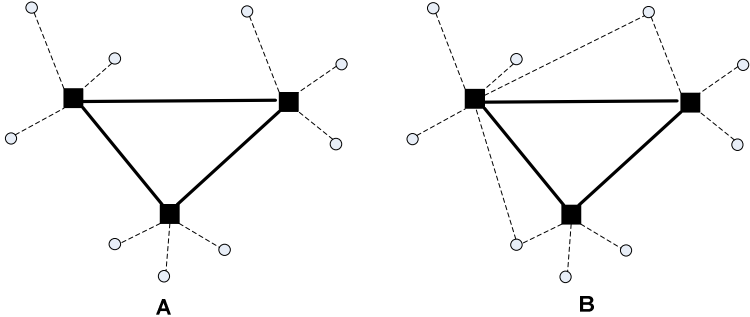
O’Kelly and Bryan (1998) explicitly emphasize the scale economies from using interhub links in the hub-and-spoke network. Due to the transshipment function and by allowing interhub costs to be a function of flows, the interhub links have the largest potential for agglomerating flow and, hence, lowering the network cost. Their results show that the optimal hub network tends to have a few interhub link(s) with large flows while the other interhub links have very slight flows.

In Table 2.2, we summarize the above reviews. An arc without an arrow indicates that aircraft fly in both directions across a link while an arc with arrow indicates that aircraft only fly in the specified direction. In addition, a box designates a hub and a circle designates a city or a nonhub airport.

Table 2.2: Summary reviews for hub network structures and characteristics

Author(s)	Problem/Network Configuration
Hall (1987)	Two-hub routing is found to be efficient for package distribution system that serves many airports; however, the result does not account for the effect of time-frame restrictions.
Hall (1989)	<p>Compares the number of required flights in different routing strategies, where multiple hubs are considered. The five strategies are described according to the time-frame restrictions and the number of airports served, which are:</p> <p>A: One-hub, shipments sent via hub closest to origin.</p> <p>B: One-hub, shipments sent via hub closest to destination.</p> <p>C: Master hub in east.</p> <p>D: One-hub west-to-east via terminal closest to origin, two-hub east-to-west.</p> <p>E: One-hub west-to-east via terminal closest to destination, two-hub east-to-west</p> 

<p>Kuby and Gray (1993)</p>	<p>Compare the stopover and feeders to the direct flights in hub-and-spoke network. Only single hub sorting is considered.</p> <div style="text-align: center;">  <p>The diagram shows two network structures. The left structure, labeled 'Pure hub-and-spoke', features a central black square hub connected by solid lines to four white circle spokes. The right structure, labeled 'Hub-and-spoke with stopovers and feeders', features a black square hub connected by solid lines to two white circle nodes. One of these nodes is further connected by a solid line to a third white circle node, which is then connected by a dashed line to a fourth white circle node, representing a stopover and feeder path.</p> </div>
<p>Aykin (1995a)</p>	<p>For each commodity, defined by the origin-destination pair, consider hub location and routing separately from the other commodities.</p> <div style="text-align: center;">  <p>The diagram shows a network with three white circle nodes and two black square nodes. A solid line connects one of the black square nodes to one of the white circle nodes. Dashed lines connect the other two white circle nodes to each other and to both black square nodes, illustrating a routing path for a commodity that may involve a hub.</p> </div>

<p>Aykin (1995b)</p>	<p>Consider two network policies: (A) nonstrict hubbing and (B) strict and restrictive hubbing.</p> <p>A: Flows channeling through hubs are not required but chosen if found less costly.</p> <p>B: All flows to/from a node must be channeled through the same hub.</p> 
<p>O'Kelly et. al (1996)</p>	<p>Discuss the sensitivity of hub location solution to the <i>interhub discount factor</i>. The single (A) and multiple hub (B) assignment models are considered. A multihub network is considered.</p> 
<p>O'Kelly and Bryan (1998)</p>	<p>Present the hub location model that accounts for scale economies by allowing interhub costs to be functions of flows.</p>

2.5 Solution Approaches

In this section, due to the nature of express package shipment delivery, we review the solution approaches related to multicommodity network flow problem (MCNF). As in section 2.1, there are several surveys on MCNF models and solution approaches (see Kennington 1978, Assad 1978, Ahuja et al. 1993.)

Ahuja et al. (1993) describe three general approaches for solving a multicommodity flow problem, including:

- Price-directive decomposition. The capacity constraints are relaxed and placed on the objective function by using Lagrangian multipliers (or prices).
- Resource-directive decomposition. This can be viewed as a capacity allocation problem. It allocates capacities to the commodities, and then uses information from the resulting single-commodity problem as subgradient direction to reallocate capacity to improve the overall system cost.
- Partition method. The approach attempts to work on each small individual single-commodity flow problems, where the bundle constraints are required to tie the individual solutions together. The solutions can be updated by special network simplex operations.

The column generation approach, first suggested by Ford and Fulkerson (1958) and by Tomlin (1966), is another promising method to solve multicommodity flow problem, as shown in Barnhart et al. (1995), and in Holmberg and Yuan (2003). Barnhart et al. (2000) apply branch-and-price-and-cut to this problem.

Crainic et al. (2000) proposed the tabu search metaheuristics for the path-based formulation of the fixed-charge capacitated multicommodity network design problem. The method explores feasible solution space of path-flow variables by using a tabu search framework combining pivot moves with column generation. The method considers the impact of changing the flow of only one commodity for each search. Recently, Ghamlouche et al. (2003) present a new cycle-based neighborhood for a tabu search metaheuristic that takes into account the impact on the total design cost when modifying the flow distribution of several commodities simultaneously. When a design arc is closed or opened, the algorithm will redirect flow around that arc accordingly.

Solution approaches applying to the specific express shipment service network design are sequentially summarized in Table 2.3.

2.6 Summary

Several past studies have focused on interhub links, which could potentially decrease the overall transportation cost. With more cities served, a two-hub sorting operation should eventually become preferable. However, as stated in Hall (1989), it is difficult to implement such a two-hub operation in a limited time frame, given a fixed sorting capacity. Even if we can conduct such an operation, the cost of the sorting operations would increase. In addition, aircraft rotation is another obstacle when the number of cities served is imbalanced between east and west regions. Therefore, with a fixed hub sorting capacity, several works on air express network design only consider one-hub operation.

If the incremental cost of a higher sorting rate is reasonable, there might be the possibility of implementing a two-stage sorting operation. Moreover, the coordination of hub sorting operations and aircraft schedules for such operation should then be explored.

Table 2.3: Summarized solution approach applied to express shipment service network design

Author(s)	Solution Approach
Barnhart and Schneur (1996)	Apply explicit column generation approach to find candidate aircraft route, while package paths are not considered.
Kim et al. (1999)	Use derived schedule network to represent the time-space network of the problem, and then apply a network reduction method with a node consolidation approach. Apply column and row generation for solving LP relaxation. Explicit column generation is applied to find candidate aircraft route, while implicit column generation is applied on package movement problem. With a large gap in IP-LP solution after using branch-and-bound method, a heuristic solution approach is applied. To do so, they first solve the approximate aircraft route network that can serve all demand with O-D cutsets and satisfy the operational constraints. Later, with the resulting approximate air network, package routes can be solved to identify the paths.
Barnhart et al. (2002)	Develop a different solution approach than Kim et al. (1999). Route generation and shipment movement subproblems are introduced. The route generation subproblem is solved using branch-and-price-and-cut, while branch-and-price is used to solve shipment movement subproblem. In Kim et al. (1999), shipment movement does not influence the decision at the route level. Therefore, a sequential approach is implemented by iterating between route and shipment movement generation to allow shipment movement to affect route generation.

Armacost et al. (2002)	The <i>composite variable</i> formulation is introduced, in which the variable represents the combination of aircraft routes and implicitly capture package flows. Package flow variables are no longer presented as separate decision variables. The resulting LP relaxation gives stronger lower bounds in solving a restricted version of express shipment service network design.
Smilowitz et al. (2003)	A two-stage solution approach is proposed. Apply column generation and cutting plane method to find the lower-bound solution for the LP relaxation. To obtain upper-bound solution or a feasible integer solution, several rounding approaches are described.

Chapter 3

Problem Definitions

In this section, we first provide an overview of the current next day air shipment delivery operations. The integration of hub sorting operation to air network is then demonstrated, in which a two-stage sorting operation is mainly focused. At a hub, the detailed FIFO sorting process is presented, and the resulting effect of this operation on the air network and package flows is described. Later in Chapter 5, the air network design, hub sorting and pricing sub problems will be incorporated at the new tactical planning to optimize the total system cost.

3.1 Problem Characteristics

3.1.1 Overview of Current Next-day Air Shipment Operation

Next-day shipment delivery is one of several shipment services provided by the dominant package delivery companies. With a service commitment in which packages must be picked up and delivered within a limited time window in which a carrier has enough time to provide such service, associated times to each service center, e.g. a spoke airport, are defined, i.e., *earliest pickup time* (EPT) and *latest delivery time* (LDT). EPT denotes the earliest time when an aircraft can depart from the origin service center, while LDT specifies the latest time at which packages can be delivered to the destination service center. Figure 3.1 demonstrates the existing or single-stage sorting operation. In Figure 3.1, after arriving from a *ground center* via trucks or small aircraft, packages are loaded onto an aircraft at an airport service center, which serves as entry and exit point of packages to the air network. Then aircraft can fly either directly to a hub sorting facility, or via a single intermediate service center. After packages arrive at the hub, they are sorted and loaded onto departing flights for the delivery service. *During the sorting operation, all planes remain at the hub and wait until "all" packages are loaded before departing.* At each hub, the *sort end time* (SET) represents the latest time at which planes can arrive from pickup routes, and also denotes the earliest time when planes may depart on delivery routes.

Early studies of the air express network design problem, including Barnhart and Schneur (1996), Kim and Barnhart (1999), Kim et al. (1999), Armacost (2002), Barnhart et al. (2002), focus specifically on single-stage operations.

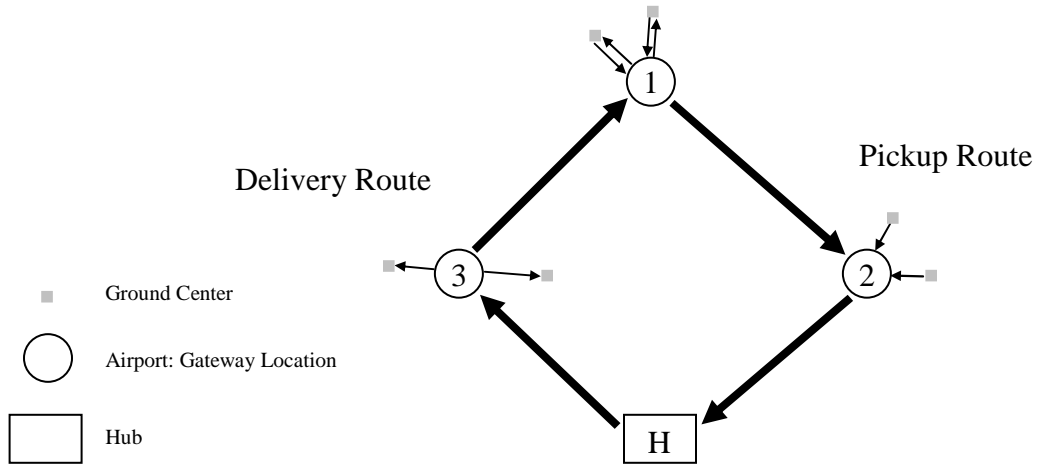


Figure 3.1: Existing next day air operation

3.1.2 Integration of Hub Operation and Air Routing: Concepts and Contributions

Before demonstrating all the concepts and assumptions in the proposed model, a preliminary analysis can demonstrate the major cost savings of the two-stage sorting operation. The following discussion will mainly focus on a distribution network with two or more hubs, in which physical service center locations and demands may justify additional hubs. Furthermore, examination of small networks will reveal principles that apply to larger networks. In the proposed operation, aircraft are allowed to depart earlier than the SET so that they can meet the second hub's requirement (SET).

Let d^k denote the demand of commodity $k, k \in K$, where an origin-destination market pair defines each commodity, $O(k)$ and $D(k)$ define the origin and destination of commodity k , respectively. Also let S and H be the set of service centers and hubs, and assume the aircraft capacity u^f exceeds the demand of any

airport i , which is $\sum_{k \in K \cap \{O(k)=i\}} d^k < u^f$ on the pickup side or $\sum_{k \in K \cap \{D(k)=i\}} d^k < u^f$ on the delivery side. In the *worst-case scenario* where only single leg flights are allowed due to the limited time span between any service center's EPT and hub's SET, we can determine the number of flight legs and the number of aircraft required for both systems as follow.

In the current practice, i.e., single-stage sorting operation (without integrated air express network design and hub sorting), as shown in Figures 3.2 and 3.4, the worst-case number of flight legs ($L_{current}$) and aircraft ($N_{current}$) required can be determined from equations (3.1) and (3.2), respectively. It is noted that the number of flight legs, which comprises flight legs on the pickup and delivery sides, can simply be determined from the number of hubs $|H|$ and the number of service centers $|S|$.

$$\begin{aligned}
 L_{current} &= \text{The worst-case number of flight legs in current practice} \\
 &= |H||S|_{pickup} + |H||S|_{delivery} = 2|H||S| \tag{3.1}
 \end{aligned}$$

$$\begin{aligned}
 N_{current} &= \text{The worst-case number of aircraft used in current practice} \\
 &= |S||H| \tag{3.2}
 \end{aligned}$$

With the proposed model or two-stage sorting operation, where integrated air network with hub sorting operation is considered as shown in Figures 3.3 and 3.5, the maximum number of flight legs ($L_{proposed}$) and the aircraft ($N_{proposed}$) required can be determined from equations (3.3) and (3.4), respectively. Assume that in the two-stage sorting operation each service center is served by aircraft connected to its hub's territory, which is defined as the set of service centers having demand going to or

from the hub. Therefore, the number of flight legs comprises both flight legs between service centers and hubs, and flight legs between hubs.

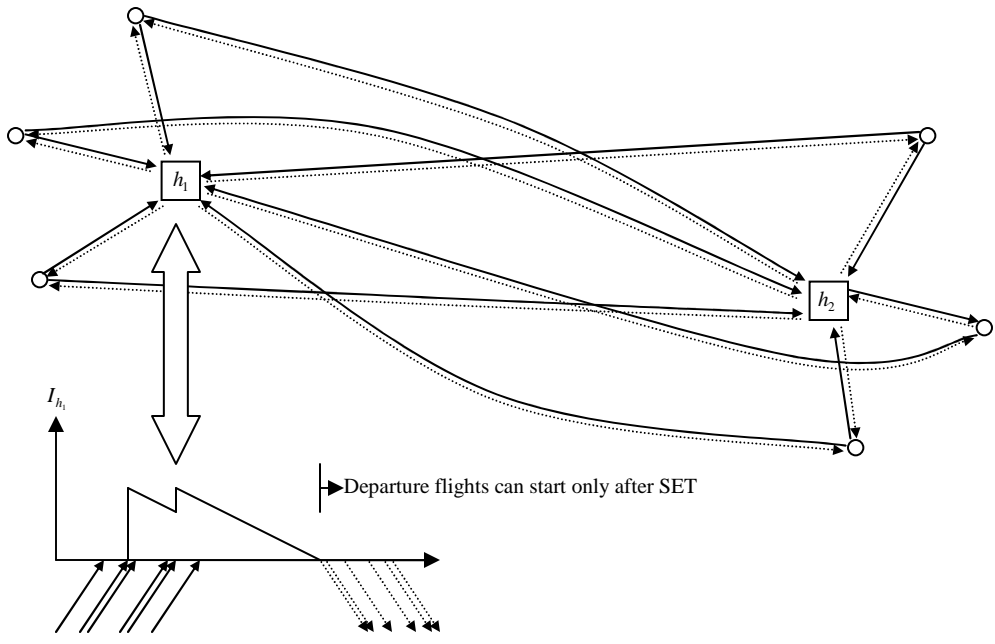


Figure 3.2: Worst-case scenario for the current number of flight legs (without integrated hub sorting operation)

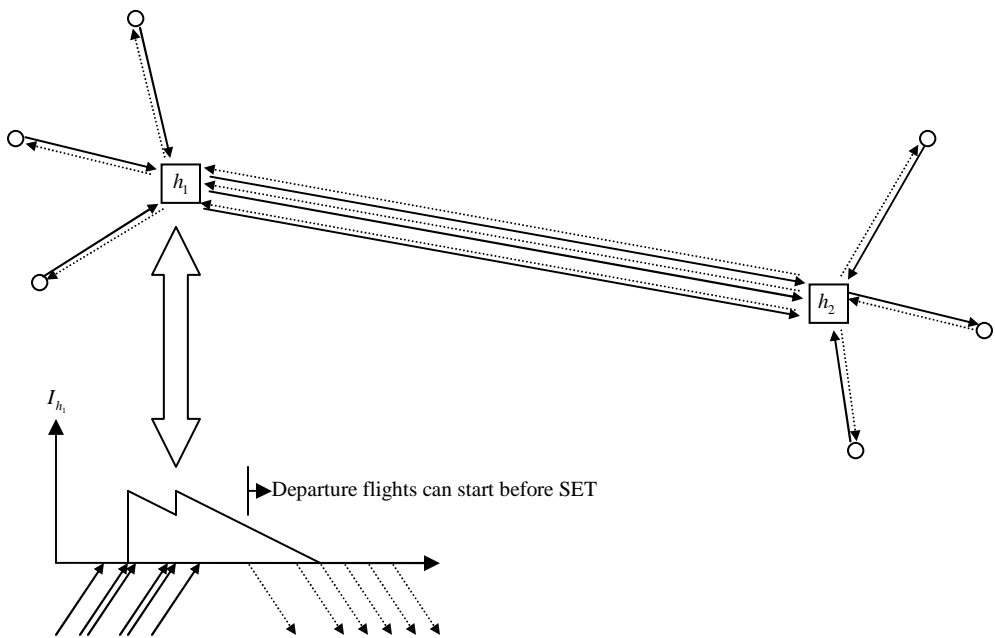


Figure 3.3: Worst-case scenario for the proposed number of flight legs (with integrated hub sorting operation)

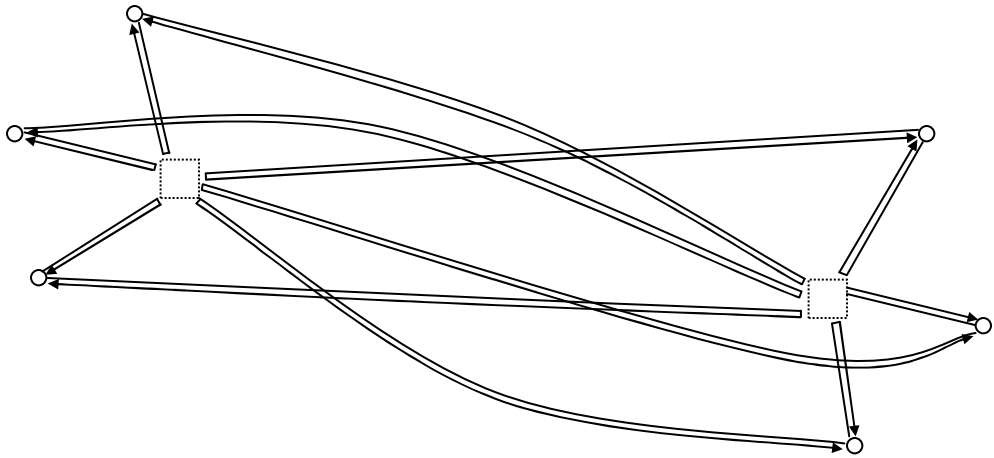


Figure 3.4: Worst-case scenario for the current number of aircraft required (without integrated hub sorting operation)

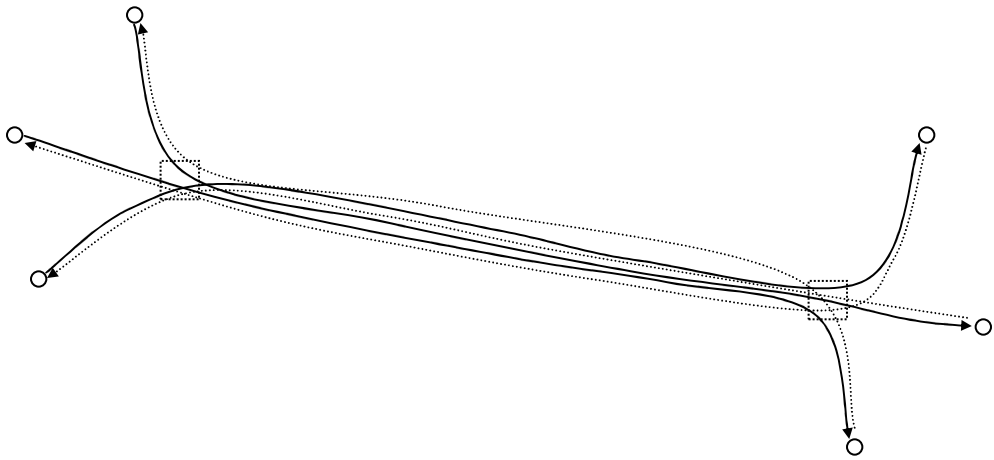


Figure 3.5: Worst-case scenario for the proposed number of aircraft required (with integrated hub sorting operation)

The first component can simply be determined by the number of service centers served on pickup and delivery sides. In the second component, the number of interhub flight legs depends on the aircraft load factor, ρ , defined by the actual load as a percentage of the aircraft capacity. To simplify the explanation, consider the two-hub network with equally sized hub territories, and aircraft transporting their shipments from the east hub to the west, $E \rightarrow W$, and vice versa. Under an assumption that aircraft capacity is greater than any service center's demand, the upper bound aircraft load factor for interhub flights is 1.

$$\begin{aligned}
L_{proposed} &= |S|_{pickup} + |S|_{delivery} + \lceil \rho \rceil_{E \rightarrow W} |S|_{delivery, E \rightarrow W} + \lceil \rho \rceil_{W \rightarrow E} |S|_{delivery, W \rightarrow E} \\
&= |S|_{pickup} + |S|_{delivery} + |S|_{delivery, E \rightarrow W} + |S|_{delivery, W \rightarrow E} \\
&= |S|_{pickup} + |S|_{delivery} + |S|_{delivery} = 3|S|
\end{aligned} \tag{3.3}$$

$$N_{proposed} = |S|_{pickup} = |S|_{delivery} = |S| \tag{3.4}$$

The results in equations (3.1) – (3.4) indicate the potential savings in the number of aircraft and flight legs required with the two-stage sorting operation. Clearly, the proposed aircraft route structure increase the utilization of aircraft by flying on pickup, interhub and delivery routes, when there is enough time. In addition, the aircraft load factor, ρ , is one of the core elements in reducing the number of flight legs, as shown in equation 3.3. To efficiently manage the interhub aircraft load factor in such a limited time frame for next day delivery, an aircraft dispatch time must be carefully selected so that an aircraft's capacity is optimally utilized while meeting the second hub's SET. Those savings are very unlikely unless hub sorting and air network design are efficiently integrated.

However, with a limited time span, the drawbacks of this proposed model are the increase in hub sorting time and/or sorting rate, given that the level-of-service at each service center remains unchanged (fixed EPT and LDT). To make the proposed operation feasible at the first sorting process, the hub sort start time (SST) must be set earlier so that, when sorted packages are available, an aircraft can depart and meet the sort end time for the second sorting process. Similarly, the hub sort end time (SET) should be extended so that all interhub flights can arrive on time and their carried packages can be sorted. Even if hub sorting hours are extended, a two-stage sorting operation might be impossible if the sorting rate at each hub is low. Consequently, the sorting rate may have to increase to speed up the whole operation. In addition, the size of sorting facility may have to increase so that all unloaded packages can be held.

Note that the two-stage sorting operation is applicable only to the multiple-hub network. The integrated hub sorting operation, however, could benefit the single-hub network. In a case where a service center's demand exceeds the assigned aircraft's capacity, two or more flights must serve that particular service center. The first aircraft, whose capacity is completely utilized, can depart before SET. This could reduce the departure congestion when takeoff capacity is limited. Departing earlier than SET can be considered for any delivery route not serving as the last flight to its service center.

3.2 Hub Sorting Subproblem

To properly incorporate hub sorting operation with air express network design, the hub sorting subproblem must be described, in which underlying concepts and assumptions are stated. The discussions mainly focus on the multi-hub network, where the integration benefits single-hub operation when having more than one flight serving any single service center, as stated in section 3.1.

Concepts:

1. In the current practice of next day delivery service, once all inbound planes unload their packages at a hub, they will wait until all packages are sorted before beginning their delivery routes. With the proposed two-stage sorting operation, some aircraft that will transport sorted packages among hubs for the second sorting process may depart before the SET. To identify the appropriate dispatch time for those interhub flights, the information about sorted package ODs is essential for identifying when there are enough loads to be carried.
2. From Concept 1, at the first hub sorting, packages may need to arrive earlier, and be consolidated with other packages having the same secondary hub sorting location. As a result, interhub flights can depart earlier, thus making the two-stage sorting process more feasible, especially in a limited time frame.
3. Within the hub sorting process, the destinations of sorted packages and the time when they are ready to be flown away is important. To properly estimate that information, when packages are sorted is needed. In this study, we model the hub sorting process as *FIFO inventory sorting model* (First in, First out - packages arriving earlier are sorted first), as shown in Figure 3.6.

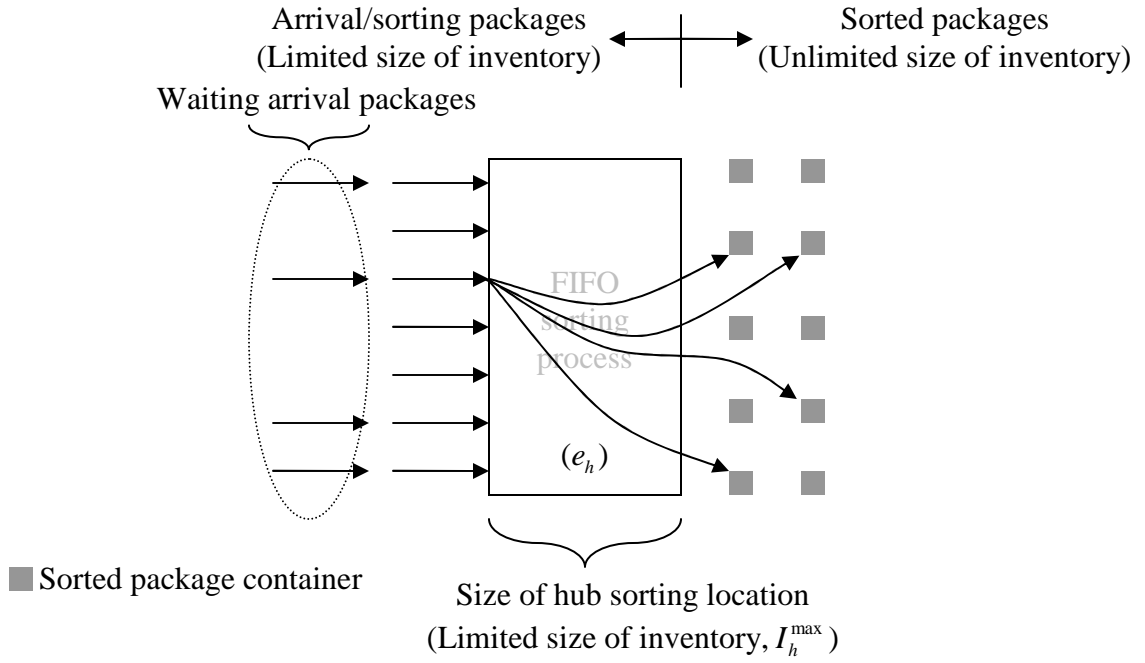


Figure 3.6: Arrival/sorting and sorted packages in FIFO sorting process at hub location

4. To reflect the expected higher hub sorting rate and storage size for the two-stage sorting operation, we model the hub sorting model as a FIFO inventory model, which follows the concepts of general inventory model (GIP) in supply chain management. At hub h , the hub sorting rate (e_h) is comparable to a constant demand rate that reduces the inventory level, while arrival packages at hub are treated as inventory fulfillment in GIP. In addition, the hub storage (I_h^{\max}) or the maximum number of unsorted package in the hub can be viewed as the maximum inventory in GIP. Figure 3.7 demonstrates the FIFO inventory sorting model, where $x_{h(t_m)}^k$ denotes the number of packages of commodity k that arrives to be sorted at hub h at time t_m . Also note that the unused sorting period is analogous to stock-out duration in GIP.

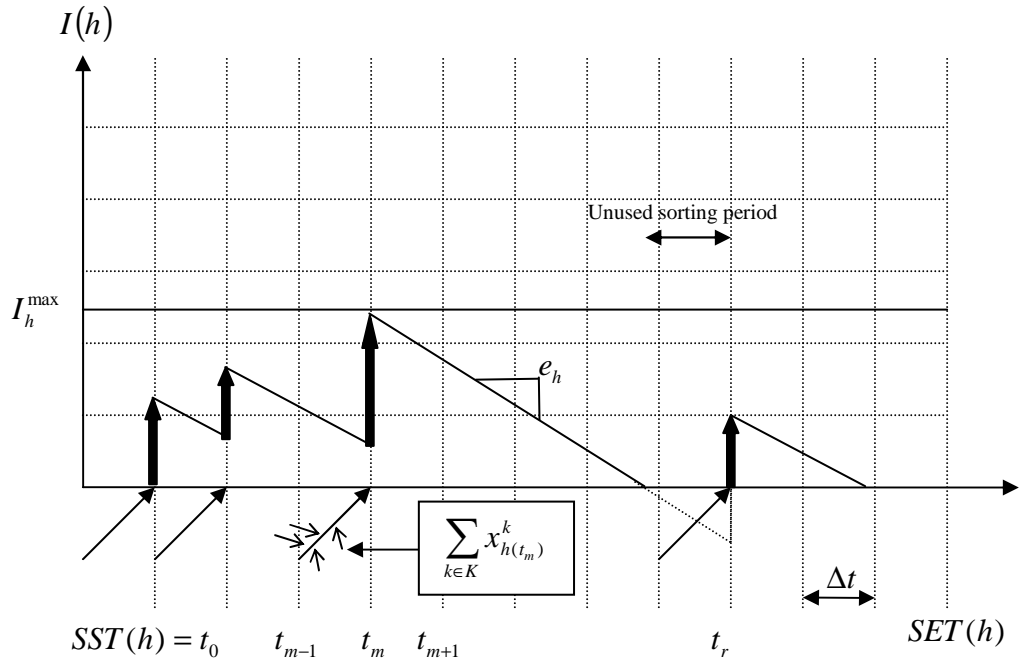


Figure 3.7: Inventory sorting model for hub sorting process

5. To reuse an aircraft from the pickup route after it unloads its packages, the aircraft can be utilized to serve an interhub route when needed. Clearly, this will increase aircraft utilization, thus reducing the number of aircraft required. However, given a hub storage (I_h^{\max}) and the current number of packages waiting to be sorted (I_h^t), an aircraft cannot be reutilized before it unloads all its packages. That is, the total number of packages carried exceeds $I_h^{\max} - I_h^t$. Therefore, that particular aircraft must be held until it unloads its packages. In Figure 3.8, aircraft No. 5 must wait until the next grid time for unloading, while in Figure 3.9, all arrival aircraft can unload their packages without waiting. Let $X(h_1(t_1) \rightarrow h_2(t_2))$ represent the total number of packages

leaving from hub h_1 at time t_1 , and arriving at hub h_2 at time t_2 . Figure 3.10 (a) illustrates the inventory sorting profile resulting from the example in Figure 3.9. In addition, Figure 3.10 (b) shows the sorted package inventory ($P(h)$) and how the information is used to identify the aircraft dispatch time, as stated in Concept 1. It is noted that $\Delta_1 + \Delta_2 + \Delta_3$ represents the number of sorted packages during $SET(h_1)$ and t_i .

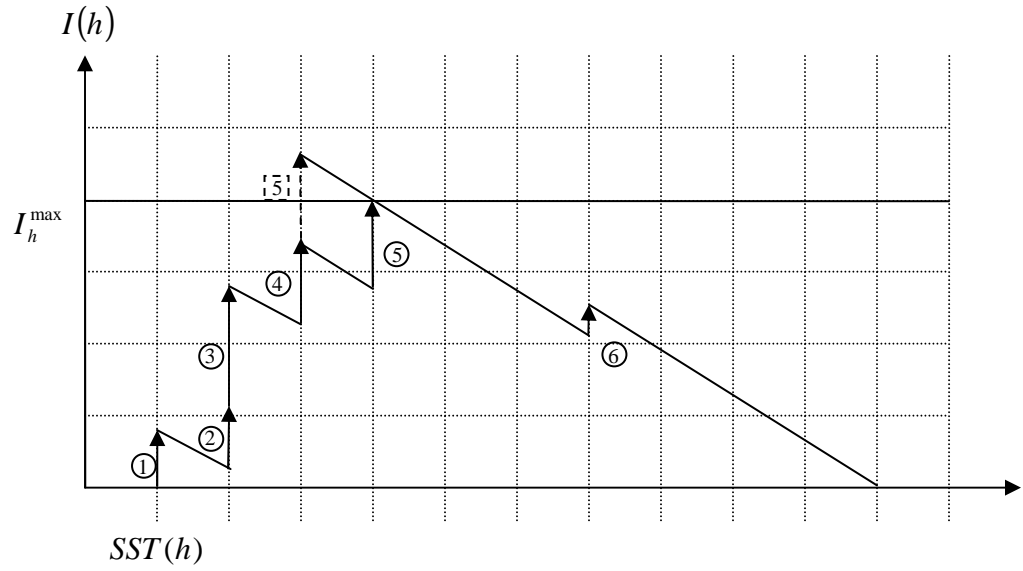


Figure 3.8: One arrival aircraft waits until the next grid time to unload packages

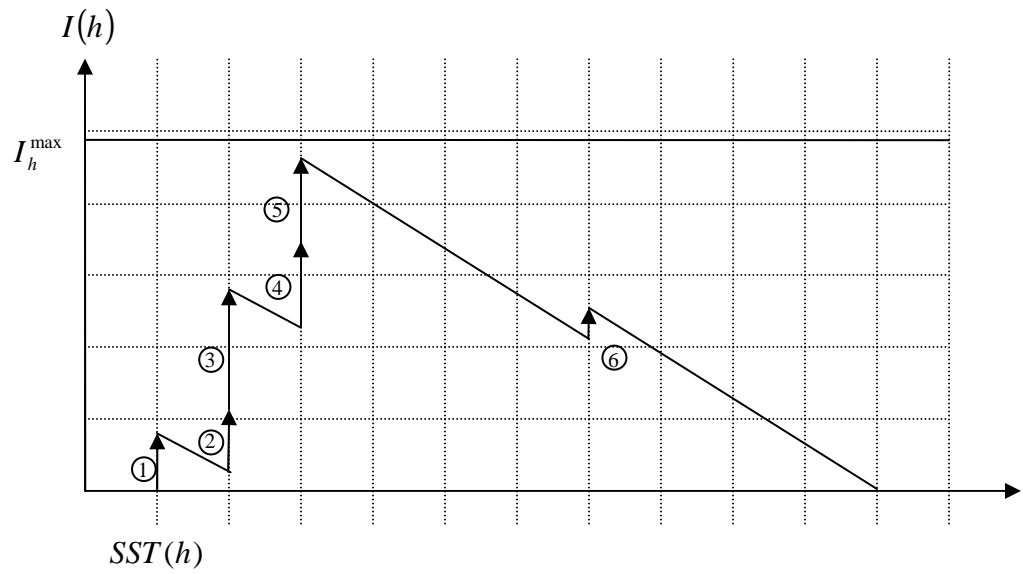


Figure 3.9: All aircraft unload packages immediately after arriving

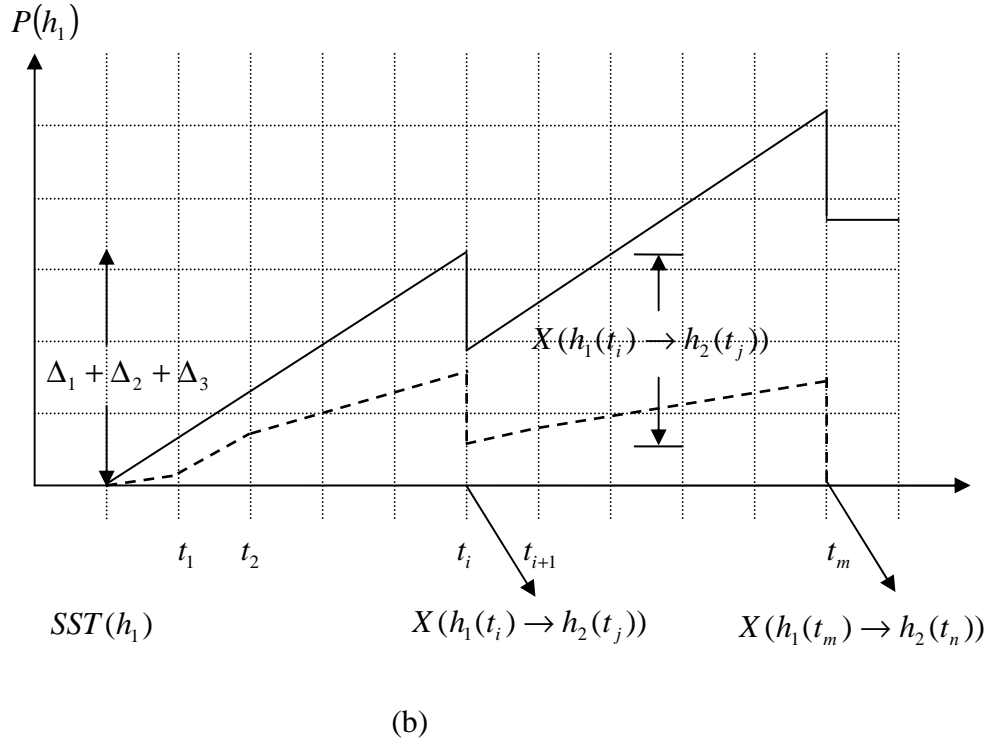
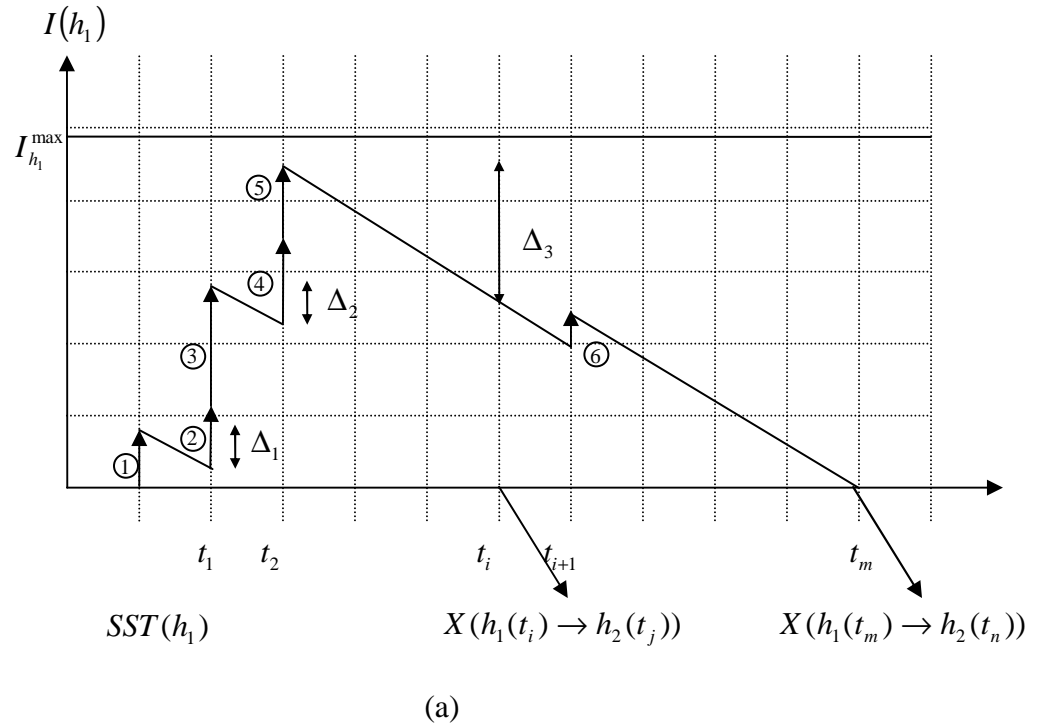


Figure 3.10: Using knowledge of sorted package ODs to identify an aircraft dispatch time

6. The integration of hub sorting operation with air network design should be able to identify the best operation to maximize the overall efficiency of package delivery system. For example, in Figure 3.8, let us assume that flights 4 and 5 are served by different aircraft types. If it is optimal to operate the interhub flight departing on the next grid time by using the same aircraft type as flight 5, then flight 5 should unload its packages first and flight 4 should be held until the next grid time. It is notable that I_h^{\max} does not affect the unloading sequence of flights 2 and 3, although the two flights are served by different aircraft types. In addition, if flight 5 carries more packages than flight 4 for the second sorting process, then flight 5 might be favored to unload first (using knowledge of package ODs on the arrival aircraft to identify which aircraft should unload first)

7. To further optimize the system performance, we should consider not only the integration within each individual hub but also the coordination among hubs. With the coordination of sorting operations among hubs, expected hub sorting inventory levels are shown in Figure 3.11. In Figure 3.11, the latest outbound interhub flights at hubs h_1 and h_2 , depart at t_b and t_c , respectively. Given a hub's territory and FIFO sorting process, the hub should first sort all packages from its hub territory (all incoming pickup routes) before the ones that do not belong to itself (the interhub flights.) For example, in Figure 3.11 at hub h_1 , all packages arriving after t_b (since t_c) will be sorted and delivered only to hub h_1 's territory. Therefore, at each hub, the integrated operation should be

able to schedule all the interhub routes arriving after pickup routes (service center to hub routes) so that the pickup packages are first sorted to identify whether they must be transported to the secondary hubs.

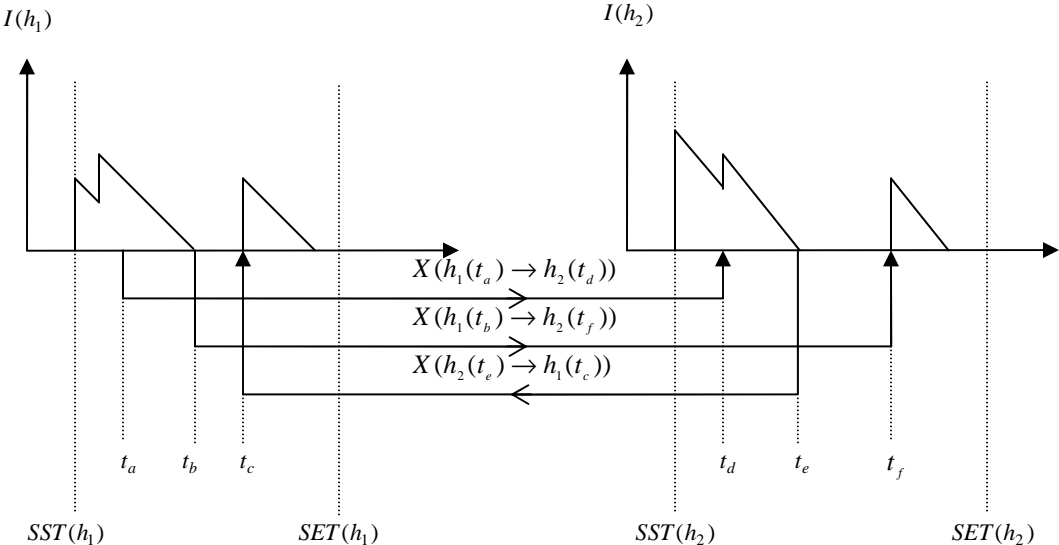


Figure 3.11: Coordination between hub sorting operations and air route design

Assumptions:

1. In this study, the SST and SET associated with each hub are fixed and given, while I_h^{\max} and e_h are considered as the designed elements.
2. At each hub h , all arrival packages will be sorted in a FIFO process. Given a hub sorting rate, e_h , the expected sorted time of the prospective set of arrival packages, $E[T(e_h)]$, can simply be determined from equation 3.5, as illustrated in Figure 3.12.

$$E[T(e_h)] = \frac{I_h^{t_m} + \sum_{k \in K} x_{h(t_m)}^k}{e_h} \tag{3.5}$$

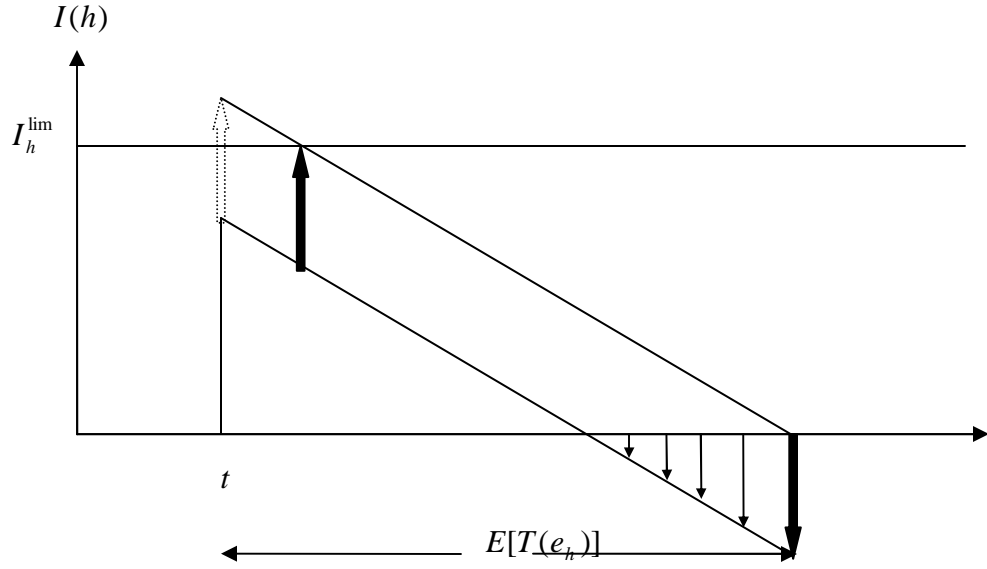


Figure 3.12: Expected sorting end time

3. Given SST and SET for each hub h , the sorting time interval is divided into equal time intervals (Δt) for modeling purposes. All the arrival or departure flights will therefore be assigned to the next nearest grid time. Let the set of grid time for hub h is defined as:

$$G(h) = \{SST = t_0, t_1, t_2, \dots, t_i, \dots, SET\}$$

4. After an aircraft unloads its packages, it will be available to fly on the delivery or interhub route at the next grid time.
5. The capacity of all aircraft type $f, f \in F$ is considerably less than the hub sorting inventory, $u^f \ll I_h^{\max}, \forall f \in F, \forall h \in H$

Chapter 4

Network Representations

Time and space are essential elements for many transportation-related scheduling problems. These problems are modeled by having a time-space structure, with nodes representing time and space, and arcs representing movement in time and possibly space. Specifically to our models, each node in the time-space network corresponds to the origin or destination of an aircraft and a package movement at some point in time, and each arc represents the movement at a particular time of an aircraft or a package. Furthermore, to properly integrate the hub sorting model with the conventional time-space network, the way packages are sorted over time at a hub should also be modeled in the same time-space structure. In this study, the time-space network can be categorized into three parts, as follows:

1. Hub Sorting Network (HSN)
2. Aircraft Route Network (ARN) and
3. Package Movement Network (PMN).

4.1 Hub Sorting Network (HSN)

To model the HSN having the FIFO sorting process, the conventional time-space network is applied where its nodes correspond to time and sorting sequence, while arcs represent the movement of packages over the hub sorting sequence. Figure 4.1 represents the HSN that can perform the FIFO sorting process as described in section 3.2. For hub h , the HSN consists of the following components:

1. The number of sorting time frames, $|G_h|$, is the time instances in which aircraft can arrive or depart for the sorting system of hub h . G_h is the set of sorting time frame of hub h . The first and last elements in G_h are SST and SET, respectively, where:

$$G_h = \{SST, SST + \Delta t, SST + 2\Delta t, \dots, SST + (|G_h| - 2)\Delta t, SET\}$$

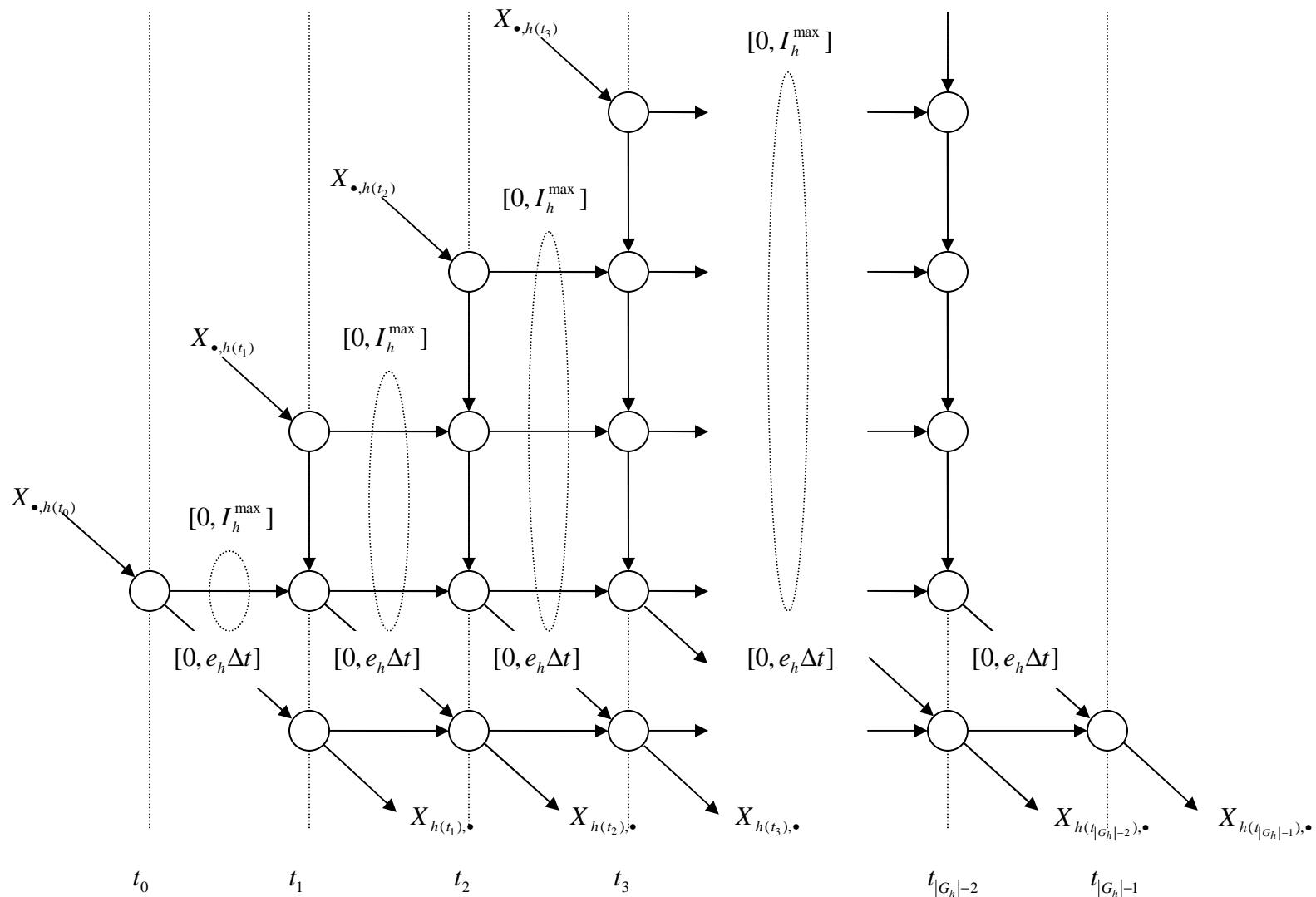


Figure 4.1: HSN representation for hub h

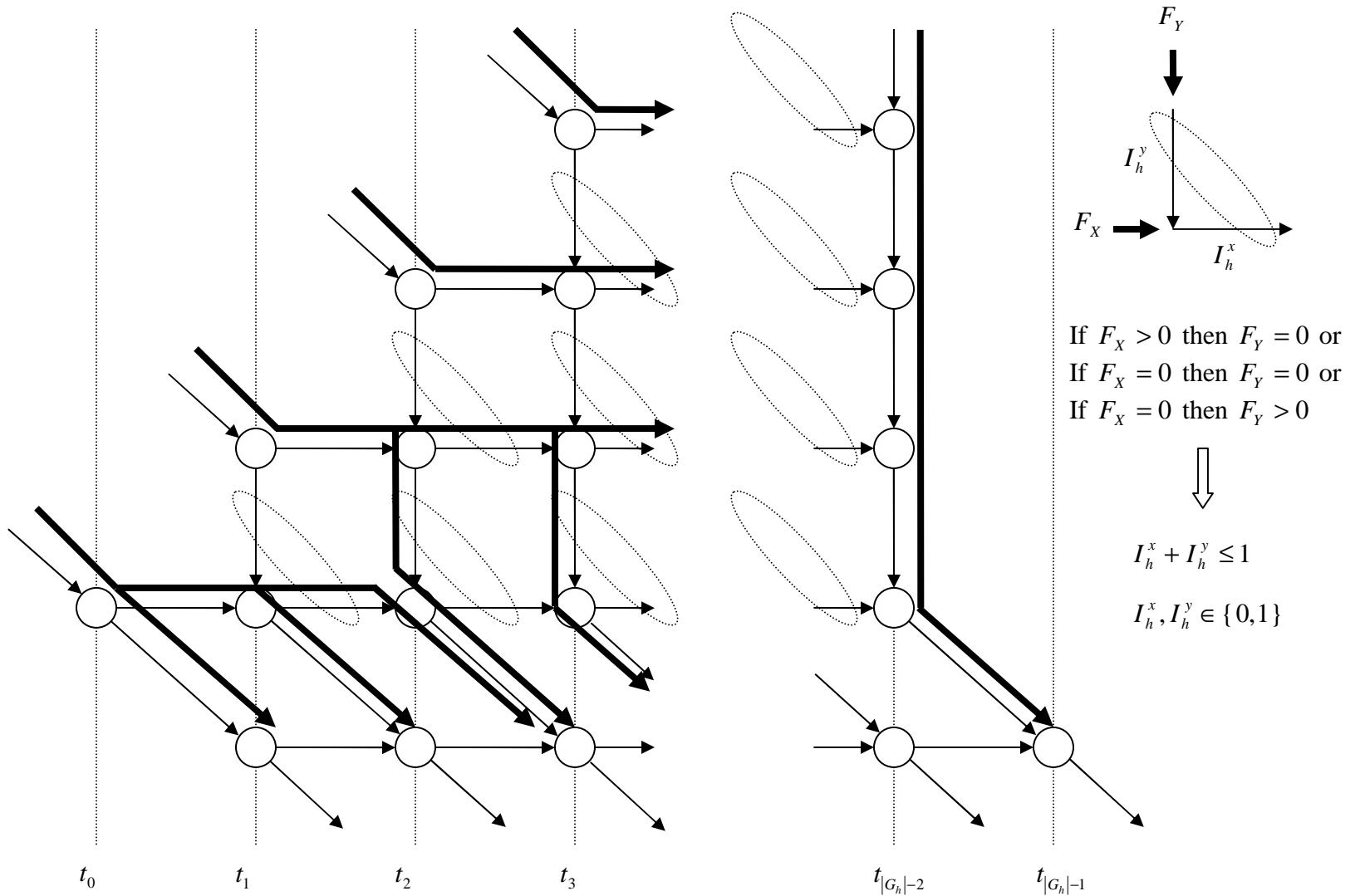


Figure 4.2: Package flow in FIFO HSN

2. The hub sorting rate, e_h , is the hourly capacity for sorting arrival packages. In Figure 4.1, because we model the hub sorting network as a set of node-arc, the hub sorting rate can be viewed as the arc capacity. Given a time interval, Δt , where $\Delta t = (SET - SST) / (|G_h| - 1)$ and $|G_h| - 1$ represents the number of sorting arcs, the sorting capacity per arc is $e_h \Delta t$. It is noted that in the capacitated network design problem the sorting capacity in each arc, $e_h \Delta t$, can be viewed as an upper bound flow on that arc.
3. The hub storage size, s_h or I_h^{\max} , is the size of hub sorting facility that can hold all the unloaded packages in the sorting queue at any given grid time interval. It is noted that, from Figure 4.1, the total number of packages waiting to be sorted in any given time interval $(t - \Delta t, t)$ must be less than I_h^{\max} , i.e.,
$$I_h^{t-\Delta t, t} \leq I_h^{\max}, \forall t \in G_h \setminus \{SST, SET\}.$$
4. A set of horizontal and vertical package flow control indicators, $\{I_h^X\}$ and $\{I_h^Y\}$, are used to control package sorting sequences in the HSN, as shown in Figure 4.2. Those indicators, using binary variables, enforce the arrival packages to be sorted in a FIFO process. For example, in Figure 4.2, at time t_1 , all packages arriving at a hub at time t_1 ($X_{\bullet, h(t_1)}$) cannot enter the sorting process right away, because some packages arriving before t_1 (which is $X_{\bullet, h(t_0)}$ in this case) are still unsorted. However, some of $X_{\bullet, h(t_1)}$ can enter the sorting process at time t_2 since $X_{\bullet, h(t_0)}$ has been completely sorted and left

some room for $X_{\bullet, h(t_1)}$ to be sorted ($3e_h \Delta t - X_{\bullet, h(t_0)} \geq 0$.) Similarly, at time t_3 , $X_{\bullet, h(t_2)}$ must wait until $X_{\bullet, h(t_1)}$ are completely sorted.

4.2 Aircraft Route Network (ARN)

In this study, the aircraft route network can be categorized into three groups, as follows:

1. Set of pickup routes (R_p),
2. Set of delivery routes (R_D), and
3. Set of interhub routes (R_H).

In the single-stage model, only R_p and R_D are considered, while all three sets of aircraft routes are included in the two-stage model. To construct the ARN with a time-space structure, associated times and physical locations of the service centers and hubs are needed. Recalling the discussion in section 3.1, each service center is associated with an earliest pickup time (EPT), and a latest delivery time (LDT), while a sort start time (SST) and a sort end time (SET) are considered at each hub location.

In the following subsections, we follow Kim et al. (1999) in constructing the ARN of R_p^f , R_D^f and R_H^f for each aircraft type f , $f \in F$.

4.2.1 Single-Stage Sorting ARN

In the single-stage sorting model, packages are sorted only once at one hub before delivered to their destinations. To ensure that all packages are sorted before starting

delivery routes, all the flights can depart only after the hub's SET. Therefore, these characteristics guide the construction of the pickup and delivery routes as follows:

4.2.1.1 Pickup Routes/Delivery Routes (ARN-P/D)

To generate the set of feasible pickup routes (the set of delivery routes can be built similarly) for each aircraft type $f, f \in F$, the network representation is constructed with three types of nodes: gateway nodes, intermediate nodes, and hub nodes. A gateway node represents the first (last) stop on a pickup (delivery) route, while a hub node is the last (first) stop on a pickup (delivery) route. To demonstrate the travel patterns of aircraft making stops before arriving at a hub on pickup routes or after departing from a hub on delivery routes, intermediate nodes are introduced. It is noted that, for each aircraft type f on pickup (delivery) routes, the number of nodes in the representation network consists of:

- The number of gateway nodes: $|S|$
- The number of intermediate nodes: $|S|^2 + |S||H|$, and
- The number of hub nodes: $\sum_{h \in H} \{G_h - 1\}$

S and H denote the set of service centers and hubs, respectively. G_h represents the set of grid time at hub h . Figure 4.3 provides an example of network representation of R_p^f , where hub nodes on the pickup side are used to determine the arrive time at the hub.

For pickup routes, arcs connecting each node in the representation network are linked when it is a feasible pickup route, i.e., route $i \rightarrow j \rightarrow h$ is feasible if:

$$\begin{aligned}
& \text{Max}(EPT(i) + t_{\text{loading}} + \text{TravelTime}(i \rightarrow j), EPT(j)) + t_{\text{loading}} + \\
& \qquad \qquad \qquad \text{TravelTime}(j \rightarrow h) + t_{\text{unloading}} \leq t_h \\
& \qquad \qquad \qquad \forall i, j \in S, \forall t_h \in G_h \setminus \{SET\}, \forall h \in H \qquad (4.1)
\end{aligned}$$

For delivery routes, arcs will be connected for route $h \rightarrow j \rightarrow i$ when equation (4.2) holds.

$$\begin{aligned}
& t_h + t_{\text{loading}} + \text{TravelTime}(h \rightarrow j) + t_{\text{unload}} + \text{TravelTime}(j \rightarrow i) + t_{\text{unload}} \leq LDT(i) \\
& \qquad \qquad \qquad \forall i, j \in S, \forall t_h \in G_h \cap \{SET\}, \forall h \in H \qquad (4.2)
\end{aligned}$$

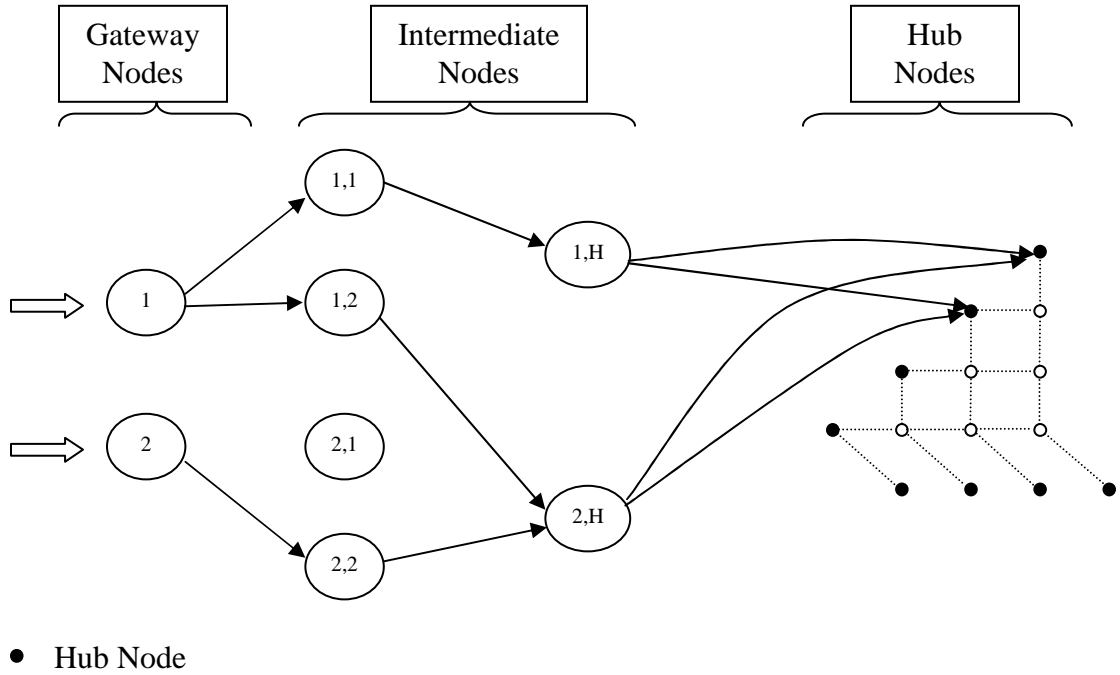


Figure 4.3: Network representation of R_p^f

4.2.2 Two-Stage Sorting ARN

In the proposed operation, each package will be sorted twice at two distinct hubs if its origin and destination are located on different hubs' territory. Still, some packages are sorted only once when their origins and destinations lie in the same hub's territory. It is noted that a hub's territory is defined as the set of service centers having demand going to or from the hub.

The characteristics of both pickup and delivery routes in this case are the same as those of a single-stage operation. To perform the second sorting process, interhub routes are needed to transport packages to the other hubs. With a limited time frame for next day delivery service, *some interhub routes are allowed to depart from the first hub before the hub's SET*. Accordingly, each of the first and last stops of an interhub route not only includes the hub location, but also the arrival/departure time.

From the above discussion, the pickup, delivery and interhub routes can be generated as follows:

4.2.2.1 Pickup Routes/Delivery Routes (ARN-P/D)

Since its characteristics are the same as that of single sorting operation, pickup and delivery arcs connecting each node can be linked using the criteria (4.1) and (4.2), respectively.

4.2.2.2 Interhub Routes (ARN-I)

Similarly, for each aircraft type f , the set of interhub routes can be constructed by using the set of sorting grid time of both origin and destination hubs, denoted the set of origin hub nodes and destination hub nodes, respectively. The set of origin hub nodes, for each hub h , are all the sorting grid time of hub h except for its SST; that is $G_h \setminus \{SST\}$. For the destination hub nodes, for each hub h , this set consists of all the sorting time of hub h except for its SET; that is $G_h \setminus \{SET\}$. Again, it is noted that the total number of nodes in the network representation for interhub routes is $2 \sum_{h \in H} \{|G_h| - 1\}$. Figure 4.4 illustrates the network representation of R_H^f .

Each arc that connects nodes in the interhub network representation is linked when there is a feasible route departing from origin hub h_o at sorting grid time t_{h_o} that can arrive at the destination hub, h_d at time t_{h_d} , as follows:

$$t_{h_o} + t_{loading} + Travel\ Time(h_o \rightarrow h_d) + t_{unloading} \leq t_{h_d}$$

$$\forall t_{h_o} \in G_{h_o} \setminus \{SST\}, \forall t_{h_d} \in G_{h_d} \setminus \{SET\}, \forall h_o, h_d \in H, h_o \neq h_d \quad (4.3)$$

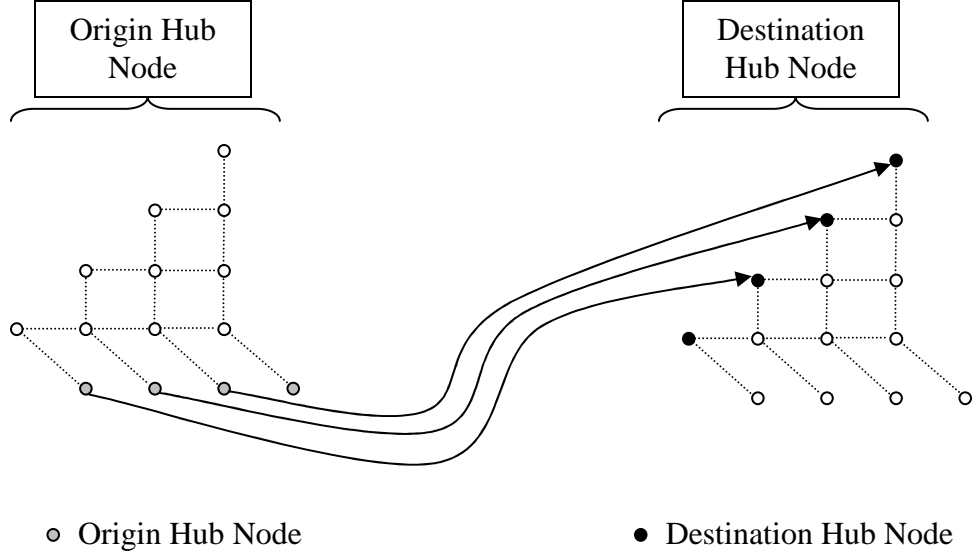


Figure 4.4: Network representation of R_H^f

4.3 Package Movement Network (PMN)

The PMN can be generated differently in the single-stage versus the two-stage model. Both are constructed by merging the HSN with ARN for each aircraft type, where ARN-I is considered only in the two-stage sorting model. Let ARN_f^P , ARN_f^D and ARN_f^I be the aircraft route network for pickup, delivery and interhub routes for aircraft type f respectively, and HSN_h denote the HSN for hub h .

In the single-stage model, we merge $ARN_f^P, \forall f \in F$ into a single ARN^P by mapping the same gateway node $i, i \in S$ into a single gateway node i in ARN^P . In addition, the same hub nodes in each $ARN_f^P, \forall f \in F$ are merged into a single hub node. The procedures are similarly applied to the ARN^D . Then, we combine the resulting ARN^P and ARN^D with $HSN_h, \forall h \in H$ by merging at the same hub node.

It is noted that a hub node represents both hub location and the associated grid time. A hub node from ARN^P is merged with a hub node in HSN_h on the pickup side, while a hub node from ARN^D is combined with HSN_h on the delivery side. Therefore, the PMN in the single-stage sorting model can be constructed by merging ARN^P , $HSN_h, \forall h \in H$, and ARN^D , as shown in equation 4.4. Figure 4.5 illustrates a single-stage-sorting PMN.

PMN in single-stage sorting model:

$$ARN^P \rightarrow HSN_h, \forall h \in H \rightarrow ARN^D \quad (4.4)$$

For the two-stage model each HSN_h is listed twice, for the first and second sorting process, where ARN^P merges with the first $HSN_h, \forall h \in H$, and ARN^D merges with the second $HSN_h, \forall h \in H$. To link between the first and second $HSN_h, \forall h \in H$, ARN^I is needed. To construct ARN^I , we merge $ARN_f^I, \forall f \in F$ into a single ARN^I when having the same origin and destination hub nodes. The resulting ARN^I is then mapped with the first $HSN_h, \forall h \in H$ when the origin hub node in ARN^I is the same as a hub node on the delivery side. Similarly, a destination hub node of ARN^I is mapped with a hub node on the origin side of the second $HSN_h, \forall h \in H$. Therefore, the PMN of the two-stage sorting model can be constructed as in equation 4.5. Figure 4.6 shows an example of two-stage-sorting PMN.

PMN in two-stage sorting model:

$$ARN^P \rightarrow (HSN_h, \forall h \in H)_{1st} \rightarrow ARN^I \rightarrow (HSN_h, \forall h \in H)_{2nd} \rightarrow ARN^D \quad (4.5)$$

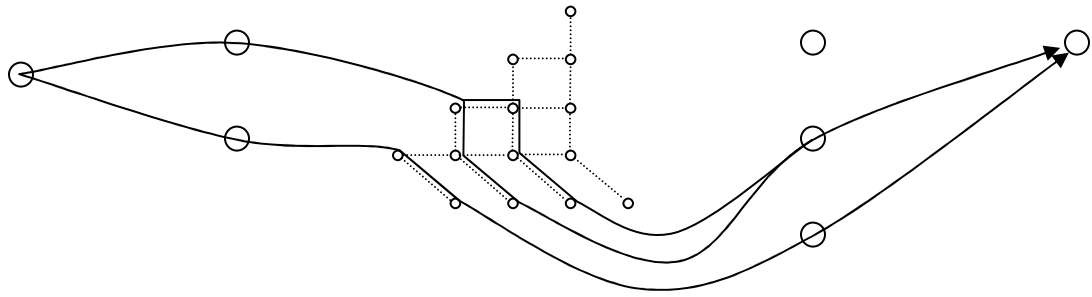


Figure 4.5: Example of single-stage-sorting PMN

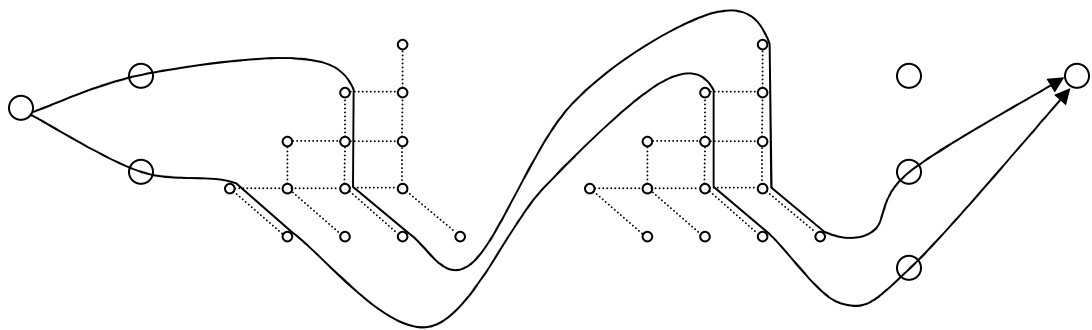


Figure 4.6: Example of two-stage-sorting PMN

Chapter 5

NH Models

The objective is to minimize total system cost while serving all the shipments from their origins to their destinations within the service commitments. The total operating cost includes aircraft operating cost and hub sorting cost. Based on problem's characteristics, it is modeled as a *mixed integer multicommodity flow (MIMCF) problem*, where an origin-destination market pair defines each commodity.

To evaluate system performance for the air network design with hub sorting (NH), four types of decision variables are included in the model. These are:

1. Aircraft route variables
2. Package flow variables
3. Hub sorting capacities

4. Hub storage sizes

5.1 NH Operational Constraints

To serve all demands within a short time window for next day delivery, all the decision variables must comply with several operational requirements, including feasible movement of packages and aircraft, fleet balance, fleet size, hub landing/take-off capacity, hub sorting capacity, hub storage capacity, and FIFO sorting process at each hub. These are detailed below.

5.1.1 Fleet Balance at Service Center

For each fleet $f \in F$, these constraints force the number of aircraft routes into and out of a service center to be equal:

$$\sum_{r \in R^f} \beta_i^r y_r^f = 0 \quad \forall i \in S, \forall f \in F \quad (5.1)$$

where

S = The set of service centers

F = The set of fleet types, $f \in F$

R^f = The set of aircraft routes for fleet f

$$\beta_i^r = \begin{cases} 1 & \text{if } i \in SC \text{ is the start node of route } r \\ -1 & \text{if } i \in SC \text{ is the end node of route } r \\ 0 & \text{otherwise} \end{cases}$$

y_r^f = The number of flights of fleet type f traveling on route r

5.1.2 Fleet Balance at Hub

To balance each fleet type $f \in F$ at a hub where the sequences of arrival and departure flight are critical, the fleet balancing concept from section 5.1.1 is modified to be compatible with HSN instead of treating a hub as a single node. For each fleet type $f \in F$ at hub h , first, the total number of inbound and outbound flights must be equal, as in section 5.1.1. Second, at any hub departure time $t_m > SST$, the total number of flights departing no later than t_m , $\forall t, t \leq t_m$, must not exceed the total number of flights arriving earlier, $\forall t, t \leq t_m - \Delta t$. Let $L_{A(h)}^t$ and $L_{D(h)}^t$ denote the set of arrival and departure aircraft at hub h at time t , respectively. In a single-stage operation, where only pickup and delivery routes are considered, the fleet balance constraints at a hub are:

$$\sum_{t=SST+\Delta t}^{t_m} \sum_{r \in R_D^f \cap L_{D(h)}^t} y_r^f \leq \sum_{t=SST}^{t_m-\Delta t} \sum_{r \in R_P^f \cap L_{A(h)}^t} y_r^f \quad \forall t_m > SST, \forall h \in H, \forall f \in F \quad (5.2)$$

For two-stage sorting, since each interhub flight departs from one hub and arrives at another, the interhub aircraft route variables can be treated as the delivery and pickup routes; this results in:

$$\sum_{t=SST+\Delta t}^{t_m} \sum_{r \in \{R_D^f \cup R_I^f\} \cap L_{D(h)}^t} y_r^f \leq \sum_{t=SST}^{t_m-\Delta t} \sum_{r \in \{R_P^f \cup R_I^f\} \cap L_{A(h)}^t} y_r^f \quad \forall t_m > SST, \forall h \in H, \forall f \in F \quad (5.3)$$

For example, in Figure 5.2, assume that, for a particular aircraft type in a hub sorting network, there are 3, 4 and 2 aircraft arriving at a hub at different times. Assume that there are 2, 3 and 4 aircraft departing from the hub, respectively. The corresponding fleet balance at hub constraints are:

$$@ SST + \Delta t : \quad 2 \leq 3$$

@ $SST + 2\Delta t$: $2 \leq 3 + 4$

@ $SST + 3\Delta t$: $2 + 3 \leq 3 + 4$

@ $SST + 4\Delta t$: $2 + 3 \leq 3 + 4 + 2$

@ SET : $2 + 3 + 4 \leq 3 + 4 + 2$

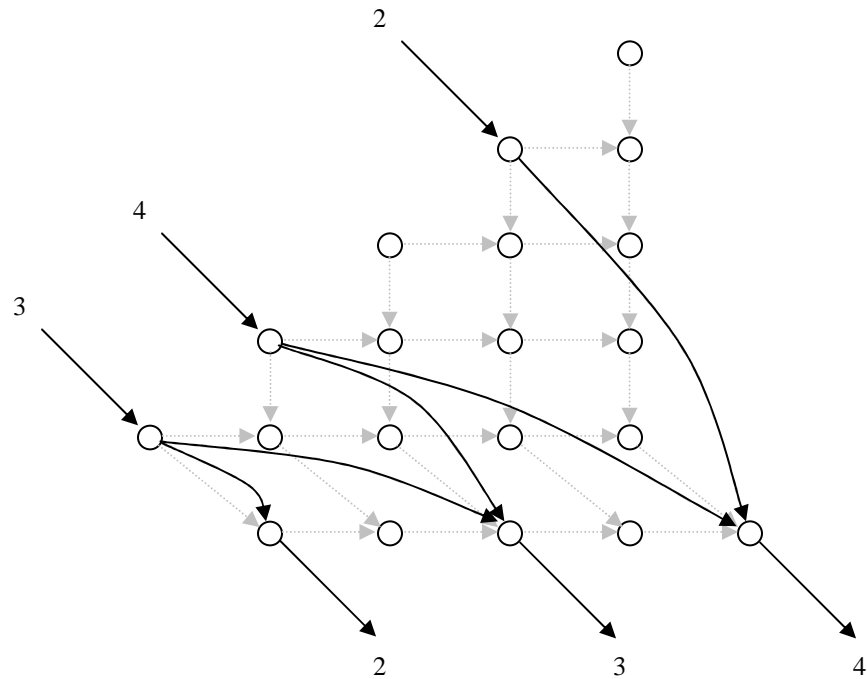


Figure 5.1: Example of fleet balancing in HSN

5.1.3 Fleet Size

For any type of aircraft, the number of aircraft used should not exceed the availability of that aircraft type. To restrict the total aircraft used, given the NH characteristics that all aircraft must start the shipment operation with a pickup route and end with a

delivery route, we can limit the number of pickup or delivery routes for each fleet type $f \in F$ to be less than n^f , the available fleet size of f . These constraints are:

$$\sum_{r \in R_p^f} y_r^f \leq n^f \text{ or } \sum_{r \in R_D^f} y_r^f \leq n^f \quad \forall f \in F \quad (5.4)$$

5.1.4 Hub Landing Capacity

At any hub, the number of aircraft that can land in an interval of time is limited by the landing capacity. Let $L_{A(h)}^t$ denote the set of arrival aircraft at hub h at time t , and a_h^t be the maximum number of aircraft that can land at hub h during the time $t - \Delta t$ and t . It is noted that the landing capacity should suffice even before the SST, i.e., $\{G_h\}_0 < SST$. Then, the hub landing capacity constraints can be represented as

$$\sum_{t=t_0}^{t_m} \sum_{f \in F} \sum_{r \in (R_p^f \cup R_D^f) \cap L_{A(h)}^t} y_r^f \leq \sum_{t=SST+\Delta t}^{t_m} a_h^t \quad \forall t_m \leq SET, \forall h \in H \quad (5.5)$$

where

$$t_0 = \text{First grid time in } G_h$$

5.1.5 Hub Take-off Capacity

Similarly, each hub has a take-off capacity that limits the number of aircraft that can take-off in an interval of time. Let $L_{D(h)}^t$ denote the set of departure aircraft at hub h at time t , and b_h^t be the maximum number of aircraft that can take-off at hub h during the time $t - \Delta t$ and t . Then, the hub take-off capacity constraints are

$$\sum_{t_m}^T \sum_{f \in F} \sum_{r \in (R_p^f \cup R_D^f) \cap L_{D(h)}^t} y_r^f \leq \sum_{t_m}^T b_h^t \quad \forall t_m > SST, \forall h \in H \quad (5.6)$$

where:

T = Last grid time in G_h

5.1.6 Hub Sorting Capacity

To model the HSN hub sorting capacity constraint, the information on when each package is sorted is very important, especially for determining the hub sorting capacity. Importantly, the hub sorting capacity is modeled as one of the decision variables in this study. In each HSN, the maximum number of packages passing through each sorting arc will determine the upper bound of that hub's sorting capacity. In this study, each package flow path contains information not only on airport/hub locations it visits, but also on when the package arrives at the hub and when it is sorted. Let $P_{(t_m - \Delta t, t_m)}^{e,h}$ be the set of package paths that is sorted at hub h during time $(t_m - \Delta t, t_m)$, and e_h be sorting capacity per hour of hub h . Then, the hub sorting capacity constraints are:

$$\sum_{k \in K} \sum_{p \in P(k)} \gamma_{k,p}^{e,h} x_p^k - e_h \Delta t \leq 0 \quad \forall t_m \in G_h \setminus \{SST\}, \forall h \in H \quad (5.7)$$

where

K = Set of package commodities, $k \in K$

$P(k)$ = Set of package routes of commodity k , $p \in P(k)$

x_p^k = Number of packages of commodity k on path p .

$$\gamma_{k,p}^{e,h} = \begin{cases} 1 & \text{if } p \in \{P_{(t_m - \Delta t, t_m)}^{e,h} \cap P(k)\} \\ 0 & \text{otherwise} \end{cases}$$

5.1.7 Hub Storage Capacity

During any time interval when packages are waiting at a hub to be sorted, these packages determine that hub's storage requirement. In our model, the hub storage capacity is also considered as one of the decision variables. Let $P_{(t_m - \Delta t, t_m)}^{s,h}$ represents the set of package paths waiting to be sorted at hub h during time $(t_m - \Delta t, t_m)$, and s_h be storage capacity (in packages) of hub h . Then, the hub storage capacity constraints are:

$$\sum_{k \in K} \sum_{p \in P(k)} \gamma_{k,p}^{s,h} x_p^k - s_h \leq 0 \quad \forall t_m \in G_h \setminus \{SST, SET\}, \forall h \in H \quad (5.8)$$

where

$$\gamma_{k,p}^{s,h} = \begin{cases} 1 & \text{if } p \in \{P_{(t_m - \Delta t, t_m)}^{s,h} \cap P(k)\} \\ 0 & \text{otherwise} \end{cases}$$

5.1.8 FIFO Package Movement in HSN

Given HSN's configuration, which contains a set of directed arcs to handle the FIFO sorting process, packages moving on the vertical arcs at any grid time $t_m \in G_h \setminus \{SST\}$ will enter a sorting channel at that time. While on the horizontal arcs, packages are moving to be sorted at a later grid time. That is, at any time $t_m \in G_h \setminus \{SST\}$, if some packages arriving at time $t_a \in G_h \setminus \{SET\}$ are left to be sorted later at $t_m + \Delta t$, no packages arriving during $(t_a, t_m]$ will be sorted during t_m . Conversely, if no packages arriving at time $t_a \in G_h \setminus \{SET\}$ are left to be processed at grid time $t_m + \Delta t$, all packages arriving during $(t_a, t_m]$ can then be sorted, but again based on FIFO.

Let $V_h^{(t_a, t_m]}$ be the set of package paths at hub h arriving during $(t_a, t_m]$ that are sorted at t_m , and $U_h^{(t_a, t_m)}$ represent the set of package paths at hub h arriving at t_a but left to be sorted after time t_m .

Let

$$V_h^{(t_a, t_m]}(x) = \{x_p^k \mid x_p^k > 0, x_p^k \in V_h^{(t_a, t_m]}, \forall k \in K, \forall p \in P(k)\} \text{ and}$$

$$U_h^{(t_a, t_m)}(x) = \{x_p^k \mid x_p^k > 0, x_p^k \in U_h^{(t_a, t_m)}, \forall k \in K, \forall p \in P(k)\},$$

then

1. If $V_h^{(t_a, t_m]}(x)$ is a non empty set, then $U_h^{(t_a, t_m)}(x)$ must be an empty set.
2. If $U_h^{(t_a, t_m)}(x)$ is a non empty set, then $V_h^{(t_a, t_m]}(x)$ must be an empty set.

To model both sets of package flows according to the above two conditions, we introduce binary decision variables to represent the indicators of those sets. Then, the FIFO package movement constraints are:

$$I[V_h^{(t_a, t_m]}(x)] + I[U_h^{(t_a, t_m)}(x)] \leq 1$$

$$\forall t_a \in G_h \setminus \{SET\}, \forall t_m \in G_h \setminus \{SST\}, \forall h \in H \quad (5.9)$$

$$\sum_{k \in K} \sum_{p \in P(k)} \gamma_{p,k}^{v,h}(t_a, t_m) x_p^k - MI[V_h^{(t_a, t_m]}(x)] \leq 0$$

$$\forall t_a \in G_h \setminus \{SET\}, \forall t_m \in G_h \setminus \{SST\}, \forall h \in H \quad (5.10)$$

$$\sum_{k \in K} \sum_{p \in P(k)} \gamma_{p,k}^{u,h}(t_a, t_m) x_p^k - MI[U_h^{(t_a, t_m)}(x)] \leq 0$$

$$\forall t_a \in G_h \setminus \{SET\}, \forall t_m \in G_h \setminus \{SST\}, \forall h \in H \quad (5.11)$$

where

$$I[V_h^{(t_a, t_m]}(x)] = \begin{cases} 1 & \text{if } V_h^{(t_a, t_m]}(x) \neq \emptyset \\ 0 & \text{otherwise} \end{cases}$$

$$I[U_h^{(t_a, t_m)}(x)] = \begin{cases} 1 & \text{if } U_h^{(t_a, t_m)}(x) \neq \emptyset \\ 0 & \text{otherwise} \end{cases}$$

$$\gamma_{p,k}^{v,h}(t_a, t_m) = \begin{cases} 1 & \text{if } x_p^k \in V_h^{(t_a, t_m)} \\ 0 & \text{otherwise} \end{cases}$$

$$\gamma_{p,k}^{u,h}(t_a, t_m) = \begin{cases} 1 & \text{if } x_p^k \in U_h^{(t_a, t_m)} \\ 0 & \text{otherwise} \end{cases}$$

M = Very large flow value, sufficient to cover all possible flow amounts in the system.

5.2 Cost Components

In this study, the system operating costs can be classified into two groups, the aircraft operating cost and hub operation cost. The aircraft operating cost consists of aircraft takeoff/landing cost (aircraft cycle cost), associated fuel cost of travel, crew cost and maintenance cost. For analyzing system performance for long term strategic planning, aircraft ownership cost is included so that aircraft mix can be optimized.

For hub operating cost, sorting and storage capacity are treated as decision variables, where given unit cost per package sorting capacity and per package storage capacity are introduced.

5.3 NH Model Formulations

We formulate the NH problem as a path-based formulation, as described in Ahuja et al. (1993), Kim and Barnhart (1999), and Kim et al. (1999). It is noted that the node-arc formulation is prohibitively large for the number of variables, even on a small problem.

To minimize the total system cost, the objective function is classified into two parts: aircraft operating cost and hub operating cost. The resulting single-stage sorting formulation is:

$$\min \sum_{f \in F} \sum_{r \in R^f} c_r^f y_r^f + \sum_{h \in H} c_h^e e_h + \sum_{h \in H} c_h^s s_h \quad (5.12.1)$$

Subject to:

$$\sum_{p \in P(k)} x_p^k = d^k \quad \forall k \in K \quad (5.12.2)$$

$$\sum_{k \in K} \sum_{p \in P(k)} \alpha_a^p x_p^k - \sum_{f \in F} \sum_{r \in R^f} \delta_a^{fr} u^f y_r^f \leq 0 \quad \forall a \in A_{ARN^{p/D}} \quad (5.12.3)$$

$$\sum_{r \in R^f} \beta_i^r y_r^f = 0 \quad \forall i \in S, \forall f \in F \quad (5.12.4)$$

$$\sum_{t=SST+\Delta t}^{t_m} \sum_{r \in R_D^f \cap L_{D(h)}^f} y_r^f - \sum_{t=SST}^{t_m-\Delta t} \sum_{r \in R_D^f \cap L_{A(h)}^f} y_r^f \leq 0 \quad \forall t_m \in G_h \setminus \{SST\}, \forall h \in H, \forall f \in F \quad (5.12.5)$$

$$\sum_{r \in R_p^f} y_r^f \leq n^f \quad \forall f \in F \quad (5.12.6)$$

$$\sum_{t=t_0}^{t_m} \sum_{f \in F} \sum_{r \in (R_p^f \cup R_f^f) \cap L_{A(h)}^f} y_r^f \leq \sum_{t=SST+\Delta t}^{t_m} a_h^t \quad \forall t_m \leq SET, \forall h \in H \quad (5.12.7)$$

$$\sum_{t_m}^T \sum_{f \in F} \sum_{r \in (R_p^f \cup R_f^f) \cap L_{D(h)}^f} y_r^f \leq \sum_{t_m}^T b_h^t \quad \forall t_m > SST, \forall h \in H \quad (5.12.8)$$

$$\sum_{k \in K} \sum_{p \in P(k)} \gamma_{k,p}^{e,h} x_p^k - e_h \Delta t \leq 0 \quad \forall t_m \in G_h \setminus \{SST\}, \forall h \in H \quad (5.12.9)$$

$$\sum_{k \in K} \sum_{p \in P(k)} \gamma_{k,p}^{s,h} x_p^k - s_h \leq 0 \quad \forall t_m \in G_h \setminus \{SST, SET\}, \forall h \in H \quad (5.12.10)$$

$$I[V_h^{(t_a, t_m)}(x)] + I[U_h^{(t_a, t_m)}(x)] \leq 1$$

$$\forall t_a \in G_h \setminus \{SET\}, \forall t_m \in G_h \setminus \{SST\}, \forall h \in H \quad (5.12.11)$$

$$\sum_{k \in K} \sum_{p \in P(k)} \gamma_{p,k}^{v,h}(t_a, t_m) x_p^k - MI[V_h^{(t_a, t_m)}(x)] \leq 0$$

$$\forall t_a \in G_h \setminus \{SET\}, \forall t_m \in G_h \setminus \{SST\}, \forall h \in H \quad (5.12.12)$$

$$\sum_{k \in K} \sum_{p \in P(k)} \gamma_{p,k}^{u,h}(t_a, t_m) x_p^k - MI[U_h^{(t_a, t_m)}(x)] \leq 0$$

$$\forall t_a \in G_h \setminus \{SET\}, \forall t_m \in G_h \setminus \{SST\}, \forall h \in H \quad (5.12.13)$$

$$x_p^k \geq 0 \quad \forall p \in P(k), k \in K \quad (5.12.14)$$

$$e_h \geq 0 \quad \forall h \in H \quad (5.12.15)$$

$$s_h \geq 0 \quad \forall h \in H \quad (5.12.16)$$

$$y_r^f \in \mathbf{Z}_+ \quad \forall r \in R^f, \forall f \in F \quad (5.12.17)$$

For the two-stage sorting formulation, since the interhub flights are included, equations (5.12.3) and (5.12.5) are changed to equations (5.12.18) and (5.12.19), respectively:

$$\sum_{k \in K} \sum_{p \in P(k)} \alpha_a^p x_p^k - \sum_{f \in F} \sum_{r \in R^f} \delta_a^{fr} u_r^f y_r^f \leq 0 \quad \forall a \in A_{ARN^{P/D/I}} \quad (5.12.18)$$

$$\sum_{t=SST+\Delta t}^{t_m} \sum_{r \in \{R_D^f \cup R_I^f\} \cap L_{D(h)}^f} y_r^f \leq \sum_{t=SST}^{t_m-\Delta t} \sum_{r \in \{R_P^f \cup R_I^f\} \cap L_{A(h)}^f} y_r^f$$

$$\forall t_m \in G_h \setminus \{SST\}, \forall h \in H, \forall f \in F \quad (5.12.19)$$

The objective function (5.12.1) minimizes the total system cost including the cost of transportation and hub operation.

Constraint set (5.12.2) states that for each commodity $k, k \in K$, the total package flows from all the paths equal the total demand. The flow of packages over any arc cannot exceed the arc capacity expressed by constraint sets (5.12.3) and

(5.12.18). It is noted that, for single-stage operation, the set of arcs in constraint set (5.12.3) contain arcs from the aircraft pickup route network (ARN^P) and aircraft delivery route network (ARN^D). For two-stage operation, the set of arcs in constraint set (5.12.18) include all aircraft route networks.

Constraint set (5.12.4) describes the fleet balancing service centers, constraints (5.12.5) and (5.12.19) impose the fleet balancing at hubs, and constraint set (5.12.6) limits the fleet size. The hub landing and take-off capacity constraints are described in equations (5.12.7) and (5.12.8), respectively.

For the HSN, constraint set (5.12.9) ensures that the total packages sorted in each sorting channel do not exceed the sorting capacity as stated in section 5.1.6. Similarly, constraint set (5.12.10) limits the hub storage capacity, as described in section 5.1.7. Constraint sets (5.12.11) - (5.12.13) impose the flow in FIFO sorting process, as discussed in section 5.1.8. Constraint set (5.12.12) provides an unlimited arc capacity if a vertical arc is selected, while similarly, constraint set (5.12.13) specifies an unbounded capacity if a horizontal arc is chosen.

Constraint sets (5.12.14 – 5.12.16) specify the bounds of the decision variables, and constraint set (5.12.17) ensures the integrality of aircraft route variables.

Chapter 6

NH Solution Approach – Column

Generation

In this section, a column generation approach for both single-stage and two-stage sorting operations will be described. Section 6.1 briefly explains the solution procedures starting from initializing and verifying input data until obtaining the IP solution. In section 6.2, after having generated possible aircraft routes, we present the procedure for identifying whether there exists a path connecting each commodity from its origin to its destination. After the feasibility of all package movements is verified, the initial network constructed by dummy aircraft routes is described in

section 6.3. A column generation approach is then described specifically for the NH in section 6.4.

6.1 Solution Procedures

Given the input data, the solution procedures start from generating feasible aircraft routes using information such as aircraft speed, location of service centers and hubs, the associated times at service centers (EPTs and LDTs) and hubs (SSTs and SETs), and the available arrival/departure times at the hubs. After enumerating all aircraft routes, the package movement connectivity procedures are performed to check whether, for each commodity k , there exists at least one package flow path from its origin to its destination. This feasibility check procedure will be described in section 6.3.

To find the LP relaxation solution of the NH, the initial service network configuration is constructed using dummy aircraft routes and the associated package flow path variables. Since cost of each dummy aircraft route is high, such routes should not be included in the final optimal solution. This initialization process is described in section 6.4.

To maintain the same LP problem structure over the solution processes, all constraints in NH must at least contain one variable. If there exists any constraint having no variables, as is true here of the bundle constraint in (5.12.3), the search algorithm for package flow path associated to that particular constraint must be applied. The completed LP problem structure will then be used as the starting restricted master problem (RMP) for NH.

During the solution processes, the column generation approach is implemented to price out the nonbasic variables or identify the potential variables, including both aircraft routes and package flow paths, as entering variables to the RMP. The column generation approach is described in section 6.4.

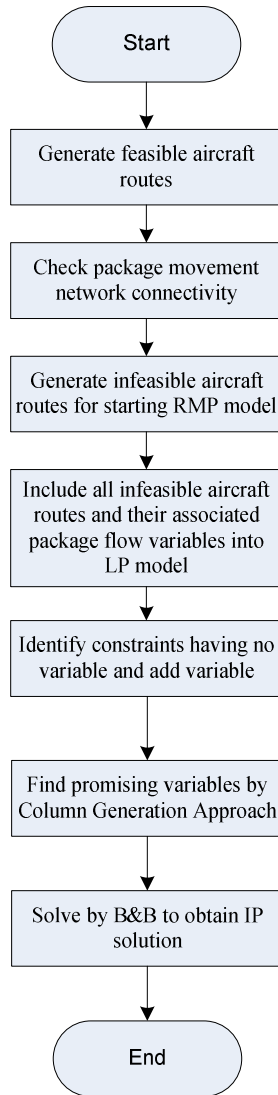


Figure 6.1: Solution procedure

6.2 Package Movement Connectivity (PMC)

As stated in section 6.1, if there is no feasible path for moving any commodity over the ARNs, the solution procedure should not proceed any further. Before comparing the system performance of single-stage and two-stage operations, some procedures should verify such infeasibility of the input data. Since network structures for single-stage and two-stage operation are different, the connectivity check of each system is separately described.

For each commodity k , let $H_{app}(k)$ be the set of approachable hubs and the associated grid times. For example in single-stage sorting operation, commodity k can be transported with the available aircraft routes (in this case via pickup routes ARN_{pickup}) to h_1 and h_2 , with associated earliest arrival times t_1 and t_2 , respectively. Therefore, $H_{app}(k)$ is $\{[h_1, t_1], [h_2, t_2]\}$. To connect $H_{app}(k)$ to its destination, there should be at least one aircraft route departing from a hub in $H_{app}(k)$ after the earliest arrival time. The algorithms are summarized in Figures 6.2 and 6.3.

```

Begin
  For each  $k \in K$ 
    Construct a set of approachable hubs and associated grid times,
     $H_{app}(k) = \{[h, \min t]\}$  via  $ARN^P$  from  $O(k)$ 
    If none exist  $y_r^f \in ARN^D$  departing from  $H_{app}(k)$  to  $D(k)$  then
      Terminate the procedure: NH is infeasible.
    End if
  Next  $k$ 
End

```

Figure 6.2: PMC for single-stage operation

```

Begin
  For each  $k \in K$ 
    Construct a set of approachable hubs and associated grid times,
     $H_{app(1)}(k) = \{[h, \min t]\}$  via  $ARN^P$  from  $O(k)$ 
    Construct a set of approachable hubs and associated grid times,
     $H_{app(2)}(k) = \{[h, \min t]\}$  via  $ARN^I$  from  $H_{app(1)}(k)$ 
    If none exist  $y_r^f \in ARN^D$  departing from  $H_{app(2)}(k)$  to  $D(k)$  then
      Terminate the procedure: NH is infeasible.
    End if
  Next  $k$ 
End

```

Figure 6.3: PMC for two-stage operation

6.3 Initial Aircraft Route Generation Procedure

The RMP must first consist of a feasible network before applying solution improvement. However, finding a starting feasible network might be as difficult as obtaining the optimal solution. In this study, we consider the dummy aircraft routes to form an initial aircraft route network for the following reasons:

1. It is easy to generate the dummy routes without considering the actual properties of the NH. In addition, to complete the RMP problem structure, dummy aircraft routes can be heuristically designed to fill any constraints that do not contain at least one variable.

2. It is difficult to generate the feasible aircraft route network, and if we can, some of these aircraft routes might not be part of the final IP solution. When having these unnecessary variables, especially if they are integer variables, it is more difficult or time-consuming to obtain the optimal IP solution during the B&B. Therefore, despite including several dummy aircraft routes, these variables will not affect the IP solution process because they are continuous variables. In addition, these should help minimize the number of actual aircraft routes at the end of the column generation procedure.

The following are the properties of the dummy aircraft routes:

1. The cost associated with each dummy variable is quite high, so that it will not be selected in the final optimal solution.
2. These dummy aircraft routes can connect from any service centers to hubs within times. That means the speed of dummy aircraft is high enough to reach any destination on time.
3. With an aircraft balancing constraint at each service center or hub, and aircraft fleet available, there exists at least one dummy aircraft route associated with those constraints.

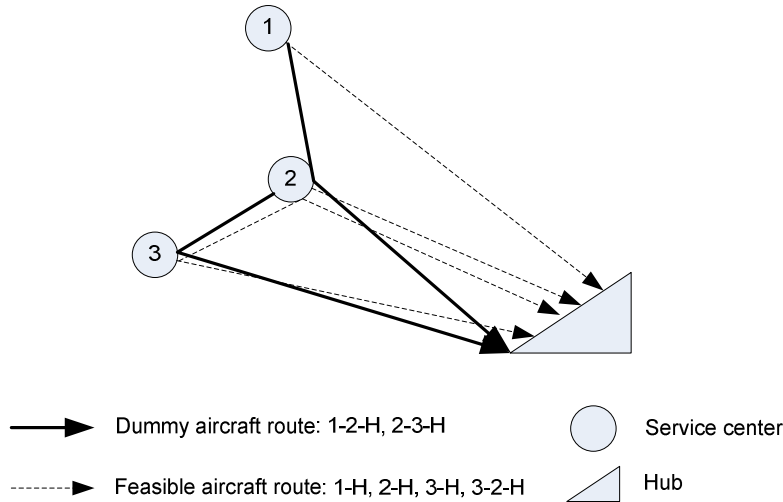


Figure 6.4: Example of dummy pickup aircraft routes

6.4 Column Generation (CG) Approach

For a practical problem size of air express network design, the time-space network results in numerous decision variables. Formulating such a problem with all possible variables yields an intractable model, which requires excessive computer memory and solution times. In this study, we consider the column generation approach (CG), which was suggested by Ford and Fulkerson (1958) and by Tomlin (1966). More details on CG are provided in Ahuja et al. (1993), Barnhart et al. (1995), Bertsimas and Tsitsiklis (1997), and Kim et al. (1999).

Because only some columns (basic variables) will be in an optimal solution, the CG approach is used to identify those columns, while all other columns (nonbasic variables) can be ignored. In CG, the *restricted master problem* (RMP), a restricted version of the original NH model with a limited number of columns, is maintained during the solution process. When solving the RMP at each so-called *master*

iteration, the dual variables are obtained. Using this set of dual variables, we can determine the potential variables that can improve the RMP's objective value explicitly or implicitly. For explicit CG, all columns are computed for the reduced costs, while for implicit CG, the potential columns are identified by solving a pricing subproblem. The latter approach is efficient if the pricing subproblem is easily formulated and solved. The process is repeated until no further column is included in the RMP, as shown in Figure 6.5. For the NH problem, CG is applied to determine two types of decision variables: aircraft route variables and package flow path variables.

The following section is applicable to both single-stage and two-stage sorting models. However, for the two-stage model, equations (5.12.3) and (5.12.5) should be changed to equations (5.12.18) and (5.12.19) in the discussion.

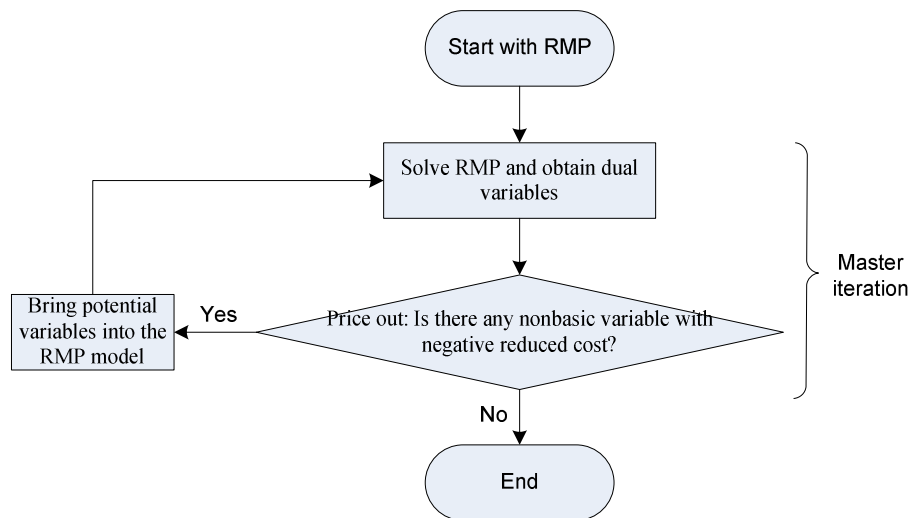


Figure 6.5: Column generation approach

6.4.1 CG Approach for Aircraft Routes

To identify the potential aircraft route variables, let \mathbf{c}_y denote the objective coefficient vector for aircraft route variables, and $\mathbf{B}_a, \mathbf{B}_{sc,b}, \mathbf{B}_{h,b}, \mathbf{B}_n, \mathbf{B}_{h,l}, \mathbf{B}_{h,t}$ be the constraint matrix for aircraft route variables in constraints (5.12.3) to (5.12.8) respectively, and let the dual vector of the corresponding constraints be $\boldsymbol{\pi}^{\mathbf{B}_a}, \boldsymbol{\pi}^{\mathbf{B}_{sc,b}}, \boldsymbol{\pi}^{\mathbf{B}_{h,b}}, \boldsymbol{\pi}^{\mathbf{B}_n}, \boldsymbol{\pi}^{\mathbf{B}_{h,l}}$ and $\boldsymbol{\pi}^{\mathbf{B}_{h,t}}$. The reduced cost vector for aircraft routes can be calculated as

$$\bar{\mathbf{c}}'_y = \mathbf{c}'_y - (\boldsymbol{\pi}^{\mathbf{B}_a})' \mathbf{B}_a - (\boldsymbol{\pi}^{\mathbf{B}_{sc,b}})' \mathbf{B}_{sc,b} - (\boldsymbol{\pi}^{\mathbf{B}_{h,b}})' \mathbf{B}_{h,b} - (\boldsymbol{\pi}^{\mathbf{B}_n})' \mathbf{B}_n - (\boldsymbol{\pi}^{\mathbf{B}_{h,l}})' \mathbf{B}_{h,l} - (\boldsymbol{\pi}^{\mathbf{B}_{h,t}})' \mathbf{B}_{h,t} \quad (6.1)$$

Because we minimize the total system cost, the aircraft route variables with negative reduced cost should be included in the RMP. The number of aircraft routes priced out in each master iteration should be properly investigated in order to limit the size of the integer programming model and obtain a good IP-LP gap. Let $\min_{\Theta(n)<0}$ be the set of first n aircraft routes with *lowest* negative reduced costs, which are currently not in RMP. The aircraft routes that should be included in the RMP can be determined from the following *pricing subproblem*:

$$\min_{\Theta(n)<0} \bar{\mathbf{c}}'_y \quad (6.2)$$

It can be seen that equation (6.2) is difficult to formulate and solve as a mathematical program. An explicit CG approach seems to be an efficient way in this situation, and there are quite a few aircraft route variables to consider.

6.4.2 CG Approach for Package Flow Paths

To determine the potential package flow path variables, let \mathbf{c}_p denote the objective coefficient vector for package flow path variables, let $\mathbf{A}_k, \mathbf{A}_a, \mathbf{A}_e, \mathbf{A}_s, \mathbf{A}_v, \mathbf{A}_u$ be the constraint matrix for package flow paths in constraints (5.12.3), (5.12.4), (5.12.8), (5.12.9), (5.12.11) and (5.12.12), respectively, and denote the dual vector corresponding those constraints as $\pi^{A_k}, \pi^{A_a}, \pi^{A_e}, \pi^{A_s}, \pi^{A_v}$ and π^{A_u} . Because we ignore the cost of moving packages over the network, the reduced cost of a package flow path can be calculated from

$$\begin{aligned}\bar{\mathbf{c}}'_p &= \mathbf{c}'_p - (\pi^{A_k})' \mathbf{A}_k - (\pi^{A_a})' \mathbf{A}_a - (\pi^{A_e})' \mathbf{A}_e - (\pi^{A_s})' \mathbf{A}_s - (\pi^{A_v})' \mathbf{A}_v - (\pi^{A_u})' \mathbf{A}_u \\ &= \mathbf{0} - (\pi^{A_k})' \mathbf{A}_k - (\pi^{A_a})' \mathbf{A}_a - (\pi^{A_e})' \mathbf{A}_e - (\pi^{A_s})' \mathbf{A}_s - (\pi^{A_v})' \mathbf{A}_v - (\pi^{A_u})' \mathbf{A}_u\end{aligned}\quad (6.3)$$

Again, only the variables with negative reduced cost should be included in RMP. To determine those variables, equation (6.3) can be decomposed into $|K|$ independent subproblems, each for a single commodity $k, k \in K$. The reduced cost for each path flow variable p of commodity k is

$$\bar{c}_p^k = 0 - \sigma_k + \sum_{(i,j) \in p} \pi_{ij} \quad \forall p \in P(k) \quad (6.4)$$

It is noted that package path p in (6.4) is a sequence of arcs contained in ARN and HSN. From (6.3), arcs in ARN are pickup and delivery arcs, while arcs in HSN comprise of sorting arcs, vertical arcs and horizontal arcs as shown in Figure 6.6. Any path p with negative reduced cost should be included in RMP, i.e.,

$$\sum_{(i,j) \in p} \pi_{ij} < \sigma_k \quad \forall p \in P(k) \quad (6.5)$$

We keep adding any paths with the condition (6.5) until no potential variables can be found. That is, we can check to see if for each commodity k

$$\bar{c}_p^k = 0 - \sigma_k + \sum_{(i,j) \in p} \pi_{ij} \geq 0 \quad \forall p \in P(k)$$

or, equivalently

$$\min_{p \in P(k)} \sum_{(i,j) \in p} \pi_{ij} \geq \sigma_k \quad (6.6)$$

The left-hand side of this inequality is just the length of the *shortest path* of commodity k . That is we solve the pricing subproblem as the *shortest path* problem for each commodity k in order to verify that we have added the potential package flow paths into the RMP. If we find any paths that violate condition (6.6), we add those paths into the RMP.

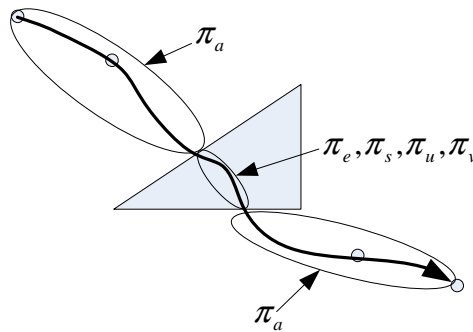


Figure 6.6: Modified arc costs associated to each type of arc

6.5 Computational Analyses

6.5.1 Case Study 1: 2 Hubs, 8 Service Centers, 1 Aircraft Type

In this case study, the column generation approach (CG) is applied to both sorting models. All runs are performed on a Pentium M 1.7 GHz processor with 1GB RAM, running CPLEX 9.0. With the available optimization software, the CG cannot be implemented at nodes within a branch-and-bound tree; therefore, we employ the CG only at the root node.

In this section, two hubs with eight service centers served by a single aircraft type are modeled for two different operations and their performances are comparatively evaluated. We distribute the O/D demand matrix so that both hubs are used to consolidate packages in a single-stage sorting operation. Since an eastern hub location is generally preferred as a master hub where all service centers are connected via at least one flight, we distribute the demands in the western service centers so that each service center is served by more than one flight. In Figure 6.5, demands from service centers No. 6, 7 and 8 should exceed an aircraft's capacity, in order to create an incentive for the network to perform two hub operations. Tables 6.1 – 6.4 are the input data for testing Case 1 scenario. Demands are randomly generated, as depicted in Table 6.1. In Table 6.4, we first consider only aircraft type 1 in order to exclude the effect of aircraft mix. It is also noted that we pre-assign each service center to its closest hub for the two-stage operation. The cost components we consider are:

- Aircraft ownership cost
- Aircraft operating cost
- Aircraft take-off/landing cost

- Hub sorting capital cost, and
- Hub storage capital cost

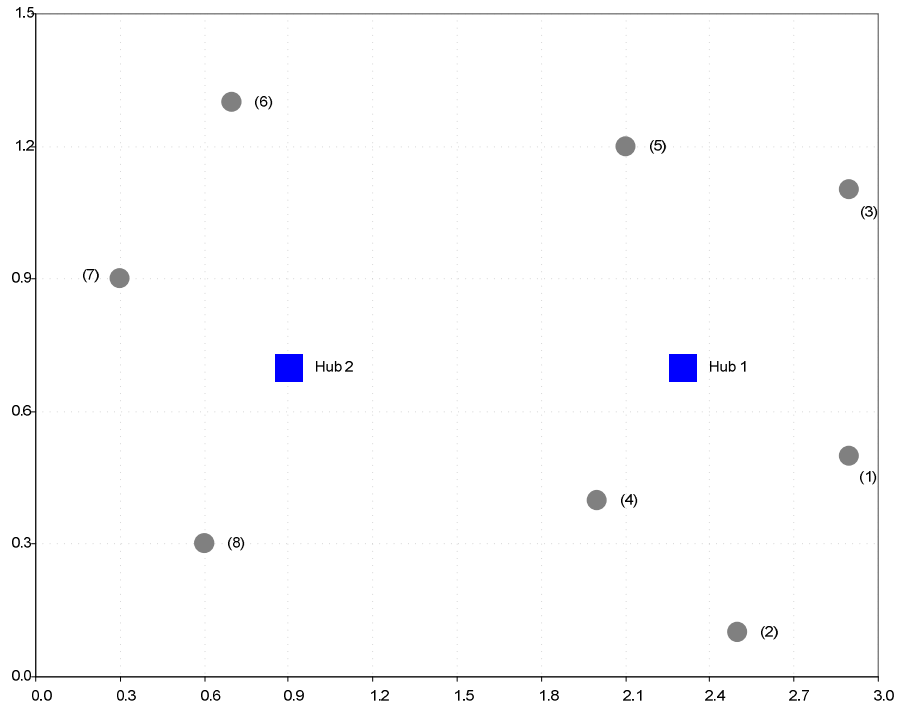


Figure 6.7: Network physical locations for Case Study 1

Table 6.1: O/D demand matrix for Case Studies 1 and 2

O/D	(1)	(2)	(3)	(4)	(5)	(6)	(7)	(8)
(1)	0	2,000	2,700	1,700	2,500	1,200	1,200	1,000
(2)	2,000	0	1,500	400	800	500	1,300	1,300
(3)	2,700	1,500	0	300	1,000	800	800	800
(4)	1,700	400	300	0	5,000	1,200	1,200	1,200
(5)	2,500	800	1,000	5,000	0	1,000	700	1,300
(6)	1,200	500	800	1,200	1,000	0	4,000	3,500
(7)	1,200	1,300	800	1,200	700	4,000	0	3,000
(8)	1,000	1,300	800	1,200	1,300	3,500	3,300	0

Table 6.2: Service center characteristics

Service Center No.	EPT	LDT	X	Y	Assigned Hub
1	8 PM (EST)	8AM (EST)	2,900	500	1
2	8 PM (EST)	8AM (EST)	2,500	100	1
3	8 PM (EST)	8AM (EST)	2,900	1,100	1
4	8 PM (EST)	8AM (EST)	2,000	400	1
5	8 PM (EST)	8AM (EST)	2,100	1,200	1
6	7 PM (PST)	6AM (PST)	700	1,300	2
7	7 PM (PST)	7AM (PST)	300	900	2
8	7 PM (PST)	6AM (PST)	600	300	2

Table 6.3: Hub characteristics

Hub No.	1	2
SST	12:00 AM	12:00 AM
SET	5:00 AM	5:00 AM
X Coordinate	2,300	900
Y Coordinate	700	700
Unit sorting cost, c_e^h (\$/package)	\$1	\$1
Unit storage cost, c_s^h (\$/package)	\$0.2	\$0.2
Number of grid time intervals ($ G_h $)	9	9

Table 6.4: Aircraft characteristics

Aircraft Type No.	1	2
Availability	20	20
Capacity (packages)	8,000	25,000
Max. Flying Range ¹ (mi.)	3,600	5,600
Avg. Cruising Speed (mph)	450	450
Operating Cost/mile	\$8	\$22
Take-Off/Landing Cost	\$300	\$600
Ownership Cost/Day/Aircraft	\$16,000	\$44,000

With this small network, we include all aircraft route variables, while we determine package flow paths using the CG approach. Although the problem size is small, we run out of the computer memory before obtaining an optimal IP solution. Therefore, for the purpose of this case study, we terminate the branch-and-bound when the IP-LP Gap is 5% for both models. The computational results are reported in

¹ Maximum flying distance at the maximum payload

Table 6.5, while the operating characteristics are shown in Table 6.6. It is noted that $|S|$ denotes the number of service centers, $|K|$ is the number of commodities, and $|AC|$ is the number of aircraft types. Detailed cost distributions are reported in Table 6.7. Figures 6.6 and 6.7 show the resulting network configurations for single-stage and two-stage sorting operation, respectively.

Table 6.5: Computational results for Case Study 1

Type of sorting operation	Single-Stage	Two-Stage
$ S $	8	8
$ K $	56	56
$ AC $	1	1
#Aircraft route variables	129	64
Termination Criteria	5% IP-LP Gap	5% IP-LP Gap
IP	483,837	475,155
LP	508,028	498,912
Gap	5%	5.0%

In Table 6.6, compared to the single-stage operation, the two-stage one reduces travel distance by 14.7% and increases average load factor (= actual package-miles / aircraft capacity package-miles) by 1.8%. However, to make such operation feasible, the hub sorting rate and storage capacity must increase so that interhub flights can arrive at the second hub before the SET. As a result in Table 6.7, the two-stage sorting operation incurs lower aircraft operating cost but higher hub operating cost compared to the single-stage operation.

Table 6.6: Comparison of operating characteristics for Case Study 1

Type of sorting operation	Single-Stage	Two-Stage	% Chg
Aircraft			
• Number of aircraft required	13	13	0%
• Total distance flown (mi.)	26,106	22,283	-14.7%
○ Pickup	14,059	8,342	-40.7%
○ Delivery	12,047	8,342	-30.8%
○ Interhub	0	5,600	NA
• Legs	31	32	3.2%
• Capacity-Miles	208.8 M	178.3 M	-14.7%
• Package-Miles	172.8M	150.7M	-12.8%
• Avg. load factor	82.7%	84.5%	1.8%
Hub No. 1			
• Sorting rate (packages/hour)	38,400	41,040	6.9%
• Storage size (packages)	24,000	25,650	6.9%
Hub No. 2			
• Sorting rate (packages/hour)	12,880	29,440	128.6%
• Storage size (packages)	8,050	18,400	128.6%

Table 6.7: Comparison of cost distributions for Case Study 1

Type of sorting operation	Single-Stage	Two-Stage	% Chg
Aircraft			
• Ownership Cost	\$208,000	\$208,000	0%
• Operating Cost	\$208,847	\$178,265	-14.7%
• Take-Off/Landing Cost	\$9,300	\$9,600	3.2%
Total Aircraft Cost	\$426,147	\$395,865	-7.1%
Hub No. 1			
• Sorting Cost	\$38,400	\$41,040	6.9%
• Storage Cost	\$4,800	\$5,130	6.9%
Total Hub No. 1 Cost	\$43,200	\$46,170	6.9%
Hub No. 2			
• Sorting Cost	\$12,880	\$29,440	128.6%
• Storage Cost	\$1,610	\$3,680	128.6%
Total Hub No. 2 Cost	\$14,490	\$33,120	128.6%
Total Operating Cost	\$483,837	\$475,155	-1.8%

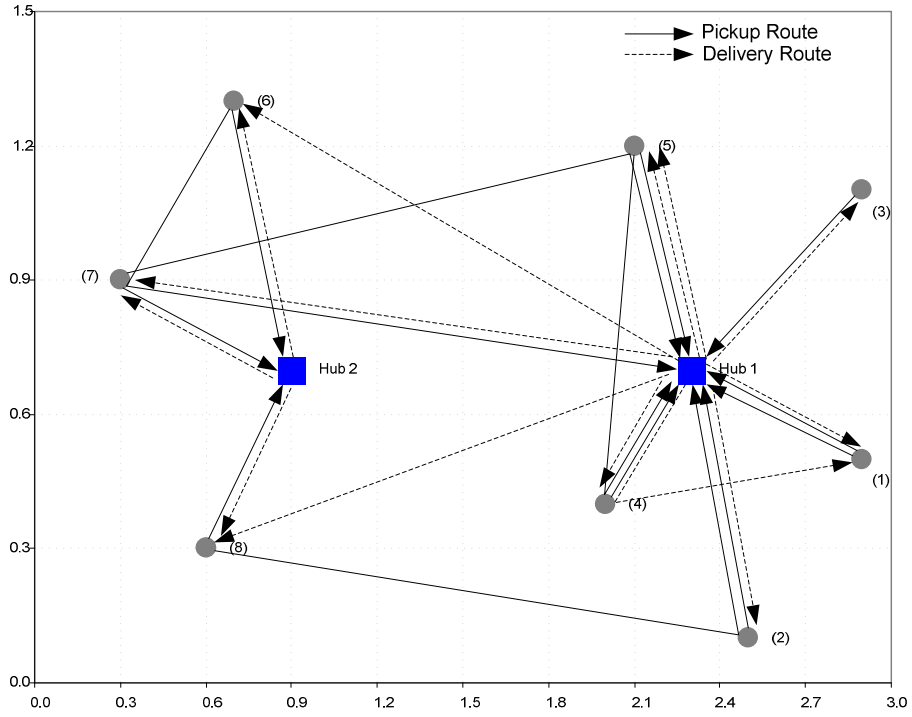


Figure 6.8: Network configuration for Case Study 1 - single-stage operation

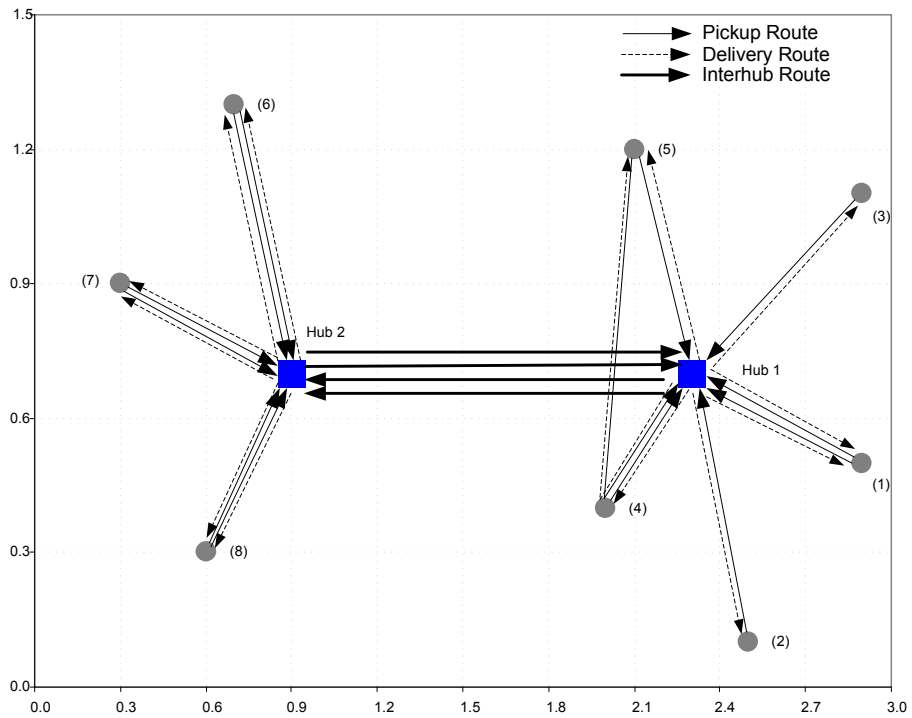


Figure 6.9: Network configuration for Case Study 1 - two-stage operation

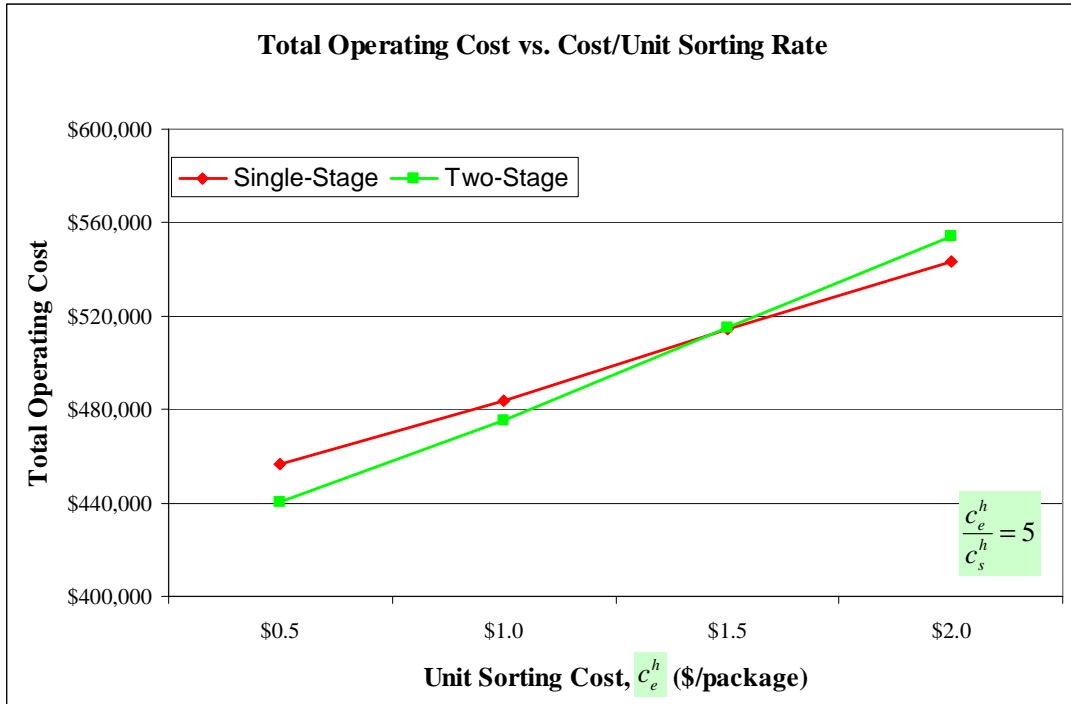


Figure 6.10: Effect of sorting cost on each operation for Case Study 1

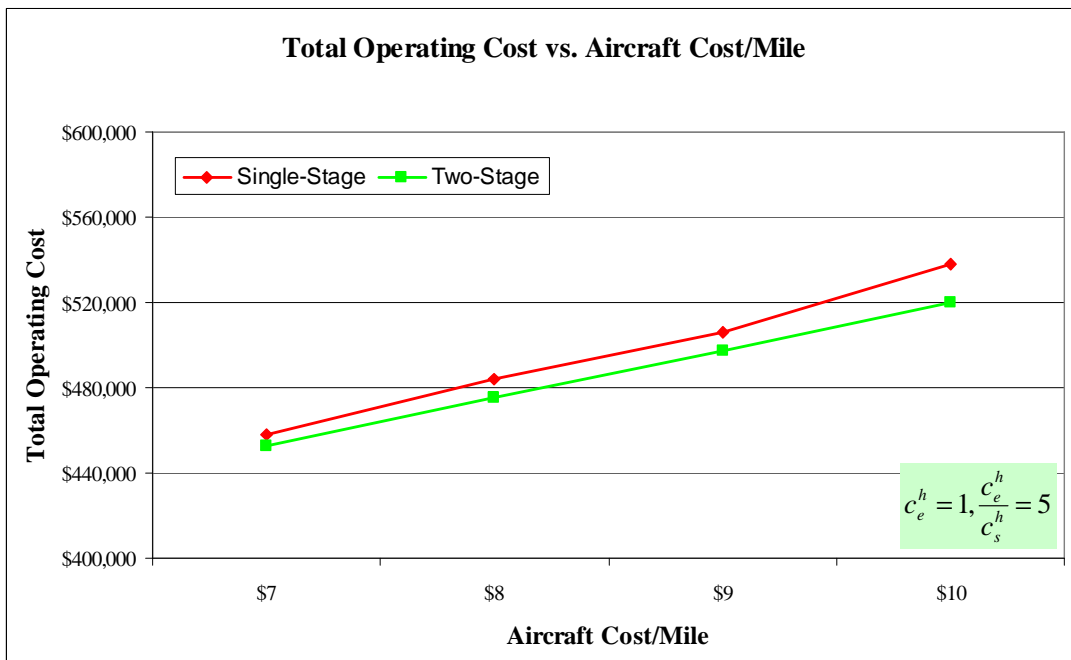


Figure 6.11: Effect of aircraft cost per mile on each operation for Case Study 1

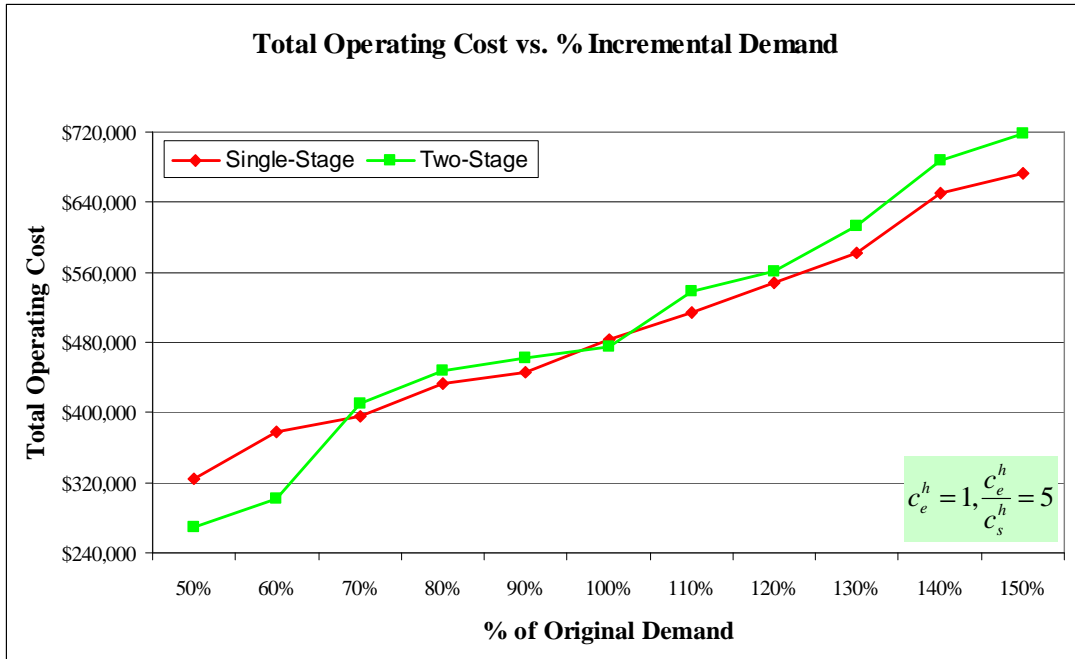


Figure 6.12: Total operating cost for each operation vs. demand for Case Study 1

Figure 6.8 shows the total operating cost of each system when varying the cost per unit sorting rate (c_e^h), given $c_e^h / c_s^h = 5$. Since the packages are sorted twice in the two-stage operation, c_e^h yields a higher total operating cost than the single-stage operation. The higher the cost of sorting, the more favored is the single-stage sorting operation. It can be seen that both systems perform equally when $c_e^h = \$1.5/\text{unit}$ sorting rate. In Figure 6.9, the two-stage sorting operation provides greater cost savings when aircraft operating cost per mile increase.

Figure 6.10 shows how the two systems compare when the demand varies from its baseline values (=100%). The total operating costs are lower with single-stage sorting at high demand, and with two-stage sorting at low demand. These results can be explained as follows:

- When the total demands of service center i exceeds an aircraft's capacity, $\sum_{k \in K \cap \{O(k)=i\}} d^k > u^f$ on the pickup side or $\sum_{k \in K \cap \{D(k)=i\}} d^k > u^f$ on the delivery side, it is not optimal to have all the demands travel farther and be consolidated twice with two-stage sorting. When demand is high, the distance-based aircraft operating cost overcomes the savings of consolidation through two-stage sorting. Thus, more direct service (single-stage sorting) is favored.
- When the total demand of service center i is below an aircraft's capacity, $\sum_{k \in K \cap \{O(k)=i\}} d^k < u^f$ on the pickup side or $\sum_{k \in K \cap \{D(k)=i\}} d^k < u^f$ on the delivery side, consolidating packages first at the nearby hub before delivering to another hub is preferable.

Given the relative advantages of each system in different situations, we can consider combinations of the two operations in a general network. If the total demands of any service center exceed the largest aircraft capacity, the demands should be separated into two groups. The first set, which completely utilizes the aircraft's capacity, are transported via single-stage sorting. For the remaining demands in the second group, $\sum_{k \in K \cap \{O(k)=i\}} d^k - u^f$ on the pickup side or $\sum_{k \in K \cap \{D(k)=i\}} d^k - u^f$ on the delivery side, if they are below an aircraft's capacity, they can benefit from a two-stage sorting operation; otherwise they are again separated into two groups, and so on.

6.5.2 Case Study 2: 2 Hubs, 8 Service Centers, 2 Aircraft Types

Case 2 is extended from Case 1. Two aircraft types are now considered. Aircraft type 2 has triple in capacity of aircraft type 1, and its unit costs are about 10% lower for both aircraft operation and ownership. This scenario thus considers the possible economies of aircraft size. The test is performed by varying the demands as in Case 1 and the results are shown in Figure 6.11. At high demand, it can be seen that the gaps in total operating cost among the two cases are less than in Case 1, as shown in Table 6.8. The two-stage sorting operation is again a good candidate when using several aircraft sizes.

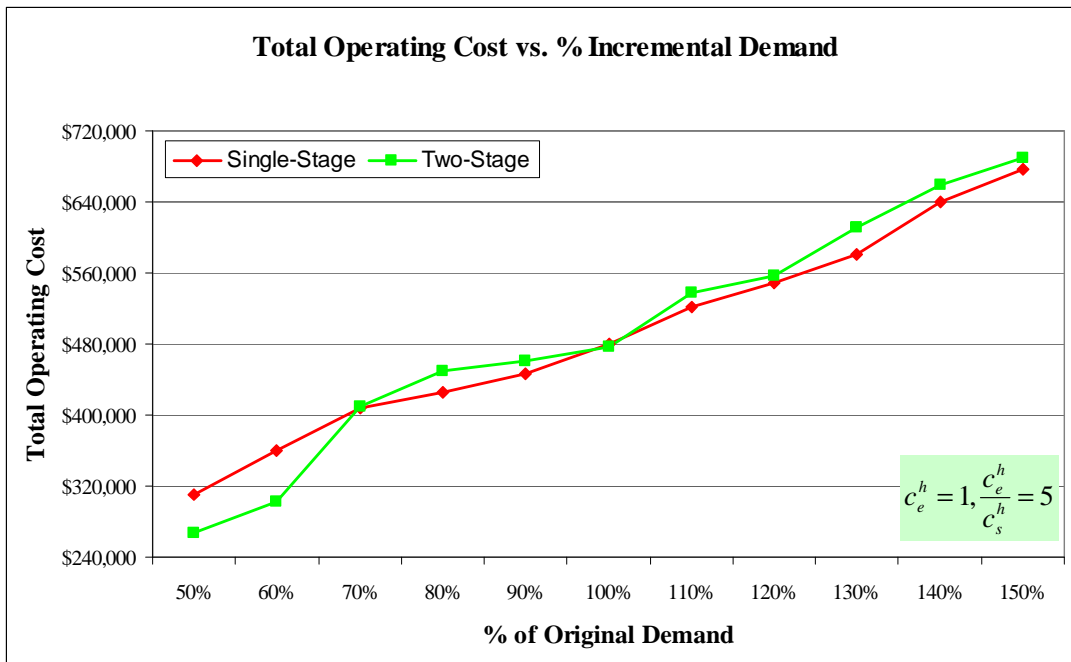


Figure 6.13: Total operating cost for each model vs. demand for Case Study 2

Table 6.8: Changes in total operating cost for Case Studies 1 and 2

% of Original Demand	Two-Stage vs. Single-Stage % Change Total Operating Cost	
	Case 1	Case 2
50%	-17.0%	-14.1%
60%	-20.1%	-16.2%
70%	4.0%	0.4%
80%	3.4%	5.8%
90%	3.7%	3.1%
100%	-1.8%	-0.7%
110%	4.7%	3.1%
120%	2.4%	1.4%
130%	5.2%	5.2%
140%	7.1%	2.9%
150%	5.1%	1.9%

To check how two-stage sorting operation benefits the distribution system, we randomly generate demands into two scenarios: (1) high demand (mean = 100% and range = 50% of demand in Table 8.1) and (2) low demand (mean = 75% and range = 50% of demand in Table 6.1). Again, two-stage sorting outperforms single-stage sorting at low demand, as shown in Table 6.9.

Table 6.9: Effect of demand level on sorting stages

Problem Label	Two-Stage vs. Single-Stage Total Operating Cost Gap		Problem Label	Two-Stage vs. Single-Stage Total Operating Cost Gap	
	1AC	2ACs		1AC	2ACs
rd_h_01 ²	1.2%	3.6%	rd_l_01 ³	-6.1%	-4.7%
rd_h_02	2.3%	1.5%	rd_l_02	2.1%	3.5%
rd_h_03	4.1%	2.8%	rd_l_03	2.0%	3.5%
rd_h_04	-0.2%	1.6%	rd_l_04	-2.2%	-2.4%
rd_h_05	4.1%	0.3%	rd_l_05	1.4%	2.4%
rd_h_06	2.9%	2.7%	rd_l_06	-3.9%	-1.4%
rd_h_07	1.6%	-0.3%	rd_l_07	-0.1%	0.2%
rd_h_08	4.2%	3.2%	rd_l_08	-3.8%	-6.4%
rd_h_09	6.8%	7.4%	rd_l_09	3.9%	3.0%
rd_h_10	8.1%	6.8%	rd_l_10	-0.8%	-2.2%
rd_h_11	1.2%	1.8%	rd_l_11	-3.8%	-9.7%
rd_h_12	6.1%	5.0%	rd_l_12	-2.1%	-8.1%
rd_h_13	1.0%	-0.8%	rd_l_13	-4.9%	-0.6%
rd_h_14	6.4%	6.9%	rd_l_14	-2.1%	-0.3%
rd_h_15	4.7%	5.6%	rd_l_15	0.3%	-1.8%
rd_h_16	3.1%	2.6%	rd_l_16	-1.9%	1.3%
rd_h_17	2.5%	0.6%	rd_l_17	-4.8%	-4.6%
rd_h_18	1.3%	2.7%	rd_l_18	-4.8%	-4.6%
rd_h_19	2.6%	0.5%	rd_l_19	4.2%	1.7%
rd_h_20	3.5%	4.1%	rd_l_20	-2.6%	1.1%
Average	3.4%	2.9%	Average	-1.5%	-1.5%

6.6 Summary

In this chapter, we present the Column Generation approach which is used to determine the promising variables for LP relaxation. The resulting problem is then embedded in a branch-and-bound approach to determine an integer solution. The model can solve both single-stage and two-stage operations, in which each service center is assign a priori to its closest hub for the two-stage case to limit the number the aircraft route variables. However, large problem instances, which result in significant size in time-space network representations, are impossible to solve using the presented solution approach. A heuristic solution approach should be considered.

² rd_h_01 = high random demand problem No.1

³ rd_l_01 = low random demand problem No.1

Chapter 7

NH Solution Approach – Genetic

Algorithm

In the last section, the column generation approach is applied at the root node of the branch and bound algorithm to identify any promising variables, which are aircraft route and package flow path variables. The approach, however, may only be used to solve a small NH problem. For a realistic instance of the NH problem, although the column generation approach can be applied, many aircraft route variables might be added in the final restricted master problem at the root node. Given the NP hard nature of the NH problem (see Ahuja et al., 1993) resulting from problem specific side constraints, i.e., aircraft balancing at hubs and service centers, landing and take-

off hub capacity, those large integer variables will result in long computation time and, in most cases, insufficient memory while running the branch and bound algorithm. Therefore, we consider a heuristic solution approach for solving a relatively large problem.

In this section, we describe “evolutionary or genetic algorithms (GAs)”, which have been successfully used for a variety of problems. Genetic algorithms are powerful search procedures motivated by ideas from the theory of evolution (Michalewicz, 1999). Let $P(t)$ be the population at generation t . Figure 7.1 shows the general GA procedure for solving an optimization problem and Figure 7.2 shows a GA procedure for our NH problem.

Due to the nature of the NH problem, each service center is connected to at least one hub. To pre-specify the hub assignment of each service center, we follow Falkenauer’s work (1996) where grouping representations are encoded to solve a capacitated tree problem. Gamvros et al. (2004) also apply a GA grouping representation for node partitioning in the multi-level capacitated minimum spanning tree problem. Their partitioning results in a smaller version of a network design problem, which can then be solved with their saving heuristic.


```

Begin
   $t \leftarrow 0$ 
  initialize  $P(t)$ 
  evaluate  $P(t)$ 
  while (not termination-condition) do
     $t \leftarrow t + 1$ 
    select  $P(t)$  solutions from  $P(t - 1)$ 
    alter  $P(t)$ 
    evaluate  $P(t)$ 
  end while
end

```

Figure 7.1: General GA solution approach

```

Begin
   $t \leftarrow 0$ 
  initialize  $P(t)$ 
  evaluate  $P(t)$ 
  while (not termination-condition) do
     $t \leftarrow t + 1$ 
    select  $r = r_1 + r_2$  parents from  $P(t - 1)$ 
    let the  $r_1$  parents crossover by randomly selecting service center locations, which
      have different hub assignment, and interchanging the assignment to generate  $r_1$ 
      offspring
    let the  $r_2$  parents mutate by randomly selecting a hub location and assigning a set of
      service centers within its hub territory to generate  $r_2$  offspring
    insert the  $r$  offspring to  $P(t)$ 
    select  $n$  individuals from  $P(t - 1)$ 
    let the  $n$  individuals mutate using developed local search operators
    insert the  $n$  mutated individuals to  $P(t)$ 
    select the best  $m$  individuals from  $P(t - 1)$ 
    let the  $m$  individuals mutate using developed local search operators
    insert the  $m$  mutated individuals to  $P(t)$ 
    select ( $popsiz e - r - n - m$ ) individuals from  $P(t - 1)$  and copy them to  $P(t)$ 
    evaluate  $P(t)$ 
  end while
end

```

Figure 7.2: Genetic Algorithm procedure for the NH problem

7.1 GA Solution Framework

As described in Chapter 5, the NH problem contains two main decision variables: aircraft route variables and package flow path variables. In this study, our GA model is mainly designed to manipulate the aircraft route variables, while we still utilize the column generation approach to determine the package flow path variables. Conceptually within our GA approach, we split the NH problem into (1) a *grouping problem* and (2) a *network design problem*. The first problem aims to find an optimal partition by means of *hub assignment*, while a later problem searches for an optimal set of aircraft routes according to the pre-specified grouping. In each problem, genetic operators are constructed using the problem content to manipulate the representation.

Figure 7.3 exhibits our GA solution framework for the NH problem. The solution process starts by assigning a grouping representation to each GA population, and then applies heuristic route construction procedure. Each population is then randomly selected proportionally to its fitness function, which in this case is the objective function value, to be applied by our developed genetic operators. At the end of each manipulation, the following system costs are also evaluated:

1. Hub sorting cost and storage cost
2. Violation cost of aircraft usage
3. Cost of violating hub landing and take-off capacity.

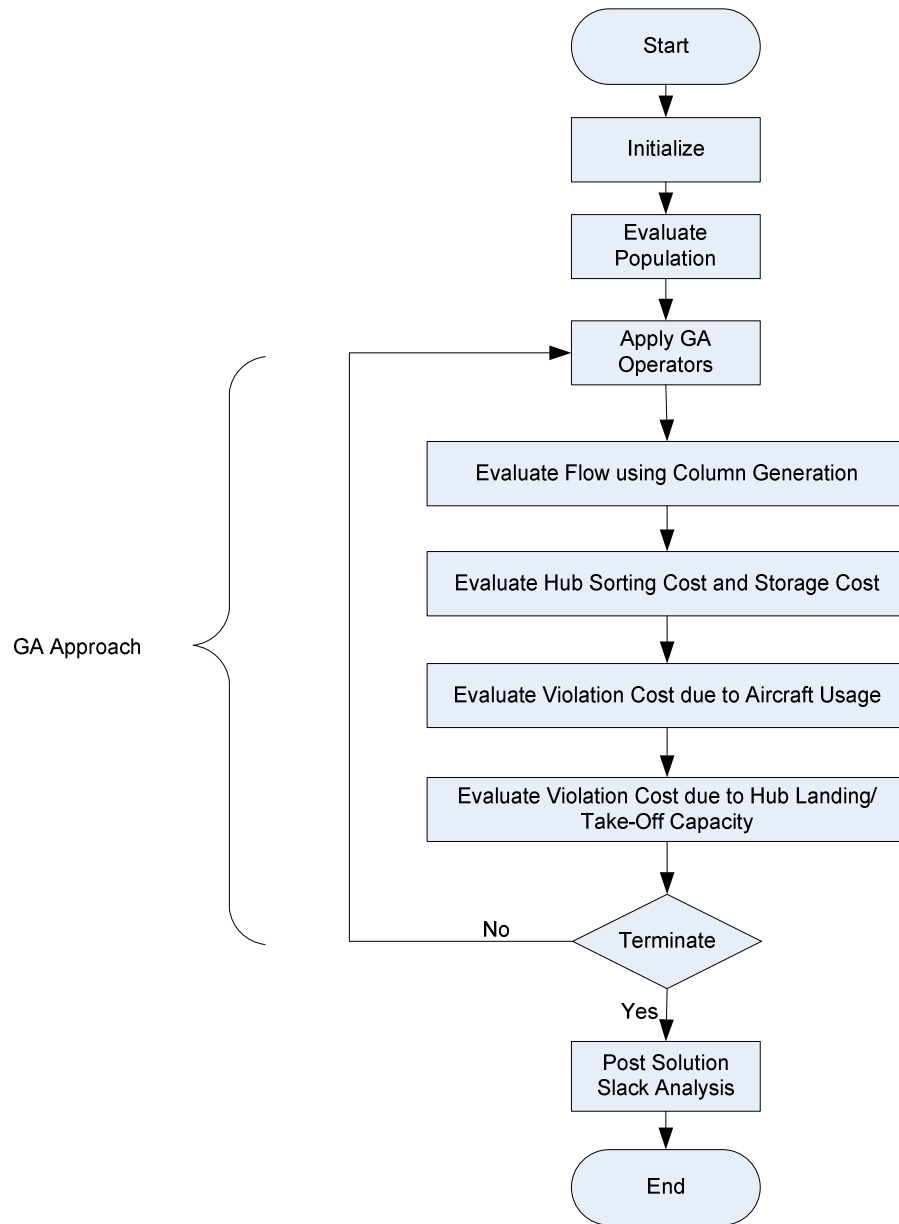


Figure 7.3: GA solution procedure for NH problem

Because we are interested in comparing the system performance between single-stage and two-stage operation, the manipulations of our GA are slightly different in (1) the initialization process, and (2) the set of GA operators applied. After obtaining an optimized solution, the model performs a post-solution analysis to analyze the system's slack, which is then used in comparing the single-stage and two-stage sorting operations.

7.2 Solution Representation

As stated, we represent each NH solution with the combined grouping and aircraft route representations. Later, genetic operators, which are designed for each specific representation, are described. Note that GA representations are applied to both single-stage and two-stage sorting operation, while we specifically design additional a GA operator to handle the two-stage operation.

7.2.1 Grouping Representation – 1st GA Layer

As discussed earlier, each service center must be connected to at least one hub. Some carriers require all-point service to and from their major hub, as described in Kim et al. (1999). Let Ω_h be the set of service centers that connect to hub h , and Λ_g define a g combination pattern of $\{\Omega_h\}$. Let h_1 be the major hub of the distribution network, and define

$$\Lambda_A = \Omega_1 = \{3, 4, 6, 7, 9\}$$

$$\Lambda_B = \Omega_1 \cup \Omega_2 = \{10, 11, 12, 13\}$$

$$\Lambda_C = \Omega_1 \cup \Omega_3 = \{1, 2, 5\}$$

$$\Lambda_D = \Omega_1 \cup \Omega_2 \cup \Omega_3 = \{8\}$$

The resulting grouping representation of NH instance is demonstrated in Figure 7.4, which is [C, C, A, A, C, A, A, D, A, B, B, B, B]. The sequence in the array represents the service center number.

Figure 7.5 shows how each service center's hub assignment is mapped with the grouping representation.

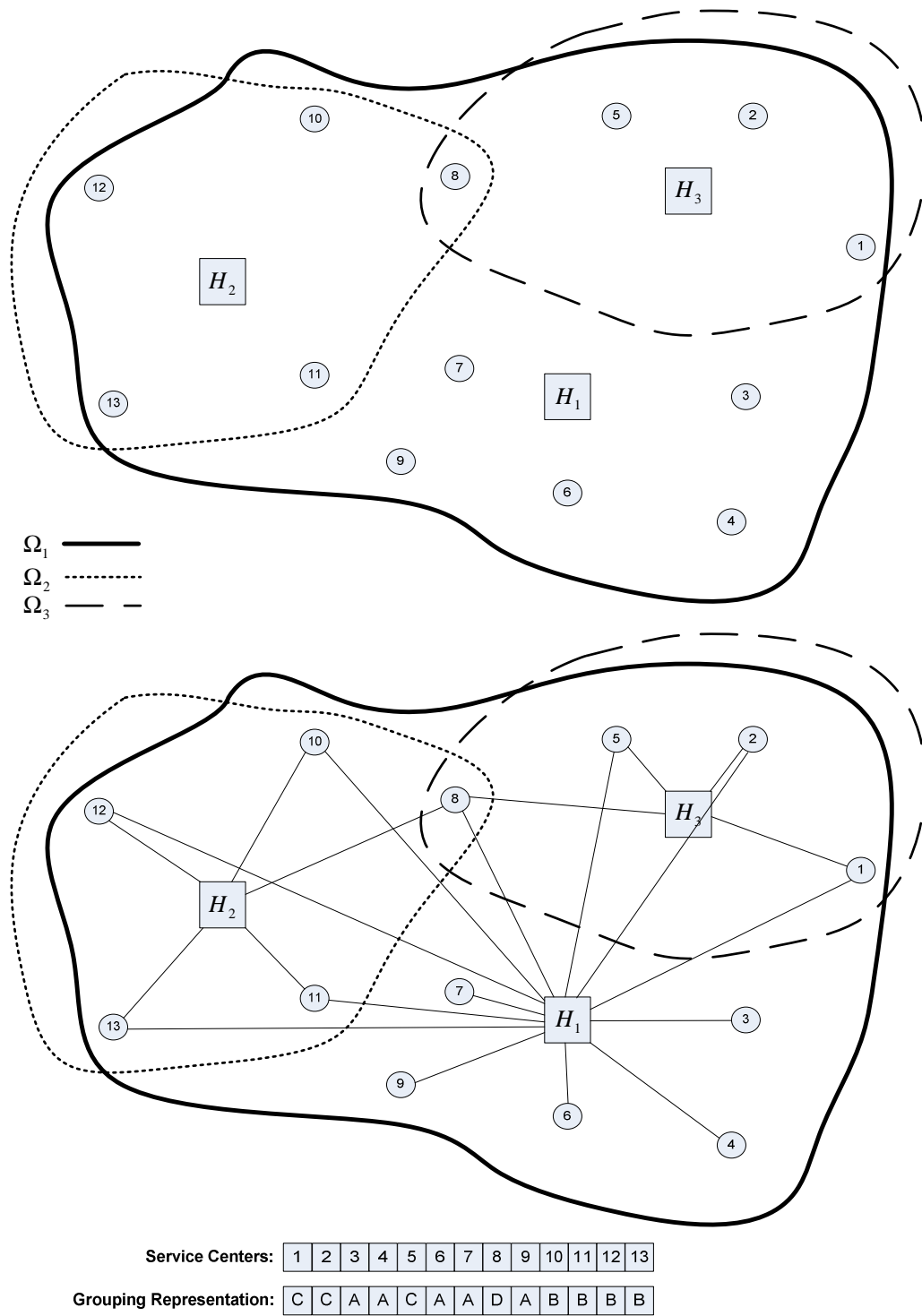


Figure 7.4: Example of GA grouping representation

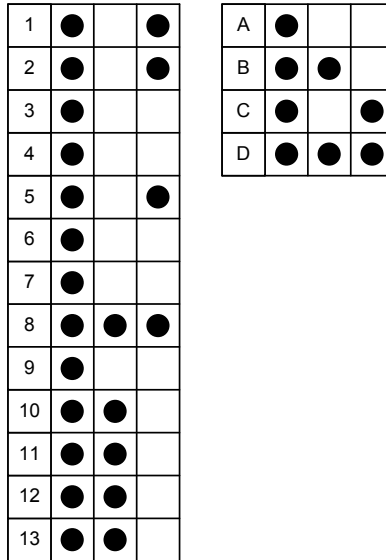


Figure 7.5: Grouping representation for Figure 7.4

7.2.2 Aircraft Route Representation – 2nd GA Layer

With the pre-specified grouping or hub assignment, a *restricted version* of the NH must be evaluated and improved where necessary. To satisfy fleet balancing constraints (5.1 – 5.3) at service centers and hubs and maintain the feasibility of solutions when applying GA operators, we define a chromosome by an aircraft route representation, where each chromosome is the collection of *cycle-based aircraft route variables*. Each cycle contains both pickup and delivery routes. It can be seen that with NH characteristics, all aircraft routes can be represented by a set of cycles, as shown in Figure 7.6.

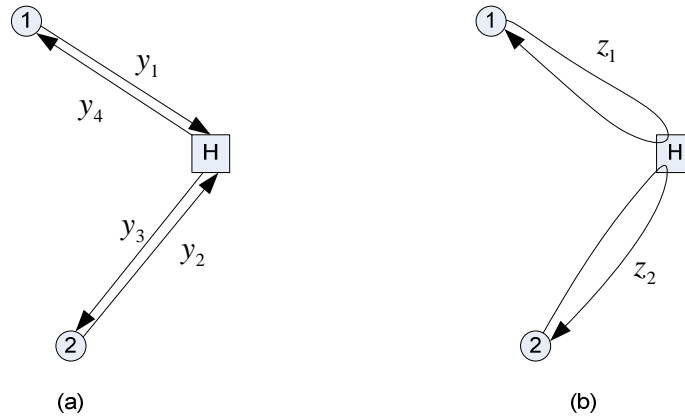


Figure 7.6: Equivalence of path-based and cycle-base aircraft routes

The cycle-based aircraft route structure in our study is represented as shown in Figure 7.7. Each cycle variable consists of 8 components:

- 1st array – origin service center on pickup route
- 2nd array – intermediate service center on pickup route
- 3rd array – hub
- 4th array – intermediate service center on delivery route
- 5th array – destination service center on delivery route
- 6th array – arrival grid time at hub
- 7th array – departure grid time at hub
- 8th array – aircraft fleet type

In the cycle's structure, the path components are the 1st – 5th arrays, and the non-path components are the 6th – 8th arrays. The purpose of maintaining the non-path 6th and 7th components is to determine the violation of (1) hub landing capacity and (2) hub take-off capacity. In addition, they can be used in post-solution slack analysis.

The non-path 8th component is used to verify the violation of aircraft fleet availability.

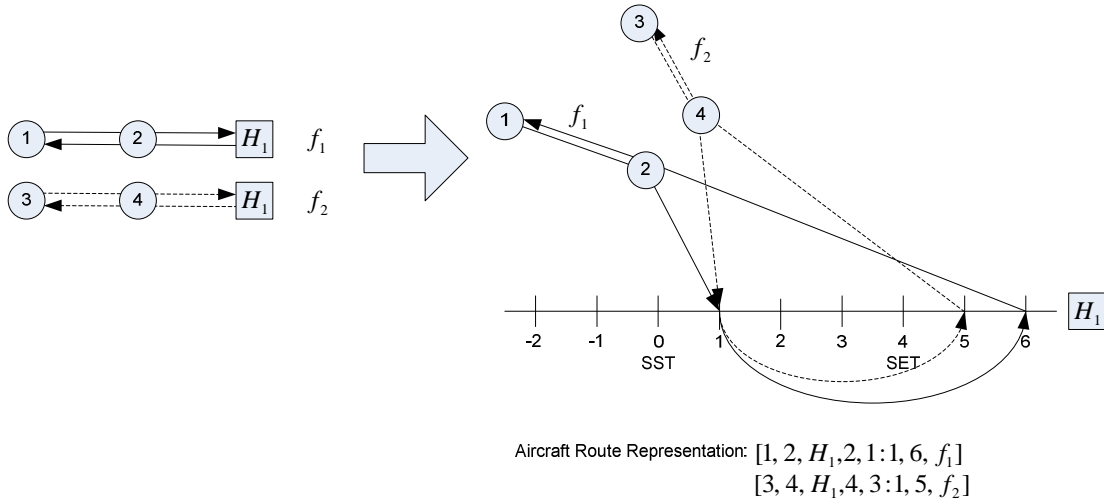


Figure 7.7: Example of aircraft route representation with cycle-based variables

7.2.3 Labeling and Encoding Scheme

Summarizing our GA solution representation, each NH solution consists of two components: grouping representation and aircraft route representation. The first representation is mainly designed to control the hub assignment for each service center, while the second is encoded by the collection of cycle-based variables. Each cycle is *dynamically* labeled according to (1) the assigned hub, (2) service center number based on pickup and delivery order, (3) arrival and departure time at the assigned hub, and (4) aircraft type.

From Figure 7.4, let the distribution network currently have only single-leg flights and a single aircraft type, and let all flights be able to arrive before the hub's

sort start time ($t_{SST} = 0$) and depart at the sort end time (e.g., $t_{SET} = 4$). Then we have

the following labeling and encoding scheme:

Grouping representation:

[C, C, A, A, C, A, A, D, A, B, B, B, B]

Aircraft route representation:

$$r[1,1] = [H_1,1,0,0,1 : 0,4,1]$$

$$r[1,2] = [H_1,2,0,0,2 : 0,4,1]$$

⋮

$$r[1,13] = [H_1,13,0,0,13 : 0,4,1]$$

$$r[2,1] = [H_2,8,0,0,8 : 0,4,1]$$

$$r[2,2] = [H_2,10,0,0,10 : 0,4,1]$$

$$r[2,3] = [H_2,11,0,0,11 : 0,4,1]$$

$$r[2,4] = [H_2,12,0,0,12 : 0,4,1]$$

$$r[2,5] = [H_2,13,0,0,13 : 0,4,1]$$

$$r[3,1] = [H_3,1,0,0,1 : 0,4,1]$$

$$r[3,2] = [H_3,2,0,0,2 : 0,4,1]$$

$$r[3,3] = [H_3,5,0,0,5 : 0,4,1]$$

$$r[3,4] = [H_3,8,0,0,8 : 0,4,1]$$

7.3 Initialization Process

The initialization process starts with constructing the territory of each hub, which is the set of service centers that can be feasibly connected to that hub. It is noted that,

the loading/unloading time of the aircraft must also be considered to verify the actual feasible connectivity. In our problem, to ensure that all packages can be served to their destinations at least via the major hub if there is no other alternative, the main hub's territory contains all the service centers. A service center that lies within more than one hub's territory is randomly assigned a grouping using (1) its feasible hub assignment and (2) the feasible hub assignment of its destination demands. For instance, from Figure 7.8(a), assume that service center i can be assigned to either hub H_1 or H_2 and service center j can only be served by hub H_1 . Because the destination of service center i (service center j) can only be shipped through hub H_1 , service center i can only be assigned to hub H_1 . In contrast, in Figure 7.8(b), service center i and k can be assigned to both hubs. However, if service center k is randomly assigned only to hub H_1 , it is useless to assign service center i to hub H_2 ; in this case, the model is designed to validate this problem. It is noted that all service centers are assigned to the major hub or H_1 to ensure the connectivity.

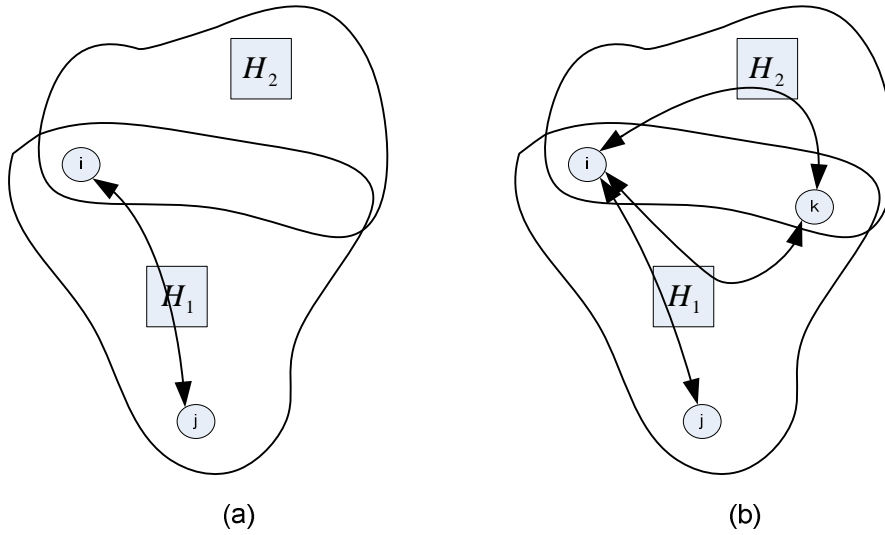


Figure 7.8: Illustration of randomly selected hub assignment

To assign aircraft to a service center, we try to use the smallest available aircraft capacity that exceeds the service center's demand. In addition, due to the limited aircraft availability constraints (5.4), the algorithm will search through the list of previously constructed cycles to check the possibility of utilizing a two-leg cycle.

```

Begin
create grouping representation according to the set of hub territories and randomly assign
demand to be transported through each connected hub
for each hub territory
    while (not all service centers are assigned by aircraft) do
        select an unassigned service center and scan through the list of previously
        constructed cycles to see whether any cycles can be inserted by the
        selected service center and meet all the operational constraints
        if insertion is possible then
            insert the selected service center into the existing cycle and form the
            cycle such that the aircraft operating cost is minimized and feasible.
        else
            select available aircraft type that can meet constrained demand and add
            the new cycle
        end if
        denoted the selected service center to be an assigned service center
    end while
end for
end

```

Figure 7.9: Initialization process

There is a difference in the initialization process for single-stage and two-stage operations. It is noted that our GA operators, which will be described in section 7.4, are designed to perform a local search using single-step improvement, i.e., applying one manipulation per one improvement. We originally designed a problem-specific GA operator using such a characteristic to search for a two-stage operation structure. However, the operator could not find a saving by both (1) constructing an interhub route and (2) diverging routes connecting to a previously constructed interhub route. Therefore, we design the initialization process for the two-stage operation by heuristically placing an interhub route using a user input. By thus initializing the two-stage operation, we are able to find a single-step improvement using our GA operator that will be described in section 7.4.2.5.

7.4 Genetic Operators

In this section the set of genetic operators, which are used to transform the current solution, are described. The operators utilize the NH problem content to guide the evolution of the solution. There are two categories of genetic operators that are designed to apply during generation improvement – grouping operators (an exchange of hub assignment) and aircraft route operators (an innovative random modification for network design). The first category consists of both crossover and mutation operators aiming to modify the grouping representation, while the second contains several mutation operators designing to optimize the network design under pre-specified grouping. Figure 7.10 summarizes problem specific genetic operators that can be applied to both single-stage and two-stage operations. We construct an additional aircraft route mutation operator for two-stage sorting operations.

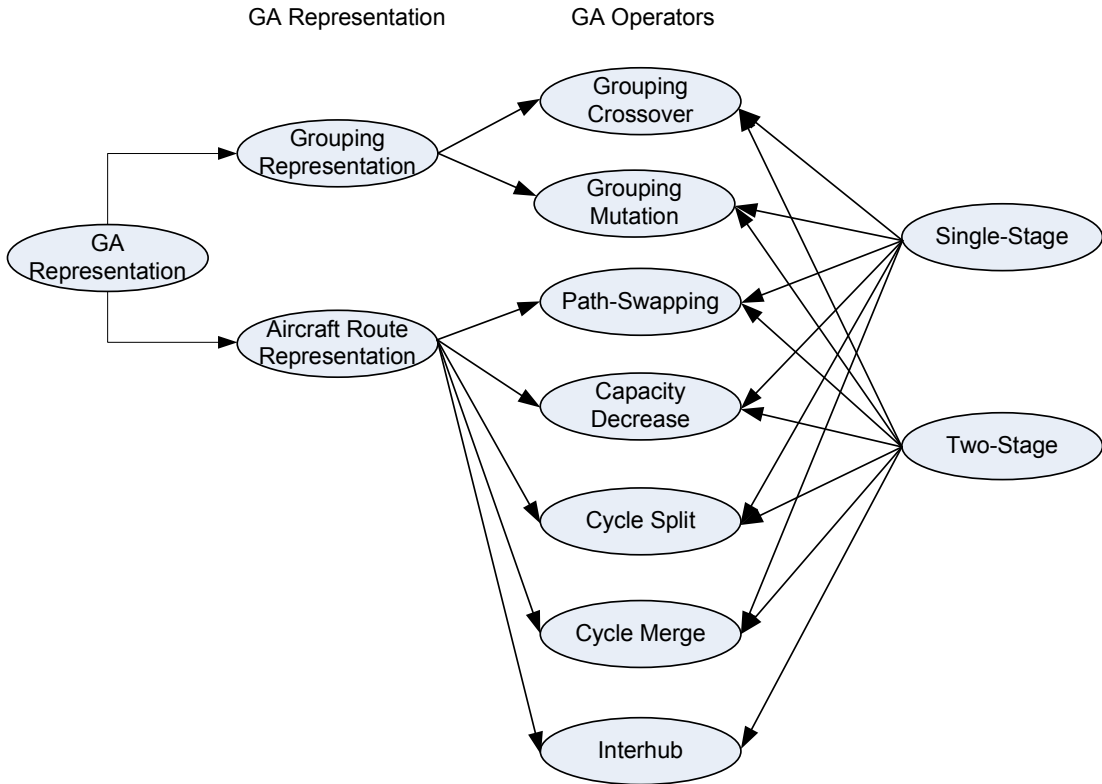


Figure 7.10: Set of GA operators applicable to different sorting policies

7.4.1 Grouping Operators

To manipulate the grouping representation, the following genetic operators are constructed to change the hub assignment. It is noted that, after applying these operator to the grouping representation, the aircraft route mutation operators are then used to optimize the network design problem under pre-specified grouping.

7.4.1.1 Grouping Crossover Operator

The general concept of a grouping crossover operator is to change solution structure significantly in order to prevent the search from getting trapped in a local optimum. In our NH problem, this can be done by modifying the grouping representation. First, two parents are selected with probabilities proportional to their fitness functions.

Second, the grouping representations of both parents are compared and identified for service center(s) having unmatched hub assignment. Now, the question becomes (1) which service centers and (2) how many of them in the unmatched list should be interchanged for hub assignment between the two groupings.

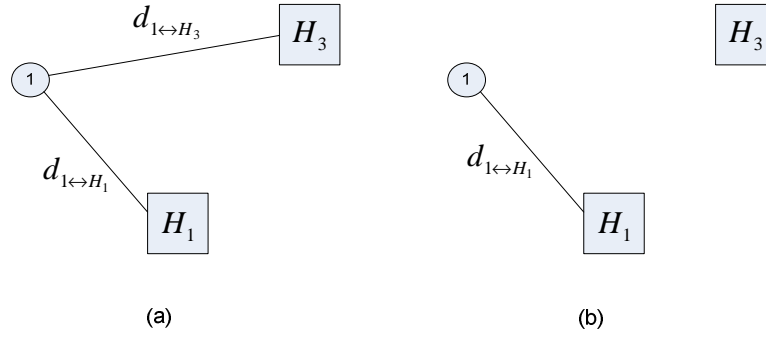
For single-point grouping crossover, we consider the *total absolute change in transferred demand at hubs* of both selected solutions to quantify how much solution structures are modified, as depicted in Figure 7.11. Therefore, although the choice of service center is made randomly, the probability is made proportional to the *total absolute change in transferred demand at hubs*:

$$\text{Prob}(\text{select } i \text{ for crossover}) = \frac{\sum_{h \in H} \Delta d_{i \leftrightarrow h}}{\sum_{j \in \{\{\Lambda\}_1 \cap \{\Lambda\}_2\}} \sum_{h \in H} \Delta d_{j \leftrightarrow h}} \quad (7.1)$$

where

$\Delta d_{i \leftrightarrow h}$ = Change of transferred demand to/from service center i to hub h

$\{\{\Lambda\}_1 \cap \{\Lambda\}_2\}$ = Set of service centers with unmatched hub assignment compared between selected parents 1 and 2.



$$\sum_{h \in H} \Delta d_{1 \leftrightarrow h} = \left| (d_{1 \leftrightarrow H_1})_{(a)} - (d_{1 \leftrightarrow H_1})_{(b)} \right| + \left| (d_{1 \leftrightarrow H_3})_{(a)} - 0 \right|$$

Figure 7.11: Total change in transferred demand at hubs

In the example below, the bold letters indicate service centers with unmatched hub assignment between the two selected parents for crossover, while the bold and underlined letter identifies the crossover location.

1st Parent: [C, C, A, A, C, A, A, **D**, A, B, **B**, B, B]

2nd Parent: [C, C, A, A, C, A, A, **C**, A, B, **A**, B, B]

1st Child: [C, C, A, A, C, A, A, **C**, A, B, **B**, B, B]

2nd Child: [C, C, A, A, C, A, A, **D**, A, B, **A**, B, B]

Figure 7.12 illustrates how the service centers are compared and selected. A question arises then about whether that particular crossover location is feasible after modification. Additional routes might need to be added or repaired to make the new solution feasible.

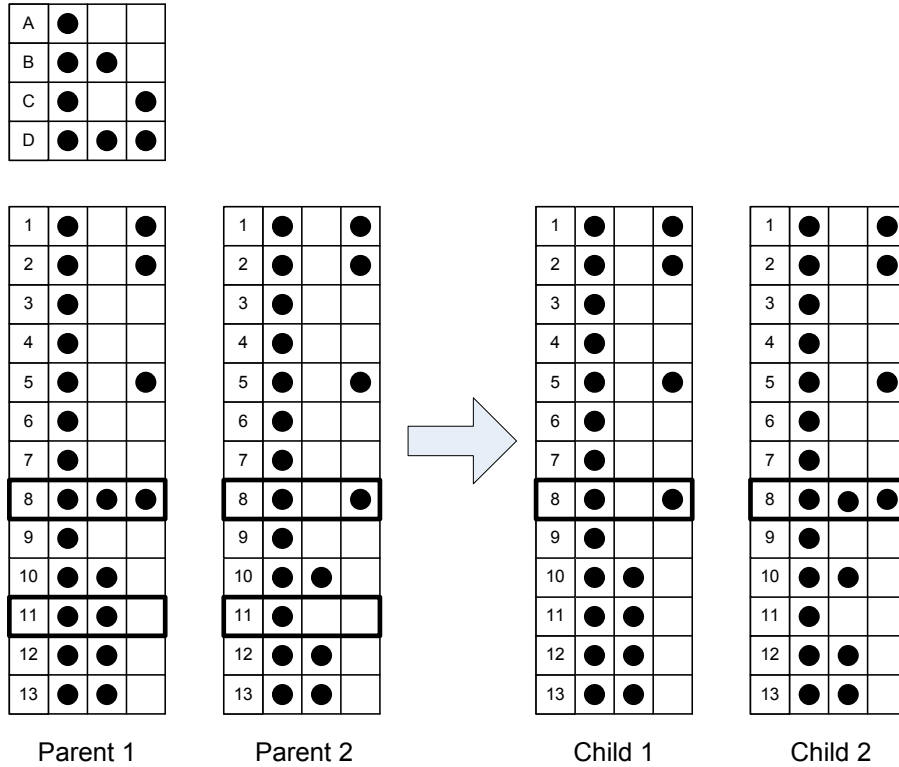


Figure 7.12: Example of single-point grouping crossover operator

One might expect an invisible impact from the single-point crossover on a large problem instance or a network containing a lot of service centers. Multiple-point grouping crossover is an alternative for modifying the hub assignment in this situation. The right hand side of equation 7.1 can be used to evaluate the selection of each individual service center that has the unmatched hub assignment between the two selected parents. The value is compared to a randomly generated number to decide the change in hub assignment.

7.4.1.2 Grouping Mutation Operator

In the grouping crossover operator, the representation is modified by considering an individual service center to two possible hub assignment. The grouping mutation manipulates the representation in a way opposite to the crossover operator. It first randomly selects a parent with probability proportional to their fitness function. Second, an individual hub is evaluated for the *maximum possible demand in its territory*, as shown Figure 7.13.

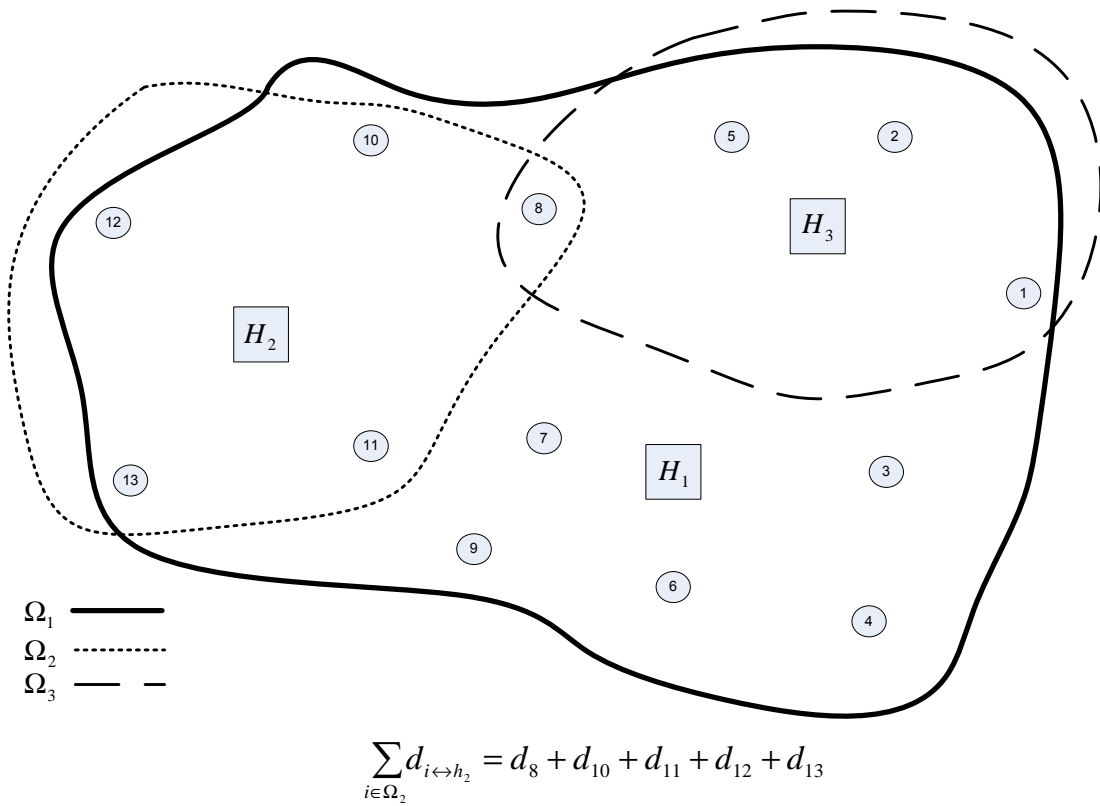


Figure 7.13: Maximum possible demand in hub territory

Therefore, although the choice of modifying a hub is made randomly, the probability is made proportional to the *maximum demand in each hub territory*:

$$\text{Prob}(\text{select } h \text{ for mutate}) = \frac{\sum_{i \in \Omega_h} d_{i \leftrightarrow h}}{\sum_{h \in H} \sum_{i \in \Omega_h} d_{i \leftrightarrow h}} \quad (7.2)$$

where

$d_{i \leftrightarrow h}$ = Total demand that can be transported from service center i to hub h

Ω_h = The set of service center that can be connected to hub h

After selecting a hub to modify the hub assignment, each service center within the hub territory is randomly assigned to that hub. One may visualize the concept as the gravity model.

7.4.2 Aircraft Route Operators

To evaluate the fitness function value of each grouping representation, although the representation results in a smaller version of the network design problem, the problem is still complex and difficult to solve. With the NP-hard nature of the network design problem, it is very difficult to design an efficient deterministic or greedy local search procedure that can consider all possible interaction within the problem characteristics. In this study, we consider the *probabilistic local search* by developing several genetic operators with all possible ways to improve the solution. With this probabilistic local search property, a single grouping representation may results in different objective functions. Therefore, for each grouping representation, the best solution can be found from performing several replications.

Note that the following GA operators only search for the feasible moves within the surrounding environment. By using problem content in guiding a search, our operators heavily utilize the information on how packages are flown through the system and on each individual route. In addition, because each gene in the chromosome is a cycle-based aircraft route and consists of mirroring pickup and delivery routes, our operators manipulate both directions at the same time.

7.4.2.1 Path-Swapping Operator

This operator is intended to interchange the path of the selected cycles that have a hub assignment in common. Generally, this manipulation benefits the overall system whenever it finds a reduction in route travel distance which decreases the aircraft operating cost. The choice of two cycles for path interchange is made randomly with a probability proportional to the expected potential benefit of the subject interchange:

$$\text{Prob}\{\text{select cycles } m \text{ and } n \text{ for path interchanges}\} = \frac{b_{swap}^{m,n}}{\sum_{r \neq s} b_{swap}^{r,s}} \quad (7.3)$$

where

$b_{swap}^{m,n}$ = Benefit or cost saving from interchange path of routes m and n .

There is a complicated situation when the two analyzed routes use different aircraft types. Let $[i, j, f]$ represent a route that departs from a service center i and have an intermediate stop at service center j before arriving to a hub, and utilizes aircraft type f . Let routes m and n consist of path and aircraft type $[a, b, f_1]$ and

$[c, d, f_2]$, respectively, and have feasibly interchangeable. There are four possible combinations that might be obtained, i.e.:

Combination 1: $[a, c, f_1]$ and $[b, d, f_2]$

Combination 2: $[a, c, f_2]$ and $[b, d, f_1]$

Combination 3: $[a, d, f_1]$ and $[b, c, f_2]$

Combination 4: $[a, d, f_{21}]$ and $[b, d, f_1]$

The algorithm is designed so that only the highest cost saving from all the possible combinations is considered. However, the two routes can interchange their paths whenever:

1. The resulting new routes can meet the operational constraint, e.g., $[a, c, f_1]$ arrive at the hub before the sort end time.
2. There is no violation in demand over new path capacity, e.g., $d(a) + d(c) \leq u(f_1)$ where $d(a)$, $d(c)$ are demands at service center a and c , respectively.

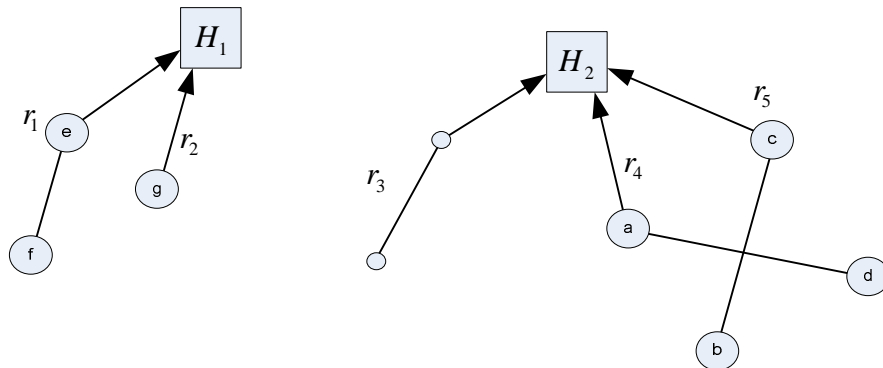


Figure 7.14: Example of path-swapping operator

From Figure 7.14, routes r_1 and r_2 cannot interchange with r_3, r_4, r_5 because they have different hub assignments. Routes r_3 and r_5 cannot interchange their paths without violating operational constraints. The resulting benefit matrix is as follows:

	r_1	r_2	r_3	r_4	r_5
r_1	0	b_{12}	—	—	—
r_2	b_{21}	0	—	—	—
r_3	—	—	0	b_{34}	—
r_4	—	—	b_{43}	0	b_{45}
r_5	—	—	—	b_{54}	0

7.4.2.2 Capacity Decrease Operator

This operator attempts to decrease aircraft route capacity when it finds a low load factor on a route. The system can benefit from this operator by (1) reducing in aircraft operating cost and (2) utilizing smaller aircraft which then save the aircraft owner cost. In addition, the operator will drop a route when there is no flow on it. This will definitely provide a significant saving.

Let $c_p(f)$ and $c_o(f)$ be aircraft operating cost per mile and aircraft ownership cost of aircraft type f . Let $u_i < u_j$ when $i < j$. Figure 7.15 demonstrates two scenarios that decrease a route's capacity. In Figure 7.15(a), it is easy to determine the saving, i.e., $c_p(f_2) + c_o(f_2) - c_p(f_1) - c_o(f_1)$. In Figure 7.15(b), one might quickly find the infeasibility of such operation. However, there might be other routes connecting those service centers, which might be able to alleviate those overflows (as shown on the dashed lines). In this study, we consider this situation to

benefit the system, but with some probability α . Therefore, the saving from Figure 7.15(b) is $\alpha(c_p(f_2) + c_o(f_2) - c_p(f_1) - c_o(f_1))$, by assuming $\alpha = 1 - X(2)/(u_2 - u_1)$. $X(2)$ denotes demands that cannot be served with a new route. Therefore, the less the flows spill over the new capacity, the more the capacity reduction benefits the system.

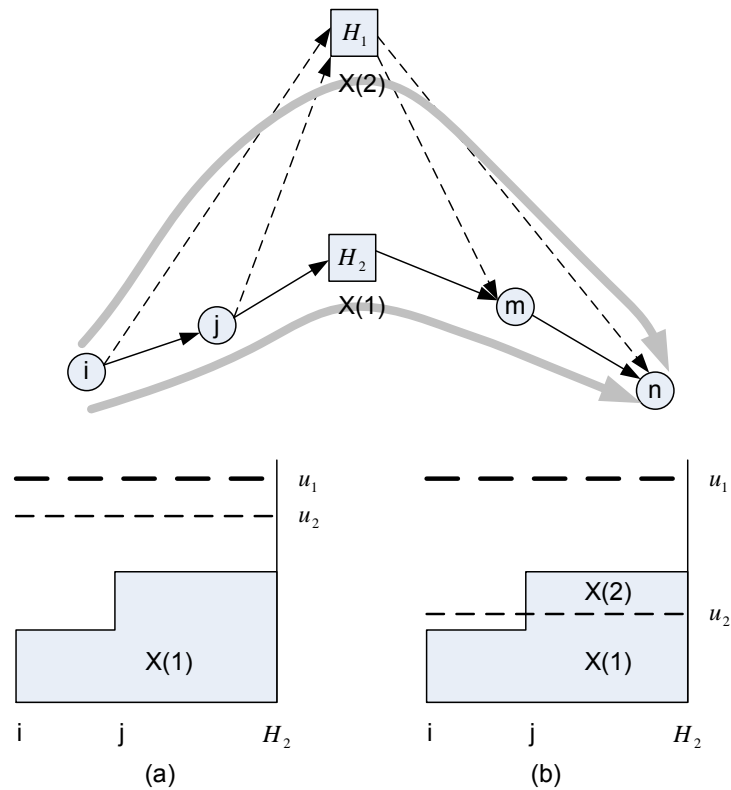


Figure 7.15: Capacity decrease operator

The operator randomly selects a cycle to change capacity, but the probability of choosing each route and the type of modification is proportional to the expected potential benefit that was previously described:

$$\text{Prob}\{\text{select route } i \text{ to change capacity from fleet } j \text{ to } k\} = \frac{b_{cap}^{i,(j \rightarrow k)}}{\sum_{n \in F_s(m)} \sum_{r \in R_Z} b_{cap}^{r,(m \rightarrow n)}} \quad (7.4)$$

where

$$F_s(m) = \{f \in F : u_f < u_m\} \cup \{u_0\}$$

= Set of aircraft types having capacity less than that of fleet type m , including a situation of completely dropping the route, (u_0) .

Let $u_1 < u_2 < u_3$. The column associated with the bold entry indicates the existing fleet type. A hypothetical matrix with nonnegative expected potential benefits when modifying aircraft capacity might be as follows:

	0	f_1	f_2	f_3
$r_1(f_1)$	b_{10}	0	-	-
$r_2(f_2)$	b_{20}	b_{21}	0	-
$r_3(f_3)$	b_{30}	b_{31}	b_{32}	0
$r_4(f_3)$	b_{40}	b_{41}	b_{42}	0
$r_5(f_2)$	b_{50}	b_{51}	0	-

7.4.2.3 Cycle Split Operator

This operator is designed to separate a two-leg cycle into two single-leg cycles whenever there is a saving. It is clear that having two single-leg cycles would increase the system operating cost because additional cycle would mean additional aircraft ownership cost, which is generally higher than the saving from aircraft operating cost. This is found during the long-term planning process. However, in the

short-term planning where aircraft ownership cost is ignored, this operator can provide savings in operational cost.

On a two-leg route r stopping at $[a,b]$ using fleet type f_i , the route can be split in several ways. For example, the new resulting route is:

$[a,0,f_i]$ and $[b,0,f_j]$ where $f_j \in F$, or

$[a,0,f_j]$ and $[b,0,f_i]$ where $f_j \in F$

To determine the benefit of such splitting, we evaluate all possible combinations and keep only the best alternative. It is noted that, when we apply this operator and there is no aircraft available, the solution will get penalized in the solution evaluation process. The cycle split operator randomly selects a cycle to be split, but the probability of choosing each route and the type of modification is proportional to the expected potential benefit that was previously described:

$$\text{Prob}\{\text{select route } r \text{ to split to routes } s \text{ and } t \text{ by adding fleet type } m\} = \frac{b_{split}^{r \rightarrow \{s,t,m\}}}{\sum_{f \in F} \sum_{l \in R_z} b_{split}^{i \rightarrow \{j,k,f\}}} \quad (7.5)$$

where

$b_{split}^{r \rightarrow \{s,t,m\}}$ = Benefit from splitting route r into routes s and t by adding fleet type m .

7.4.2.4 Cycle Merge Operator

This operator is the opposite of the cycle split operator. Whenever any two single-leg cycles can be combined to save (1) aircraft operating cost and/or (2) aircraft ownership cost, merging the two cycles will benefit the system. On any given two

single-leg cycles that can feasibly be merged their path without violating the operational constraints; there are two possible situations to consider. Let the two routes r_1 and r_2 be $[a,0,f_1]$ and $[b,0,f_2]$ having flows $d(a)$ and $d(b)$, respectively. It is noted that $d(a) \leq u_1$ and $d(b) \leq u_2$. The following possible benefits are analyzed:

1. If $d(a) + d(b) \leq u_1$, then the saving is $c(r_1) + c(r_2) - c(r_{new})$ where $r_{new} = [a,b,f_1]$.
2. If $d(a) + d(b) \leq u_2$, then the saving is $c(r_1) + c(r_2) - c(r_{new})$ where $r_{new} = [a,b,f_2]$.
3. If $d(a) + d(b) > u_1$, then the saving is $\alpha(c(r_1) + c(r_2) - c(r_{new}))$ where $r_{new} = [a,b,f_1]$ and α is the probability the exceeding flow can be served somewhere else, $1 - (d(a) + d(b) - u_1)/u_2$.
4. If $d(a) + d(b) > u_2$, then the saving is $\alpha(c(r_1) + c(r_2) - c(r_{new}))$ where $r_{new} = [a,b,f_2]$ and α is the probability the exceeding flow can be served somewhere else, $1 - (d(a) + d(b) - u_2)/u_1$.

In this study, we consider the highest potential saving, i.e., the maximum from the above four cases. The operator will randomly select two single-leg cycles to be merged, but the probability of selecting the two routes is proportional to the expected potential benefit.

$$\text{Prob}\{\text{merge route } s \text{ and } t \text{ to be route } r, \text{ using fleet type } m\} = \frac{b_{merge}^{(s,t) \rightarrow r(m)}}{\sum_{m,n \in R_z: m \neq n} \sum_{f \in \{f(s) \cup f(t)\}} b_{merge}^{(m,n) \rightarrow r(f)}} \quad (7.6)$$

where

$b_{merge}^{(s,t) \rightarrow r(m)}$ = Benefit from merging route s and t to be route r using fleet type f .

$f(s)$ = Fleet type of route s .

7.4.2.5 Interhub Operator

This operator tries to change route's hub destination or hub assignment to the nearest hub when there is an interhub route connecting the two hubs, as shown in Figure 7.16.

From Figure 7.16, route r_2 is selected by the operator to change its original hub assignment from h_1 to h_2 . It can be seen that the flows on route r_2 diverge from single-stage to two-stage flow. The saving from this operator is the reduction in distance or aircraft operating cost. Obviously, the operator can be applied to a route only when it meets the operational constraints, in which the critical one would be change in operational time when reaching its original assigned hub. Several considerations determine the savings:

1. If $d(r_2) \leq u_1 - d(r_3) - d(r_4)$, the saving is $c(r_2^{new}) - c(r_2) - \Delta e$, where Δe is the expected increase in hub sorting cost at hub h_2 .
2. If $d(r_2) > u_1 - d(r_3) - d(r_4)$, the saving is $\alpha(c(r_2^{new}) - c(r_2) - \Delta e)$, where Δe is the expected increase in hub sorting cost at hub h_2 and α is the probability that the flow on route r_2 plus the existing flow on the interhub route can meet the interhub capacity, $1 - d(r_2)/(u_1 - d(r_1))$. In this calculation, we assume that the spilled flow has a chance to be served somewhere in the system.

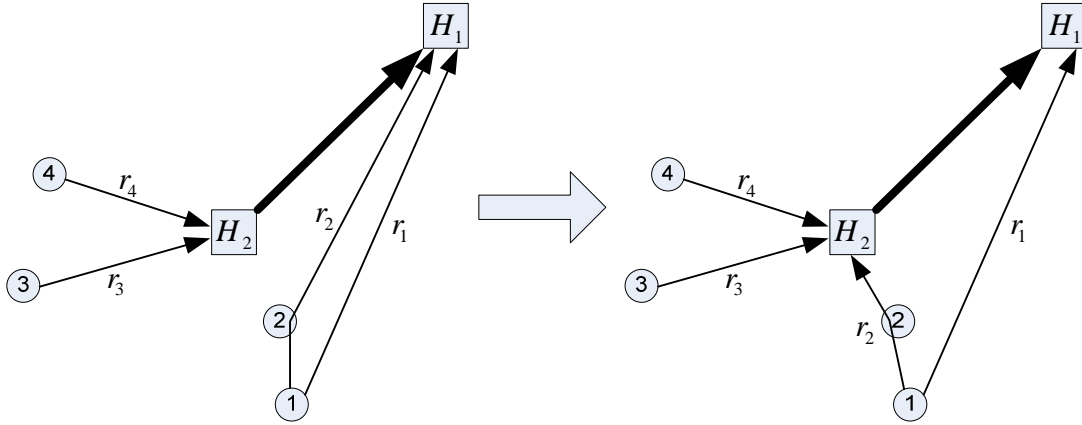


Figure 7.16: Interhub usage operator

The operator randomly diverges a route to connect to the interhub route, but the probability of selecting each route is proportional to the expected potential benefit:

$$\text{Prob}\{\text{diverge route } i \text{ to use hub } j\} = \frac{b_i^j}{\sum_{h \in H} \sum_{r \in R_z} b_r^h} \quad (7.7)$$

where

b_r^h = Benefit from diverging route r to from its original hub to hub h .

7.5 Network Evaluation Process

From Figure 7.3, to evaluate each GA solution, the following steps are performed:

1. Obtain network configuration from GA and evaluate the aircraft operating cost. Add penalty cost when the system violates (1) aircraft availability, (2) hub landing capacity, and (3) hub take-off capacity.
2. Evaluate package flow movement without considering hub sorting capacity and hub storage size.

3. Evaluate hub sorting capacity using the resulting flow from (2). Add penalty cost if the resulting hub sorting capacity exceeds the desired limit.
4. Evaluate hub storage capacity using the resulting flow from (2) and hub sorting capacity from (3). Add penalty cost if the resulting hub storage size exceeds the bound.

From the above procedures, to determine the set of optimal flow paths, step 2 can be cast as a *capacitated multicommodity network flow problem*. By separately determining the hub sorting cost in steps 3 and 4, the network flow problem is significantly smaller than the original model that was previously described in section 5.3 because the hub sorting network, HSN, can be consolidated into a single node for each hub. The problem can then be solved by using the column generation approach. The network configuration obtaining from the GA solution, however, might provide insufficient capacity to serve the required demands. Therefore, we add a set of dummy routes, R_M , to the restricted master problem, RMP-GA, as shown in equations 7.8.

$$(RMP-GA) \tag{7.8}$$

$$\min \sum_{r \in R_M} My \tag{7.8.1}$$

Subject to:

$$\sum_{p \in P(k)} x_p^k = d^k \quad \forall k \in K \tag{7.8.2}$$

$$\sum_{k \in K} \sum_{p \in P(k)} \alpha_a^p x_p^k \leq u_a \quad \forall a \in A_{ARN} \tag{7.8.3}$$

$$x_p^k \geq 0 \quad \forall p \in P(k), k \in K \tag{7.8.4}$$

where:

$\alpha_a^p = 1$ if path p consists of arc a , or 0 otherwise

$u_a =$ Total capacity on arc a

The solution to equations 7.8 is either equal to zero (sufficient capacity) or greater than zero (insufficient capacity), i.e. $\min \sum_{r \in R_M} My > 0$.

7.5.1 CG Approach for Package Flow Paths

To determine the potential package flow path variables on the consolidated network representation, we modify the approach described in section 6.4.2. Let \mathbf{c}_p be the objective coefficient vector for package flow variables, let $\mathbf{A}_k, \mathbf{A}_a$ be the constraint matrix vector for package flow paths in constraints (7.8.2) and (7.8.3), respectively, and denote the dual vector corresponding those constraints as $\boldsymbol{\pi}^{\mathbf{A}_k}, \boldsymbol{\pi}^{\mathbf{A}_a}$. Because we ignore the cost of moving packages over the network, the reduced cost of a package flow path can be calculated from

$$\begin{aligned} \bar{\mathbf{c}}'_p &= \mathbf{c}'_p - (\boldsymbol{\pi}^{\mathbf{A}_k})' \mathbf{A}_k - (\boldsymbol{\pi}^{\mathbf{A}_a})' \mathbf{A}_a \\ &= \mathbf{0} - (\boldsymbol{\pi}^{\mathbf{A}_k})' \mathbf{A}_k - (\boldsymbol{\pi}^{\mathbf{A}_a})' \mathbf{A}_a \end{aligned} \quad (7.9)$$

From equation 7.9, the problem can then be solved using the shortest path on the modified arc cost, as described in 6.4.2.

7.5.2 Analytical Model for Hub Design Characteristics

At each hub location, given known flow values for all arriving package, we can determine the required sorting rate to serve those packages. For a single-stage operation, the sorting rate can be calculated using equation 7.10:

$$\sum_{k \in K} \sum_{p \in P(k)} \delta_t^{p,k} x_p^k \leq (|G_h| - t) e_h \Delta t \quad \forall t \in G_h \quad (7.10)$$

For example, let $\Delta t = 1$ hour; then:

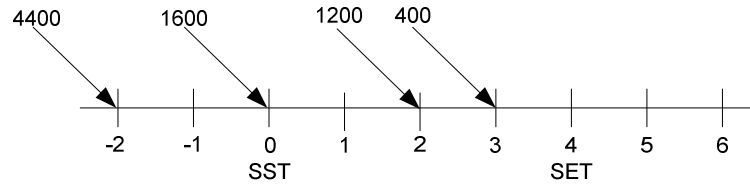


Figure 7.17: Determination of hub sorting capacity for single-stage operation

For single-stage operation:

@ $SST + 3\Delta t$:	$400 \leq e_h \Delta t$	$\Rightarrow 400 \leq e_h$
@ $SST + 2\Delta t$:	$1200 + 400 \leq 2e_h \Delta t$	$\Rightarrow 800 \leq e_h$
@ $SST + \Delta t$:	$1200 + 400 \leq 3e_h \Delta t$	$\Rightarrow 533 \leq e_h$
@ SST :	$4400 + 1600 + 1200 + 400 \leq 4e_h \Delta t$	$\Rightarrow 1900 \leq e_h$

Therefore, the required sorting rate to accommodate all the arrival packages is 1900 packages per hour.

However, for two-stage operation, we can determine the sorting capacity in two different ways: with FIFO and with TFSF (two-stage flow sorted first)

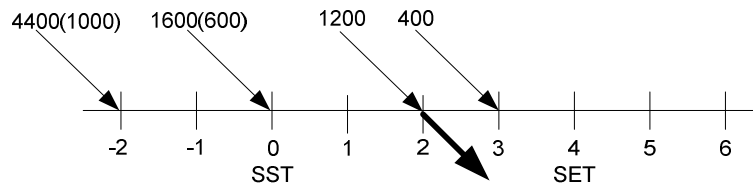


Figure 7.18: Determination of hub sorting capacity for two-stage operation

For a two-stage operation with TFSE, we expect less hub sorting capacity than with FIFO:

Two-stage hub sorting calculation with TFSE:

1. hub sorting capacity due to single-stage flow:

$$@ SST + 3\Delta t : \quad 400 \leq e_h \Delta t \quad \Rightarrow 400 \leq e_h$$

$$@ SST + 2\Delta t : \quad 1200 + 400 \leq 2e_h \Delta t \quad \Rightarrow 800 \leq e_h$$

$$@ SST + \Delta t : \quad 1200 + 400 \leq 3e_h \Delta t \quad \Rightarrow 533 \leq e_h$$

$$@ SST : \quad 3400 + 1000 + 1200 + 400 \leq 4e_h \Delta t \quad \Rightarrow 1500 \leq e_h$$

2. hub sorting capacity due to two-stage flow:

$$@ SST + 2\Delta t : \quad 1000 + 600 \leq 2e_h \Delta t \quad \Rightarrow 800 \leq e_h$$

Therefore, the sorting capacity required for the case with TFSE is $1500+800 = 2300$ packages/hour.

To determine the hub sorting capacity with FIFO, all flows before an interhub flight must be sorted:

$$@ SST + 3\Delta t : \quad 400 \leq e_h \Delta t \quad \Rightarrow 400 \leq e_h$$

$$@ SST + 2\Delta t : \quad 1200 + 400 \leq 2e_h \Delta t \quad \Rightarrow 800 \leq e_h$$

$$@ SST + \Delta t : \quad 4400 + 1600 \leq 3e_h \Delta t \quad \Rightarrow 3000 \leq e_h$$

Therefore, the sorting capacity required with FIFO is 3000 packages/hour.

After obtaining the hub sorting capacity, we can determine the hub storage size required for hub h , s_h , using the concept of the general inventory problem; that is:

$$\max \left\{ I_h^{t-1} + \sum_{k \in K} \sum_{p \in P(k)} \alpha_p^t(h) x_p^k - e_h \Delta t, 0 \right\} = I_h^t \quad \forall t \in G_h, h \in H \quad (7.11)$$

$$s_h = \max_{t \in G_h} \{ I_h^t \} \quad \forall h \in H \quad (7.12)$$

where

I_h^0 = Initial storage size = 0

$\alpha_p^t(h)$ = 1 if package path p arrives at hub h at time t , or 0 otherwise

G_h = Set of grid time at hub h

7.5.3 Other Operational Requirements

For operational constraints, the network must meet the requirement of (1) the aircraft availability constraints, (2) hub landing capacity constraints, and (3) hub take-off capacity constraints. In this study, we penalize any violations of constraints 5.4 – 5.6 accordingly using a fixed high cost value.

7.6 Slack Analysis

Slack is a measure of how much a task can be delayed without violating any constraints. Although the two-stage operation might benefit the system in term of cost savings, consolidating packages twice at two distinct hubs in the next day shipment would definitely decrease the slack within the system. In this study, we perform post-solution analysis, i.e., after obtaining an optimal solution, to determine the total system slack. To compare the slack between the two systems, we define total system slack, S , as the total slack of all commodities. Let s_p^k be the slack of commodity k

shipped through path p . For single-stage operation, s_p^k can be determined from (1) slack from pickup route and (2) slack from delivery route. On the other hand, additional slack from an interhub route is required to determine the slack for two-stage operation. It is noted that, even with a two-stage operation, the slack of a commodity can be determined only from pickup and delivery routes when its origin and destination lies within the same hub assignment. The total system slack can be determined from equation 7.13.

$$S = S_{pickup} + S_{interhub} + S_{delivery} = \sum_{k \in K} \sum_{p \in P(k)} x_p^k s_p^k \quad (7.13)$$

7.6.1 Pickup Route

After obtaining an optimal solution, we analyze the pickup slack of each route by determining the latest arrival time at hub that does not violate (or increase) the designed hub sorting rate and landing capacity, as shown in Figure 7.19. On any given route, it is important to point out that the latest arrival time at hub depends on the amount of flow the route is carrying. A route carrying fewer packages is likely to have less impact on the designed hub sorting rate, i.e., the latest arrival time at hub can be extended or delayed. Figure 7.19 demonstrates the iterative procedure in determining the latest arrival time at hub.

On a pickup route consisting of two-legs stopping at service centers i and j , as shown in Figure 7.20, there are two possibilities in determining the slack of each set of commodities originating from each location:

Case 1: when the earliest arrival time at service center j is less than the earliest pickup time at service center j , as shown in Figure 7.20(a).

Case 2: when the earliest arrival time at service center j exceeds the earliest pickup time at service center j , as show in Figure 7.20(b).

```

Begin
  let  $\Delta t =$  grid time interval
   $t_e \leftarrow$  earliest arrival time of route  $r$  at  $h$ 
   $t_l \leftarrow$  earliest grid time that is greater than or equal to  $t_e$ 
  while (not termination-condition) do
    if the next arrival grid time of package does not violate (1) hub sorting capacity and
      (2) hub landing capacity then
       $t_l \leftarrow t_l + \Delta t$ 
    else
      termination-condition = true
    end if
  end while
  return  $LAH(r, h) = t_l$ 
end

```

Figure 7.19: Determining the latest hub arrival time, $LAH(r, h)$

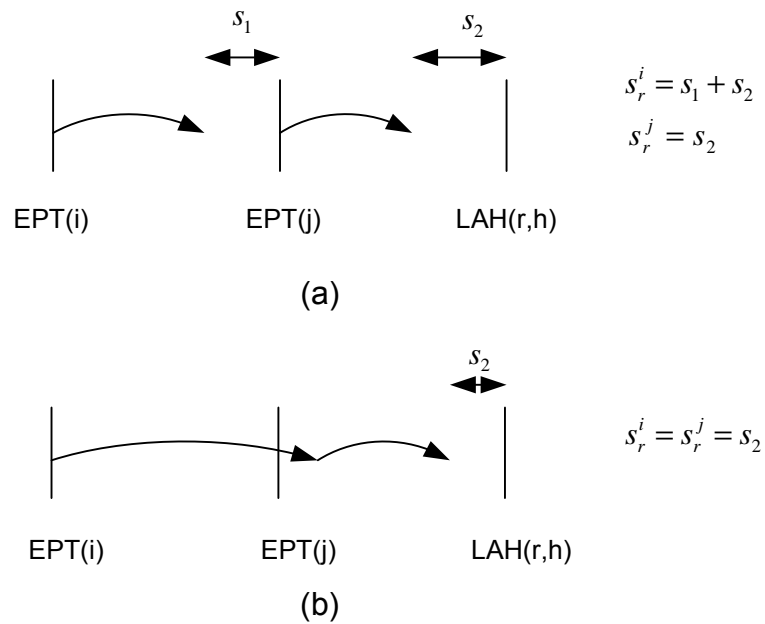


Figure 7.20: Slack analysis on pickup route

7.6.2 Delivery Route

Similarly to the analysis of the pickup route, to determine the slack of the delivery route, we iteratively change the aircraft departure time to find the earliest departure time without violating the hub take-off capacity constraints, as shown in Figure 7.21.

Figure 7.22 demonstrates the slacks for packages ending at different service centers.

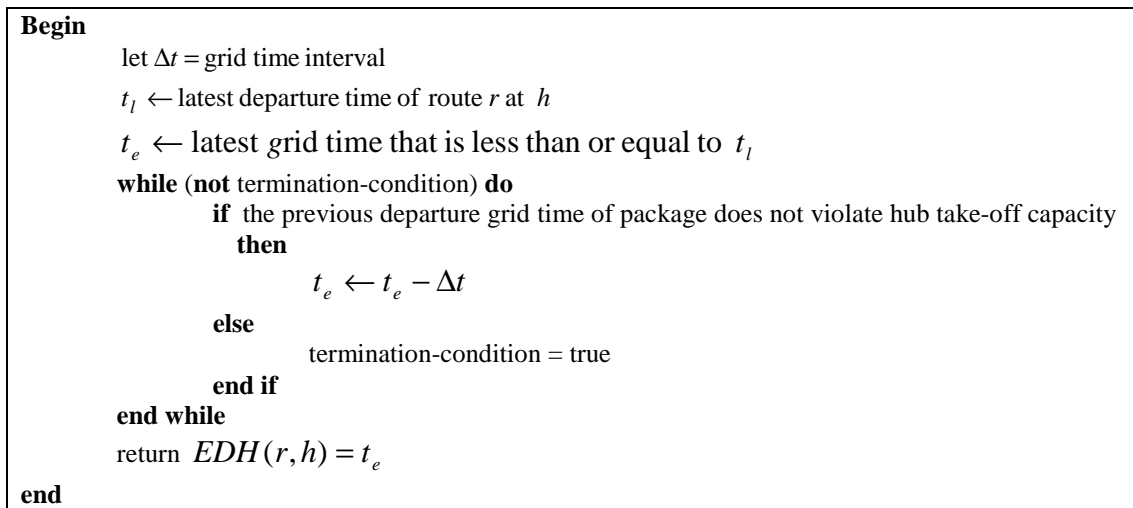


Figure 7.21: Determining the earliest delivery time, $EDH(r, h)$

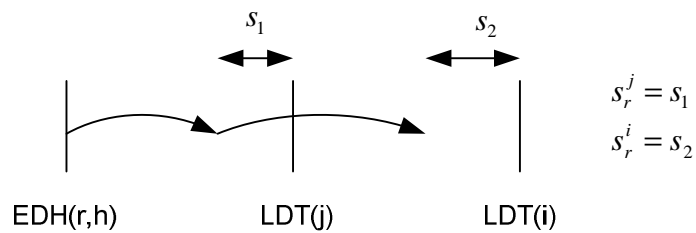


Figure 7.22: Slack analysis on delivery route

7.6.3 Interhub Route

From Figure 7.23, the slack of an interhub route r destined to hub h can be determined from the time interval between the earliest arrival time, $EAT(r,h)$, and the latest arrival time, $LAT(r,h)$, i.e.:

$$s_{\text{interhub}} = LAT(r,h) - EAT(r,h) \quad (7.14)$$

where:

$$EAT(r,h) = t_{\text{earliest}} + t_{\text{loading}} + t_{\text{unloading}} + \text{travel time between hub}$$

$LAT(r,h)$ = Latest arrival time for which packages can still be sorted at the second hub

t_{earliest} = The earliest departure time for which the interhub flight can carry all the interhub packages. In this study, we assume t_{earliest} to be the next grid time after the *latest entry interhub flow*. We can determine the latest entry interhub flow as soon as we know the optimal flow paths. The *latest entry interhub flow* from hub h_j to h_i is the latest arrival time of any routes carrying packages that will be transported using the interhub flight.

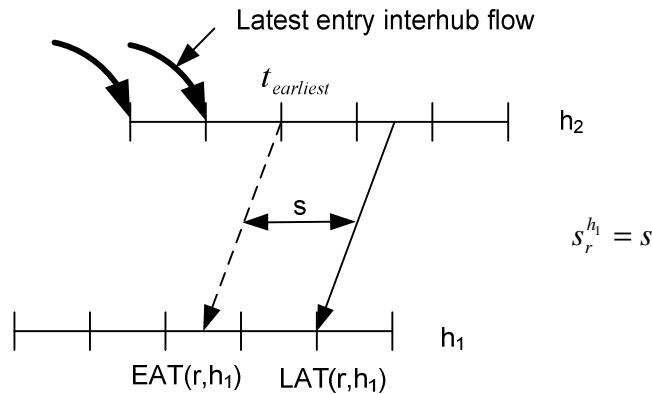


Figure 7.23: Slack analysis on interhub route

7.7 GA Performance Validation

The immediate task after developing the proposed GA solution approach is to validate and evaluate its solution quality by comparing it to the previously constructed column generation approach. Because, in our GA model, two-stage operations are only formed when they improve the total system cost, we simplify our test validation to only involve the single-stage operation. In addition, with a capability in solving only a small problem of the column generation approach, we only validate our GA model on a small arbitrary network. Tables 7.1 and 7.2 are our GA input parameters and the comparison results, respectively. In Table 7.1, we limit the population size to exhibit the performance of our GA operators. In addition, due to a probabilistic local search procedure, we allow the re-evaluation process by randomly selecting a set of population, n , and by selecting the set of best m population. These replications are performed to obtain the better or true solution value of the existing grouping representations. The followings are our problem characteristics:

- Problem set 1, “bench01” through “bench05”, have the same network configuration with a single hub, but their demands are increased accordingly.
- Problem set 2, “bench06” through “bench10”, have the same input data as those of problem set 1, but with an additional hub.
- All random selections throughout the algorithm are done with regard to the fitness values, i.e., objective functions, of the individuals which include the aircraft operating cost, aircraft ownership cost and hub sorting and storage cost.

- On evaluating each population, all 4 aircraft route operators (7.4.2.1 – 7.4.2.4) are equally and randomly selected.
- For each problem, 10 runs are performed with different random seeds

Table 7.1: GA parameters for performance validation

Population Size	20
#Population for grouping crossover, r_1	4
#Population for grouping mutation, r_2	2
#Population for randomly mutate, n	4
#Population for best mutate, m	2
Termination	20 generations w/o improvement

Table 7.2: GA performance evaluation

Problem Name	# Hubs	# SCs	CG and B&B			GA			
			IP	LP	Time (sec)	Best IP	Avg IP	Worst IP	Avg Time (sec)
bench01	1	9	\$228,602	\$189,754	7,200	\$215,382	\$215,382	\$215,382	31
bench02	1	9	\$261,089	\$227,533	7,200	\$260,488	\$260,488	\$260,488	40
bench03	1	9	\$317,206	\$270,554	7,200	\$301,444	\$301,444	\$301,444	84
bench04	1	9	\$378,587	\$316,595	7,200	\$351,378	\$351,378	\$351,378	83
bench05	1	9	\$401,146	\$363,047	7,200	\$394,923	\$394,923	\$394,923	101
bench06	2	9	\$250,616	\$166,716	7,200	\$215,382	\$215,382	\$215,382	69
bench07	2	9	\$322,608	\$201,659	7,200	\$256,506	\$256,506	\$256,506	114
bench08	2	9	\$439,095	\$238,316	7,200	\$281,408	\$281,408	\$281,408	206
bench09	2	9	\$405,551	\$279,618	7,200	\$337,813	\$343,151	\$350,054	266
bench10	2	9	\$393,849	\$321,600	7,200	\$383,974	\$388,092	\$393,413	329

From Table 7.2, the GA model is able to find better IP solutions with significantly less run time than the bench model (the column generation approach and the branch-and-bound algorithm). In addition, the model can identify the improved objective function when having an additional hub, i.e., the objective functions of problem set 1 are upper bounds of problem set 2. For example, the objective function of “bench06” should at most equal to that of “bench01”.

When comparing the optimal solutions among the problems, the solutions from the CG&BB deteriorate when (1) having more hubs which add complexity to the problem and (2) demands increase. In contrast, the GA solutions in the second set never exceed these of the first set, as expected. In addition, although we experience longer computation times when demands increase, the GA solutions do not deteriorate.

On “bench01” through “bench06”, we obtain the same optimal solution when applying grouping crossover rate of 20%, grouping mutation rate of 10%. On “bench07” through “bench08”, we can obtain the same optimal solution when increase the grouping mutation rate to 20%. However, we can not find the same optimal solution on multi-hub congested network, “bench09” through “bench10”, despite of an increase in both grouping crossover and mutation rates.

7.8 Computational Analyses

In these analyses, we employ our GA algorithm on the selected small UPS network to better understand how two-stage operation affects the system. All runs are performed on a Pentium M 1.7 GHz processor with 1GB RAM, running CPLEX 9.0. In addition, we consider the TFSF (two-stage sorted first) sorting process so that the benefit of two-stage operation from all analyses can be clearly identified. Otherwise, with FIFO, the total hub sorting cost might outweigh the distance saving from two-stage operation.

7.8.1 Case Study 3: 2 Hubs at Louisville, KY and Dallas, TX

In this section, two hubs with nine service centers served by a single aircraft type are evaluated for both single-stage and two-stage operation. The objectives of this analysis are to:

1. Examine sensitivity to various input parameters to understand when the two-stage operation benefits the system, and verify the conclusion found in section 6.5.1
2. Understand the changes in network configuration due to different inputs.
3. Understand the impact of two-stage operation on the system.

The following are the input characteristics:

1. No hub demands
2. Because the physical location is defined by latitude and longitude, we calculate the distance between any pair of locations using the Great Circle Distance Formula in equation 7.15.

$$3963 \arccos(\sin(\text{lat1})\sin(\text{lat2}) + \cos(\text{lat1})\cos(\text{lat2})\cos(\text{lon2} - \text{lon1})) \quad (7.15)$$

where:

lat1, lon1 = Latitude and longitude of the first location, in radians

lat2, lon2 = Latitude and longitude of the second location, in radians

3963 = The radius of the earth in statute miles

3. As in current practice, whenever packages can be transported via ground service without jeopardizing their critical time requirements, we exclude those packages from the analysis of air network. In this study, we ignore the OD demands for distances below 400 miles.

Table 7.3: Selected service centers for Case Study 3

No.	Location	EPT	LDT	Longitude	Latitude
1	Indianapolis, IN	8PM	6AM	-86.29	39.73
2	Chicago, IL	8PM	6AM	-87.65	41.90
3	Detroit, MI	8PM	6AM	-83.18	42.32
4	Pittsburg, PA	8PM	6AM	-80.08	40.43
5	Houston, TX	8PM	6AM	-95.35	29.97
6	San Antonio, TX	8PM	6AM	-98.47	29.53
7	Austin, TX	8PM	6AM	-97.70	30.30
8	Oklahoma City, OK	8PM	6AM	-97.60	35.40
9	Jackson, MS	8PM	6AM	-90.08	32.32
10	New Orleans, LA	8PM	6AM	-90.10	29.95
11	El Paso, TX	8PM	6AM	-106.40	31.80

Table 7.4: Selected hubs for Case Study 3

No.	Location	SST	SET	Longitude	Latitude
1	Louisville, KY	11PM	3AM	-85.70	38.21
2	Dallas, TX	10PM	3AM	-97.03	32.90

Note: All times are local standard times.

Table 7.5: O/D demand matrix for Case Study 3

O/D	(1)	(2)	(3)	(4)	(5)	(6)	(7)	(8)	(9)	(10)	(11)
(1)	0	0	0	0	2,596	491	519	599	1,169	599	1,169
(2)	0	0	0	0	907	236	761	1,238	1,276	1,238	1,276
(3)	0	0	0	0	547	738	872	836	307	836	307
(4)	0	0	0	0	2,433	664	803	801	775	801	775
(5)	1,006	720	587	3,333	0	0	0	0	0	0	0
(6)	791	362	778	966	0	0	0	0	2,827	0	0
(7)	1,169	1,276	307	775	0	0	0	0	0	0	0
(8)	548	771	773	921	0	0	0	0	0	0	0
(9)	1,169	1,276	307	775	0	2,827	0	0	0	0	0
(10)	548	771	773	921	0	0	0	0	0	0	0
(11)	1,169	1,276	307	775	0	0	0	0	0	0	0

Table 7.6: Hub characteristics for Case Study 3

Hub No.	1	2
Unit sorting cost, c_e^h (\$/package)	\$0.10-0.60	\$0.10-0.60
Unit storage cost, c_s^h (\$/package)	\$0.02-0.12	\$0.02-0.12
Landing capacity (#aircraft/hour)	40	40
Take-off capacity (#aircraft/hour)	50	50

Table 7.7: Aircraft characteristics for Case Study 3

Aircraft Type No.	1
Availability	20
Capacity (packages)	50,000
Avg. Cruising Speed (mph)	550
Aircraft Loading/Unloading Time (min)	20
Operating Cost/mile (\$/mile)	\$7-12
Take-Off/Landing Cost	\$300
Ownership Cost/Day/Aircraft	\$16,000

Table 7.8: GA parameters for Case Study 3

Population Size	20
#Population for crossover, r	6
#Population for randomly mutation, n	4
#Population for best mutation, m	2
Termination	20 generations w/o improvement

We vary the input data along three dimensions: hub operating cost, aircraft operating cost and demand levels. Figures 7.24 – 7.29 demonstrate the results of the variation. It can be seen that:

1. Two-stage operation benefits the system when having lower hub operating cost or higher aircraft operating cost, as was previously concluded in section 6.5.1.
2. Two-stage operation benefits the system at low demand, as described in section 6.5.1.

In Figures 7.25, 7.27 and 7.29, the formation of routes connecting to the interhub route and the percentage of hub sorting cost compared to the total system cost are analyzed. We define $n(\text{Pattern})$ to be a number of flights connecting to the interhub route.

In Figure 7.25 when demand level = 100%, we categorize the route formation into two groups, A and B, where $n(A) = 2$ and $n(B) = 3$. In group A, the two-stage

operation can benefit the system despite low aircraft operating cost (\$7/aircraft-mile) by having only two routes connecting to the interhub route. At \$7/aircraft-mile, having more than two routes would increase hub operating cost and a single-stage would be preferred. In the case of higher aircraft unit operating cost (above \$7), consolidating packages for two-stage operation with three routes, which results in less lower aircraft operating cost, overcomes the additional hub operating cost.

In Figure 7.27 when demand level = 150%, the route formation is classified into three groups, A, B and C, where $n(A) = n(B) = 2$ and $n(C) = 3$. The discussion in Figure 7.25 is also applicable for comparing A and B to C. Although the number of routes connecting to an interhub route is the same for groups A and B, the package flows in case A are less than in case B.

In Figure 7.29 when demand level = 200%, we only find one pattern of route formation, $n(A) = 2$. At higher demand level, diverging routes to consolidate twice is not favorable due to high hub operating cost. It is noted that the hub operating cost depends of the amount of package flows that are consolidated.

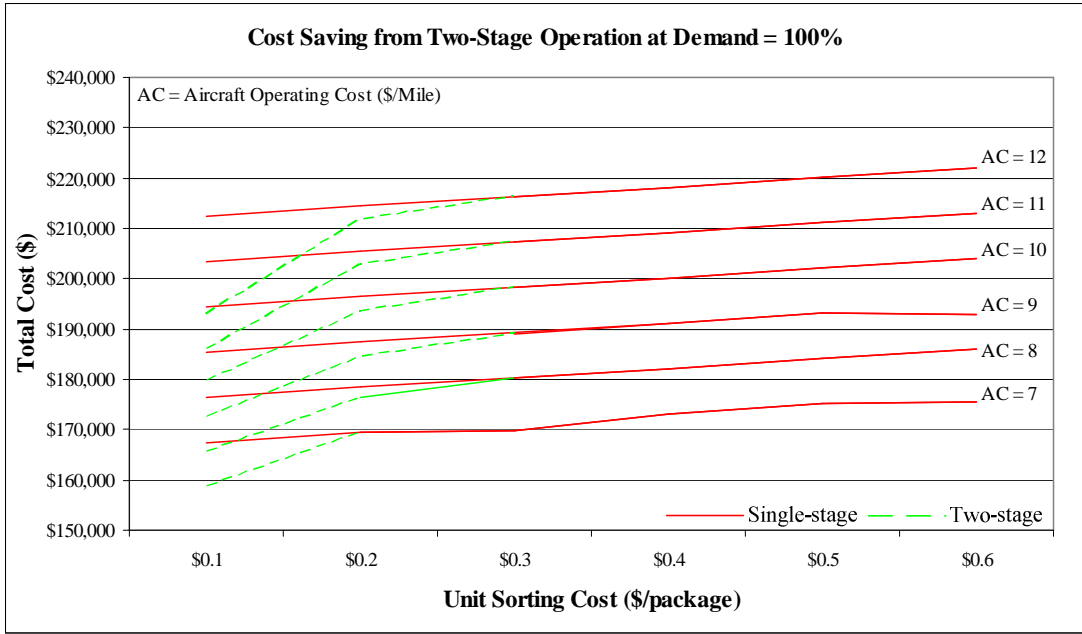


Figure 7.24: Cost saving from two-stage operation at 100% demand

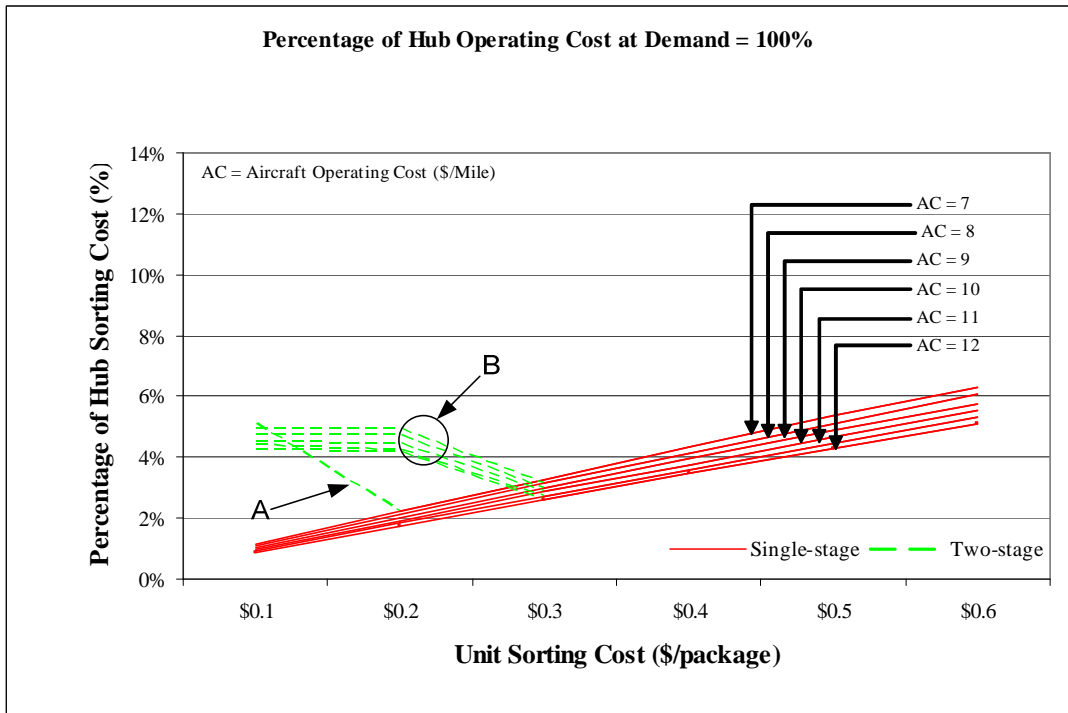


Figure 7.25: Percentage of hub sorting cost at 100% demand

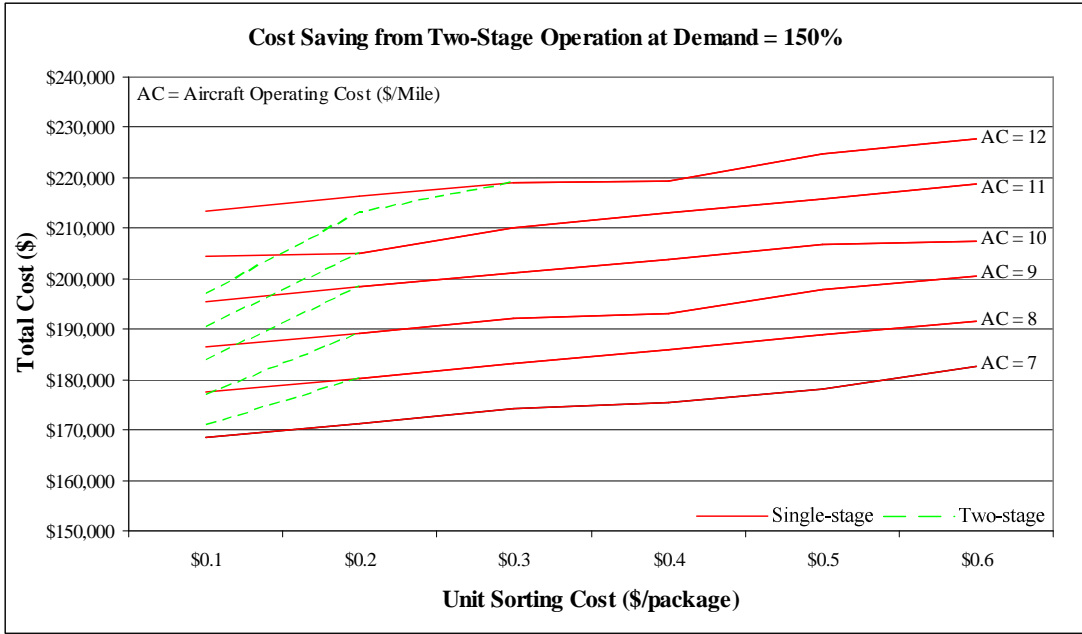


Figure 7.26: Cost saving from two-stage operation at 150% demand

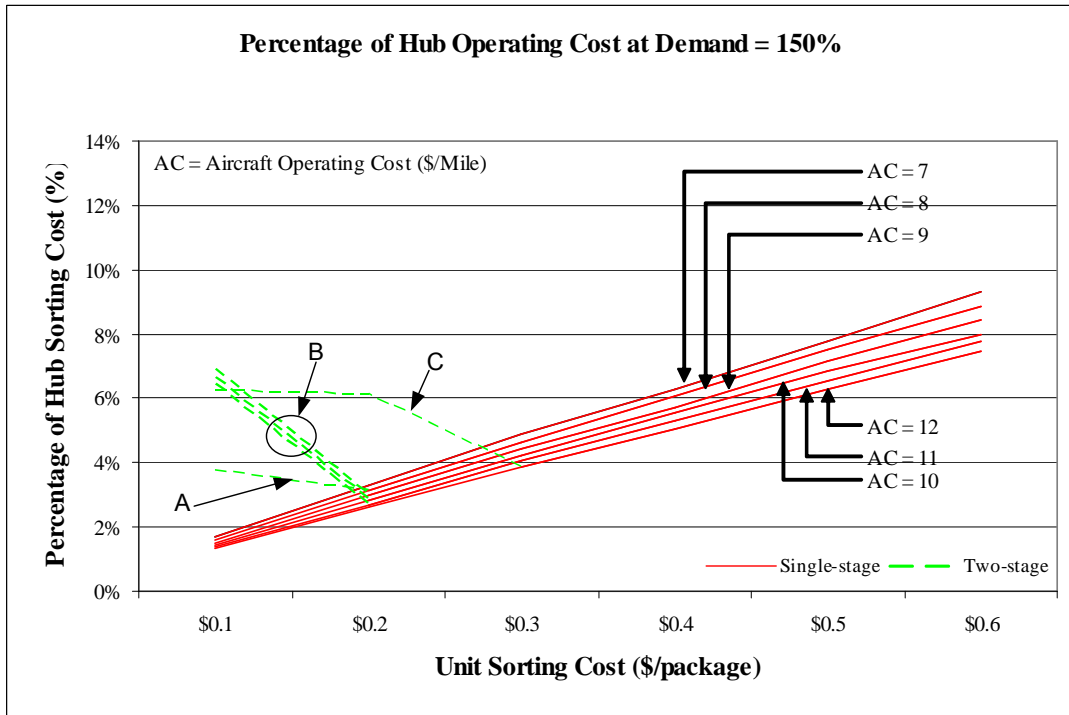


Figure 7.27: Percentage of hub sorting cost at 150% demand

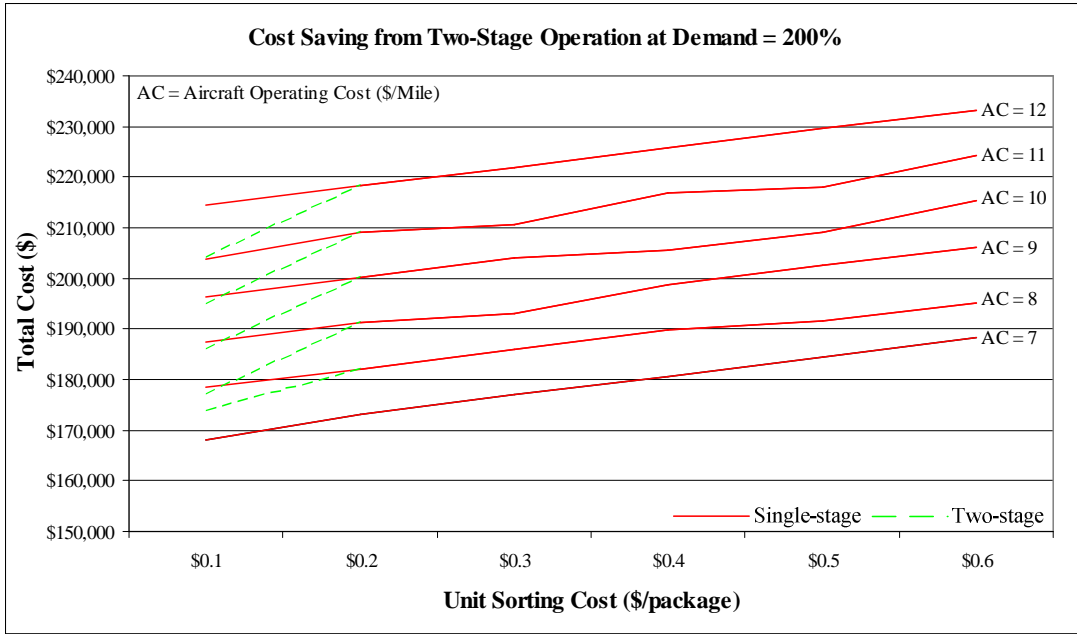


Figure 7.28: Cost saving from two-stage operation at 200% demand

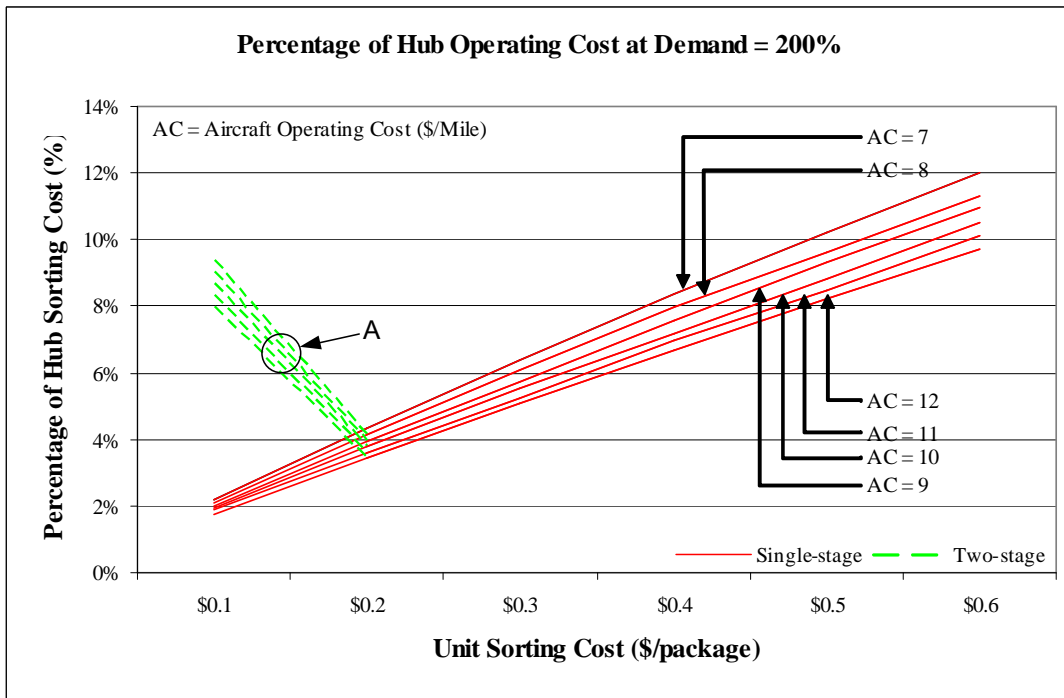


Figure 7.29: Percentage of hub sorting cost at 200% demand

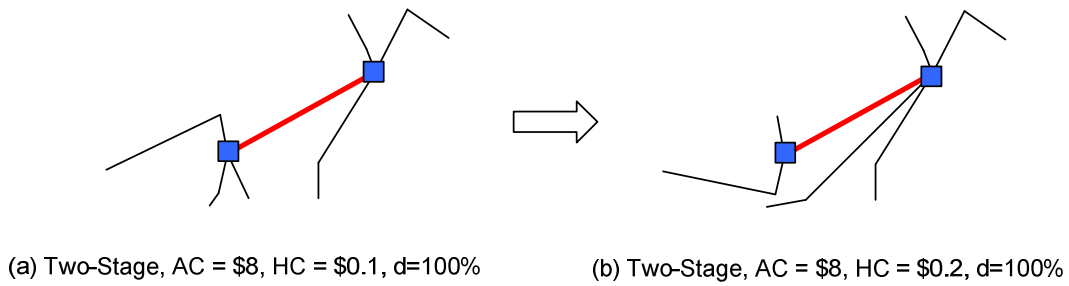


Figure 7.30: Change in two-stage network configuration when unit hub sorting cost increases

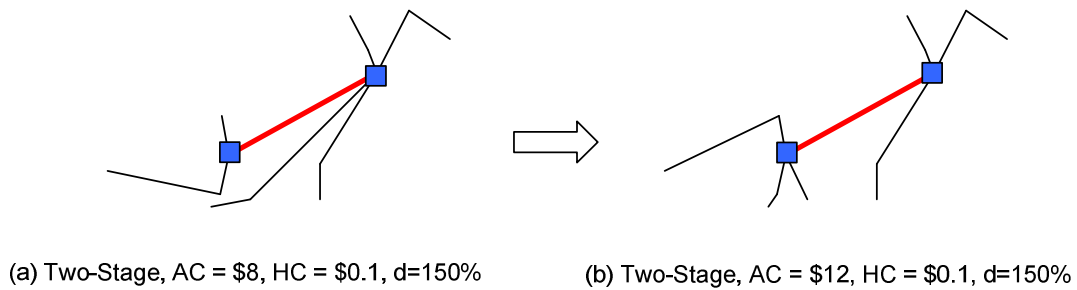


Figure 7.31: Change in two-stage network configuration when unit aircraft operating cost increases

Figures 7.30 and 7.31 depict the change in route formation when (1) unit hub operating cost and (2) unit aircraft operating cost vary, respectively.

We earlier (in section 6.5.1) concluded that the two-stage operation benefits the system when demands are low (comparing to the aircraft capacity). However, as we keep increasing the demand level, we find the savings at demand levels of 1050% (A), 1100% (B), and 1300% (C), as shown in Figure 7.32.

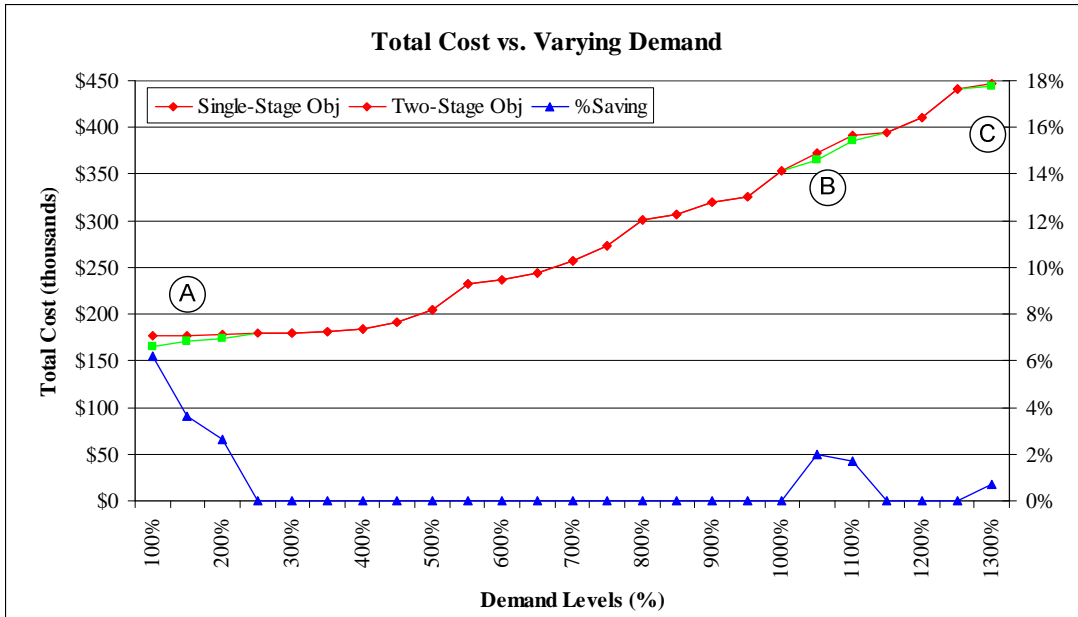


Figure 7.32: Cost saving from two-stage operation as demand increases

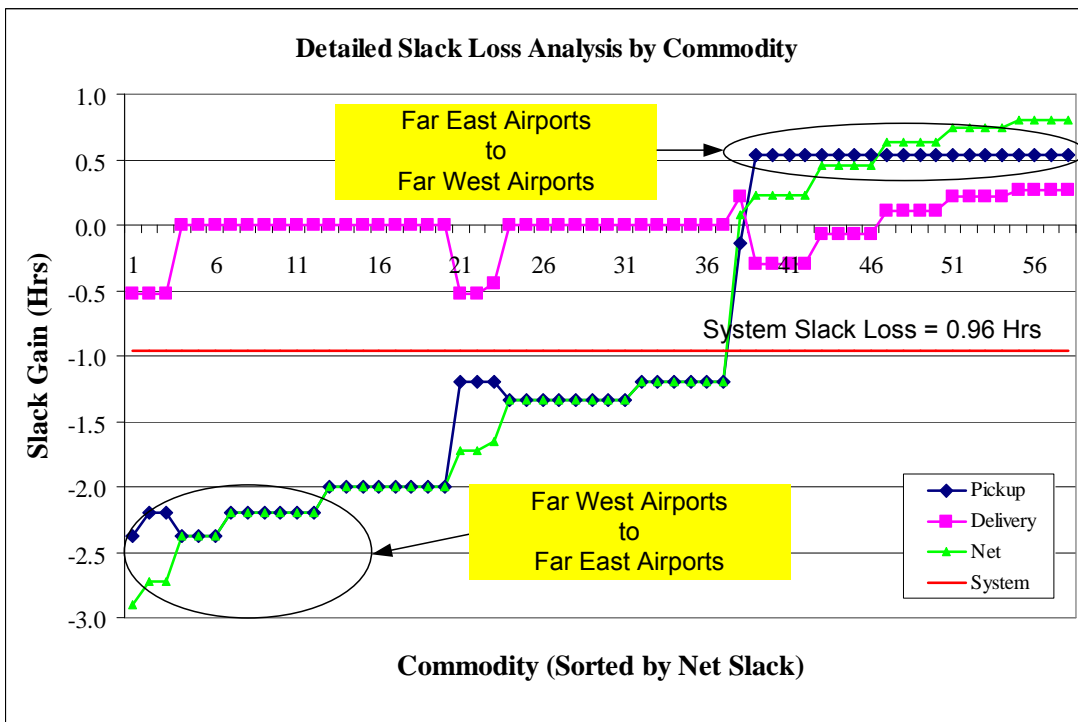


Figure 7.33: Detailed slack gain/loss analysis by commodity

From Figure 7.33, we demonstrate the detailed slack gain/loss by commodity when unit aircraft operating cost = \$10/mile, unit hub sorting cost = \$0.1/package, and demand level = 100%. For side-by-side comparison of operations, we combine the pickup and interhub slacks and represent them as pickup slack. Although the two-stage operation saves about 7.6% of total cost (from Figure 7.24), the overall system slack decreased by about 0.96 hours/package or about 17.5%. The highest slack loss occurs when shipping from Oklahoma City, OK to Detroit, MI with 2.96 hours/package, while we surprisingly gain slack for packages originating in Indianapolis, IN, Chicago, IL, Detroit, MI or Pittsburg, PA to a western destination at El Paso, TX. The gain in slack when shipping from east to west is from the additional slack from interhub route due to the difference in sorting time windows in different time zones.

In addition, the high variation in slack occurs toward pickup portions (including interhub route for two-stage), while the variation in slack on the delivery routes is significantly small. This is quite unsurprising. By using the hub sort end time as the reference point, both single-stage and two-stage operate after this point for delivery routes similarly. On the contrary, before the hub sort end time, the single-stage only consists of pickup routes, while both pickup and interhub routes are operated in two-stage.

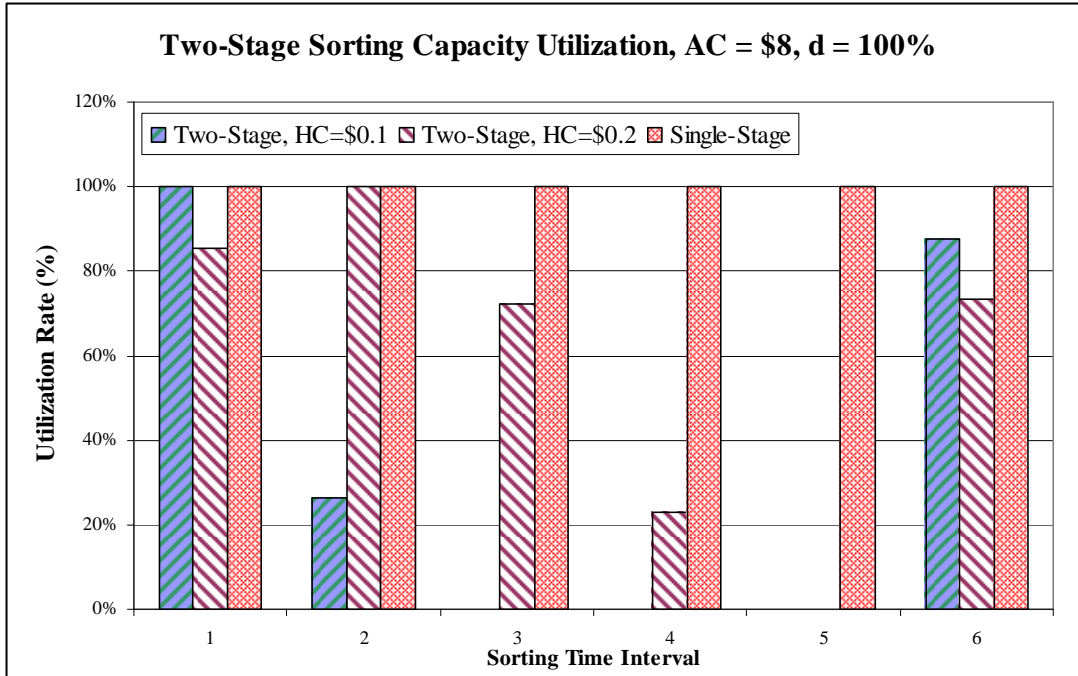


Figure 7.34: Utilization of hub sorting capacity

Figure 7.34 compares the utilization of hub sorting capacities in the two systems. In our study, the utilization of hub sorting capacity is defined as the percentage of sorting capacity used compared to the designed sorting capacity. Given a fixed sorting time window and having an objective to minimize the hub sorting cost, the utilization in the single-stage operation is likely to be constant at 100% because (1) most of packages arrive close to the sort start time (SST) and (2) they have enough sorting time until the sort end time (SET). On the other hand, the utilization of hub sorting capacity for two-stage operation significantly varies from 21% and 41% when unit hub sorting costs are \$0.1/package and \$0.2/package, respectively. This occurs because the system must provide higher than normal capacity to speed up the completion time so that packages can be transported via interhub flights, as expected from Figure 3.11. At a unit hub sorting cost of \$0.1, more packages connect to an

interhub flight than at unit hub sorting cost of \$0.2. Therefore, as more packages connect to interhub flights, the variation in utilization increases.

7.8.2 Case Study 4: 2 Hubs at Louisville, KY and Columbia, SC

In this study, we consider the regional hub in Columbia, SC and its nearby service centers. The purpose of this case study is to explore how slack affects the system when a regional hub is located east of the major hub. Tables 7.9 – 7.11 are the new input data for Case Study 4, while other inputs are as in Case Study 3.

To be able to compare the benefit/impact of the two-stage operation, we select the service centers so that they can benefit from the interhub route. One interesting finding is that the two-stage network requires more service centers to outperform the single-stage one, i.e., 13 service centers compared to 9 in Case Study 3. This is due to lesser distance saving between Louisville, KY and Columbia, SC compared to the greater distance saving between Louisville, KY and Dallas, TX. Figure 7.35 depicts the saving from the two-stage operation for Case Study 4.

Table 7.9: Selected service centers for Case Study 4

No.	Location	EPT	LDT	Longitude	Latitude
1	Indianapolis, IN	8PM	6AM	-86.29	39.73
2	Chicago, IL	8PM	6AM	-87.65	41.9
3	Milwaukee, WI	8PM	6AM	-87.98	43.04
4	Minneapolis, MN	8PM	6AM	-93.36	44.93
5	St. Louis, MO	8PM	6AM	-90.37	38.75
6	Kansas City, MO	8PM	6AM	-94.66	39.22
7	Orlando, FL	8PM	6AM	-81.32	28.43
8	Atlanta, GA	8PM	6AM	-84.42	33.65
9	Jacksonville, FL	8PM	6AM	-81.63	30.35
10	Savannah, GA	8PM	6AM	-81.2	32.13
11	Charlotte, NC	8PM	6AM	-80.93	35.22
12	Charleston, SC	8PM	6AM	-80.03	32.9
13	Tampa, FL	8PM	6AM	-82.53	27.97

Table 7.10: Selected hubs for Case Study 4

No.	Location	SST	SET	Longitude	Latitude
1	Louisville, KY	11PM	3AM	-85.70	38.21
2	Columbia, SC	11PM	3AM	-81.12	33.95

Note: All times are local standard times.

Table 7.11: O/D demand matrix for Case Study 4

	(1)	(2)	(3)	(4)	(5)	(6)	(7)	(8)	(9)	(10)	(11)	(12)	(13)
(1)	0	0	0	771	0	0	1,284	0	672	102	0	204	1,281
(2)	0	0	0	0	0	0	143	1,341	201	166	527	216	434
(3)	0	0	0	0	0	0	200	807	1,249	313	763	238	908
(4)	714	0	0	0	0	0	306	149	1,194	157	1,128	1,316	772
(5)	0	0	0	0	0	0	932	0	814	742	625	15	802
(6)	0	0	0	0	0	0	755	234	233	1,379	1,265	524	1,316
(7)	656	1,141	978	1,016	381	881	0	0	0	0	0	0	0
(8)	0	269	1,150	397	0	750	0	0	0	0	0	0	0
(9)	269	189	253	1,389	526	1,200	0	0	0	0	0	0	0
(10)	416	1,167	579	517	1,417	648	0	0	0	0	0	0	0
(11)	0	1,388	1,161	161	162	184	0	0	0	0	0	0	760
(12)	1,158	1,442	762	872	1,203	1,388	0	0	0	0	0	0	0
(13)	190	1,094	1,003	361	1,096	1,006	0	0	0	0	621	0	0

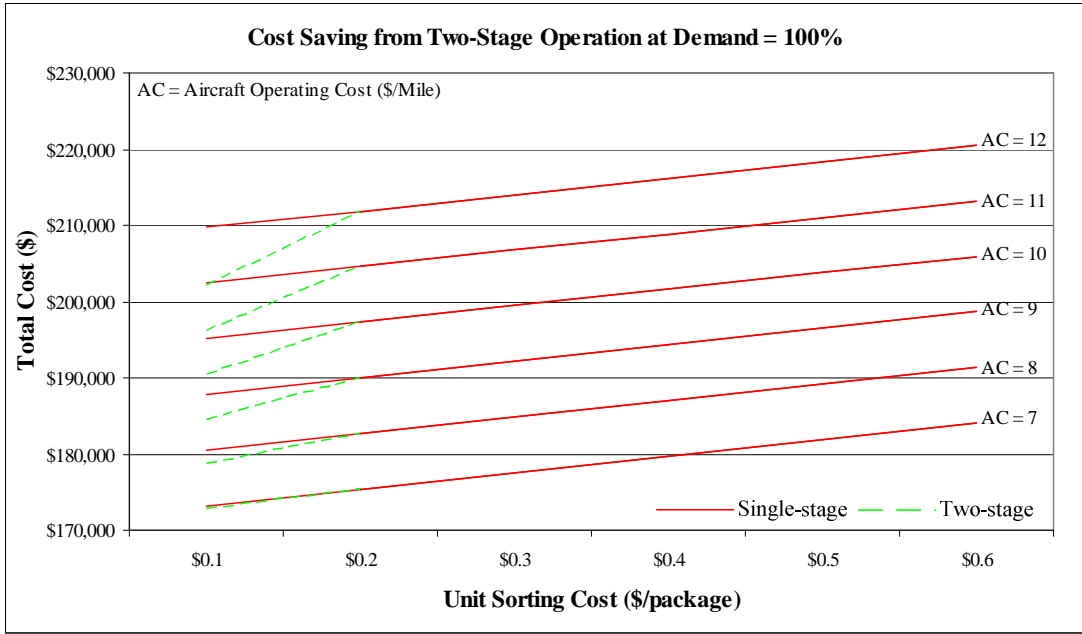


Figure 7.35: Cost saving from two-stage operation for Case Study 4

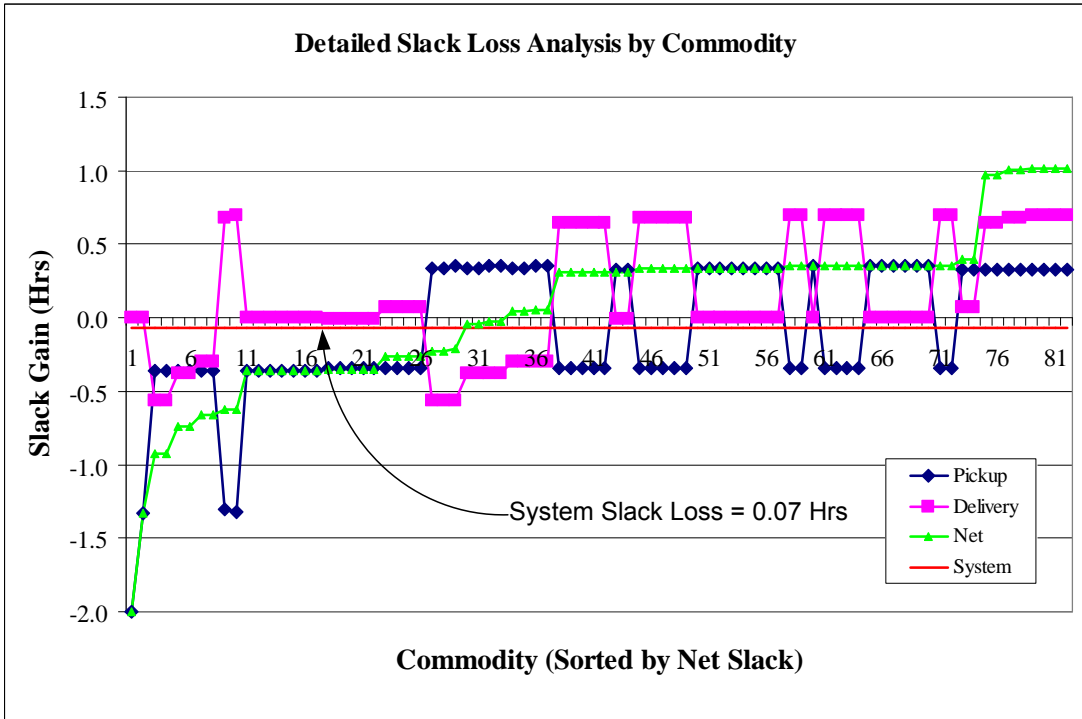


Figure 7.36: Detailed slack gain/loss analysis by commodity, Case Study 4

Figure 7.36 demonstrates the detailed slack analysis for a unit aircraft operating cost = \$10/mile, and a unit hub sorting cost = \$0.1/package. We find another interesting point in slack loss when the regional hub is located east of the main hub. In Case Study 4, the two-stage operation yields a small loss in slack of about 0.07 hours/package or 1%. This is significantly less than for Case Study 3.

7.9 Summary

In this chapter, we present the Genetic Algorithm for solving the air express network design problem, including both single and two-stage operation. The model representation consists of two parts: grouping representation and aircraft route representation. The first representation controls the search space by means of the hub assignment problem, while the second is used to determine the optimal network design according to the grouping representation. Several operators are developed for both representations to facilitate the search. Due to the complexity in forming the two-stage operation, user-defined interhub routing is considered to guide the search. The model also captures several operational practices, including aircraft balancing at each service center and hub, aircraft availability, hub sorting capacity and storage size. In addition, post-solution analysis was introduced to determine system slack. Importantly, the GA model demonstrates significantly less computational time and is able to find a good optimal solution compared to the exact model using the Column Generation Approach.

Chapter 8

Large System Computational Analyses

In chapters 6 and 7, two different solution approaches, namely column generation and GA, were exploited to analyze the possible benefits of two-stage operation in small problems. In the performance comparison of the two approaches in section 7.7, a good optimal solution is obtained with significantly less computational time when employing the GA model. In this chapter, we apply the GA approach to solve relatively large problems using the data from the top 150 metropolitan areas in the United States, as shown in Table 8.1. It is noted that the longitude and latitude in Table 8.1 indicate the nearest airport location to that particular metropolitan area.

The objectives of solving these large problems are:

1. To illustrate the applicability and reasonableness of the GA model developed in the previous chapter.
2. To verify the findings from the small problem and gain more insights on the effects of two-stage operation in a larger network.

Section 8.1 outlines the computational analyses and inputs of this chapter. We first demonstrate the computation performance by varying the network size in section 8.2. A numerical example is then analyzed using the single two-stage routing strategy in section 8.3, in which there are interhub flights only from one regional hub to the main hub. The multiple two-stage routing strategy is considered in section 8.4. Additional analyses are performed for different aircraft mix and demand levels in section 8.5, and the impacts in economies of scale by aircraft mix in section 8.6. The findings are then summarized in section 8.7.

Table 8.1: Top 150 metropolitan areas in the United States

No.	Metropolitan statistical areas	Population	Long.	Lat.
1	New York-Northern New Jersey-Long Island, NY-NJ-PA	18,747,320	-73.78	40.65
2	Los Angeles-Long Beach-Santa Ana, CA	12,923,547	-118.40	33.93
3	Chicago-Naperville-Joliet, IL-IN-WI	9,443,356	-87.65	41.90
4	Philadelphia-Camden-Wilmington, PA-NJ-DE-MD	5,823,233	-75.25	39.88
5	Dallas-Fort Worth-Arlington, TX	5,819,475	-97.03	32.90
6	Miami-Fort Lauderdale-Miami Beach, FL	5,422,200	-80.28	25.82
7	Houston-Sugar Land-Baytown, TX	5,280,077	-95.35	29.97
8	Washington-Arlington-Alexandria, DC-VA-MD-WV	5,214,666	-77.46	38.95
9	Atlanta-Sandy Springs-Marietta, GA	4,917,717	-84.42	33.65
10	Detroit-Warren-Livonia, MI	4,488,335	-83.18	42.33
11	Boston-Cambridge-Quincy, MA-NH	4,411,835	-71.03	42.37
12	San Francisco-Oakland-Fremont, CA	4,152,688	-122.53	37.69
13	Riverside-San Bernardino-Ontario, CA	3,909,954	-117.45	33.95
14	Phoenix-Mesa-Scottsdale, AZ	3,865,077	-112.02	33.43
15	Seattle-Tacoma-Bellevue, WA	3,203,314	-122.30	47.45
16	Minneapolis-St. Paul-Bloomington, MN-WI	3,142,779	-93.36	44.93
17	San Diego-Carlsbad-San Marcos, CA	2,933,462	-117.05	32.70
18	St. Louis, MO-IL	2,778,518	-90.37	38.75
19	Baltimore-Towson, MD	2,655,675	-76.59	39.23
20	Tampa-St. Petersburg-Clearwater, FL	2,647,658	-82.53	27.97
21	Pittsburgh, PA	2,386,074	-80.08	40.43
22	Denver-Aurora, CO1	2,359,994	-104.87	39.75
23	Cleveland-Elyria-Mentor, OH	2,126,318	-81.68	41.50
24	Portland-Vancouver-Beaverton, OR-WA	2,095,861	-122.60	45.60
25	Cincinnati-Middletown, OH-KY-IN	2,070,441	-84.55	39.08
26	Sacramento--Arden-Arcade--Roseville, CA	2,042,283	-121.55	38.61
27	Kansas City, MO-KS	1,947,694	-94.66	39.22
28	Orlando-Kissimmee, FL	1,933,255	-81.33	28.49
29	San Antonio, TX	1,889,797	-98.47	29.53
30	San Jose-Sunnyvale-Santa Clara, CA	1,754,988	-121.92	37.37
31	Las Vegas-Paradise, NV	1,710,551	-115.17	36.08
32	Columbus, OH	1,708,625	-82.88	40.00
33	Virginia Beach-Norfolk-Newport News, VA-NC	1,647,346	-76.28	36.93
34	Indianapolis-Carmel, IN	1,640,591	-86.27	39.73
35	Providence-New Bedford-Fall River, RI-MA	1,622,520	-71.43	41.73
36	Charlotte-Gastonia-Concord, NC-SC	1,521,278	-80.93	35.22
37	Milwaukee-Waukesha-West Allis, WI	1,512,855	-87.98	43.04
38	Austin-Round Rock, TX	1,452,529	-97.70	30.30
39	Nashville-Davidson--Murfreesboro, TN	1,422,544	-86.68	36.12
40	New Orleans-Metairie-Kenner, LA	1,319,367	-90.10	29.95
41	Memphis, TN-MS-AR	1,260,905	-90.00	35.05
42	Jacksonville, FL	1,248,371	-81.63	30.35
43	Louisville-Jefferson County, KY-IN	1,208,452	-85.70	38.21
44	Hartford-West Hartford-East Hartford, CT	1,188,241	-72.65	41.73
45	Richmond, VA	1,175,654	-77.33	37.50
46	Oklahoma City, OK	1,156,812	-97.60	35.40
47	Buffalo-Niagara Falls, NY	1,147,711	-78.73	42.93
48	Birmingham-Hoover, AL	1,090,126	-86.75	33.57
49	Rochester, NY	1,039,028	-77.67	43.12
50	Salt Lake City, UT	1,034,484	-111.97	40.78

Source: Annual Estimates of the Population of Metropolitan and Micropolitan Statistical Areas: April 1, 2000 to July 1, 2005, U.S. Census Bureau

Table 8.1: Top 150 metropolitan area in the United States (Cont.)

No.	Metropolitan statistical areas	Population	Long.	Lat.
51	Raleigh-Cary, NC	949,681	-78.78	35.87
52	Tucson, AZ	924,786	-110.93	32.12
53	Bridgeport-Stamford-Norwalk, CT	902,775	-73.13	41.17
54	Tulsa, OK	887,715	-95.90	36.20
55	Fresno, CA	877,584	-119.72	36.77
56	Albany-Schenectady-Troy, NY	848,879	-73.80	42.75
57	New Haven-Milford, CT	846,766	-72.67	41.22
58	Dayton, OH	843,577	-84.20	39.90
59	Omaha-Council Bluffs, NE-IA	813,170	-95.90	41.30
60	Albuquerque, NM	797,940	-106.60	35.05
61	Oxnard-Thousand Oaks-Ventura, CA	796,106	-119.20	34.20
62	Allentown-Bethlehem-Easton, PA-NJ	790,535	-75.43	40.65
63	Worcester, MA	783,262	-71.87	42.27
64	Grand Rapids-Wyoming, MI	771,185	-85.52	42.88
65	Bakersfield, CA	756,825	-119.05	35.43
66	Baton Rouge, LA	733,802	-91.15	30.53
67	El Paso, TX	721,598	-106.40	31.80
68	Akron, OH	702,235	-81.46	41.04
69	Columbia, SC	689,878	-81.12	33.95
70	Springfield, MA	687,264	-72.53	42.20
71	McAllen-Edinburg-Mission, TX	678,275	-98.23	26.18
72	Greensboro-High Point, NC	674,500	-79.95	36.08
73	Sarasota-Bradenton-Venice, FL	673,035	-82.55	27.40
74	Poughkeepsie-Newburgh-Middletown, NY	667,742	-74.10	41.50
75	Stockton, CA	664,116	-121.25	37.90
76	Toledo, OH	656,696	-83.80	41.60
77	Knoxville, TN	655,400	-83.98	35.82
78	Syracuse, NY	651,763	-76.12	43.12
79	Little Rock-North Little Rock, AR	643,272	-92.15	34.92
80	Charleston-North Charleston, SC	594,899	-80.03	32.90
81	Youngstown-Warren-Boardman, OH-PA	593,168	-80.67	41.27
82	Greenville, SC	591,251	-82.35	34.85
83	Colorado Springs, CO	587,500	-104.72	38.82
84	Wichita, KS	587,055	-97.43	37.65
85	Scranton-Wilkes-Barre, PA	550,546	-75.73	41.33
86	Cape Coral-Fort Myers, FL	544,758	-81.87	26.58
87	Boise City-Nampa, ID	544,201	-116.22	43.57
88	Lakeland, FL	542,912	-81.95	28.03
89	Madison, WI	537,039	-89.33	43.13
90	Palm Bay-Melbourne-Titusville, FL	531,250	-80.63	28.10
91	Jackson, MS	522,580	-90.08	32.32
92	Des Moines-West Des Moines, IA	522,454	-93.65	41.53
93	Harrisburg-Carlisle, PA	521,812	-77.42	40.37
94	Augusta-Richmond County, GA-SC	520,332	-81.97	33.37
95	Portland-South Portland-Biddeford, ME	514,227	-70.32	43.65
96	Modesto, CA	505,505	-120.95	37.63
97	Chattanooga, TN-GA	492,126	-85.20	35.03
98	Lancaster, PA	490,562	-76.30	40.13
99	Deltona-Daytona Beach-Ormond Beach, FL	490,055	-81.05	29.18
100	Ogden-Clearfield, UT	486,842	-112.02	41.18

Source: Annual Estimates of the Population of Metropolitan and Micropolitan Statistical Areas: April 1, 2000 to July 1, 2005, U.S. Census Bureau

Table 8.1: Top 150 metropolitan area in the United States (Cont.)

No.	Metropolitan statistical areas	Population	Long.	Lat.
101	Santa Rosa-Petaluma, CA	466,477	-122.82	38.52
102	Durham, NC	456,187	-78.78	35.87
103	Lansing-East Lansing, MI	455,315	-84.60	42.77
104	Provo-Orem, UT	452,851	-111.72	40.22
105	Winston-Salem, NC	448,629	-80.23	36.13
106	Flint, MI	443,883	-83.75	42.97
107	Spokane, WA	440,706	-117.53	47.63
108	Pensacola-Ferry Pass-Brent, FL	439,877	-87.32	30.35
109	Lexington-Fayette, KY	429,889	-85.00	38.05
110	Corpus Christi, TX	413,553	-97.50	27.77
111	Salinas, CA	412,104	-121.60	36.67
112	Vallejo-Fairfield, CA	411,593	-122.28	38.21
113	Visalia-Porterville, CA	410,874	-119.40	36.32
114	Canton-Massillon, OH	409,996	-81.43	40.92
115	York-Hanover, PA	408,801	-76.73	39.96
116	Fayetteville-Springdale-Rogers, AR-MO	405,101	-94.17	36.00
117	Fort Wayne, IN	404,414	-85.20	41.00
118	Mobile, AL	401,427	-88.25	30.68
119	Manchester-Nashua, NH	401,291	-71.43	42.93
120	Santa Barbara-Santa Maria, CA	400,762	-119.83	34.43
121	Springfield, MO	398,124	-93.38	37.23
122	Reading, PA	396,314	-75.97	40.38
123	Reno-Sparks, NV	393,946	-119.78	39.50
124	Asheville, NC	392,831	-82.55	35.43
125	Beaumont-Port Arthur, TX	383,530	-94.02	30.58
126	Shreveport-Bossier City, LA	383,233	-93.75	32.52
127	Port St. Lucie-Fort Pierce, FL	381,033	-80.37	27.50
128	Brownsville-Harlingen, TX	378,311	-97.43	25.90
129	Davenport-Moline-Rock Island, IA-IL	376,309	-90.52	41.45
130	Salem, OR	375,560	-123.00	44.92
131	Peoria, IL	369,161	-89.68	40.67
132	Huntsville, AL	368,661	-86.77	34.65
133	Trenton-Ewing, NJ	366,256	-74.82	40.28
134	Montgomery, AL	357,244	-86.40	32.30
135	Hickory-Lenoir-Morganton, NC	355,654	-81.38	35.75
136	Killeen-Temple-Fort Hood, TX	351,528	-97.68	31.08
137	Anchorage, AK	351,049	-150.02	61.17
138	Evansville, IN-KY	349,543	-87.53	38.05
139	Fayetteville, NC	345,536	-78.88	35.00
140	Ann Arbor, MI	341,847	-83.75	42.22
141	Rockford, IL	339,178	-89.10	42.20
142	Eugene-Springfield, OR	335,180	-123.22	44.12
143	Tallahassee, FL	334,886	-84.37	30.38
144	Kalamazoo-Portage, MI	319,348	-85.55	42.23
145	South Bend-Mishawaka, IN-MI	318,156	-86.32	41.70
146	Wilmington, NC	315,144	-77.92	34.27
147	Savannah, GA	313,883	-81.20	32.13
148	Naples-Marco Island, FL	307,242	-81.80	26.13
149	Charleston, WV	306,435	-81.60	38.37
150	Ocala, FL	303,442	-82.22	29.17

Source: Annual Estimates of the Population of Metropolitan and Micropolitan Statistical Areas: April 1, 2000 to July 1, 2005, U.S. Census Bureau

8.1 Outline of Computational Analyses and Inputs

According to the UPS 2005 Annual Report, the average daily package volume for next day air is 1.23 millions, with a 3.4% increase compared to year 2004. In sections 8.3, we compare the single-stage operation to the two-stage operation, in which the single two-stage routing is considered. A scenario of the UPS network is analyzed using the top 100 locations from Table 8.1 by assuming 0.8 million total daily packages, respectively. After analyzing the potential cost saving of individual regional hubs, the two-stage operation with multiple two-stage routings to the promising regional hubs is considered in section 8.4, in which five scenarios with different demand levels, ranging from 0.8 million to 1.2 million are analyzed. In section 8.5, impacts of congested networks and aircraft mix on the two systems are examined on the randomly selected 40 locations from Table 8.1. Using the same selected 40 service centers, additional tests are performed to better understand the effects of economies of scale in aircraft in section 8.6.

O/D demand matrices are generated for each case, with the following characteristics:

1. A gravity model is used to generate demand of each O/D pair by assuming the total number of packages shipping through the distribution network to be Q .
2. As in current practice, whenever packages can be transported via ground service without jeopardizing their critical time requirements, we exclude those packages from the air network. In this study, those OD flows with distances under 400 miles are neglected.
3. Hub demands are excluded from this study.

From (1) and (2), let l_k and d_k be the distance between commodity k and its demand, respectively. Let P_i be the number of population in metropolitan area i . We have

$$\sum_{k \in K} \alpha \beta_k P_{O(k)} P_{D(k)} = \sum_{k \in K} d^k = Q \quad (8.1)$$

where

α = Constant factor that meets equation 8.1

β_k = 1 if $l_k \geq 400$, 0 otherwise

$O(k)$ = Origin of commodity k

$D(k)$ = Destination of commodity k

The UPS air hubs within the United States are located in Louisville, KY (main US hub), Philadelphia, PA, Dallas, TX, Ontario, CA, Rockford, IL, Columbia, SC, and Hartford, CT. In this study, we consider 5 hubs, which are located quite far apart, as shown in Table 8.2. The earliest pickup time (EPT) and latest delivery time (LDT) for all service centers by time zones are shown in Table 8.3. Table 8.4 provides the input data for aircraft characteristics, in which aircraft types 1 and 2 represent Boeing 757-200 and 747-400, respectively. Because the available information about the maximum payload is in pound units and this entire analysis focuses on number of packages, we obtain the aircraft capacity by assuming an average weight of 5 lbs/package. Table 8.5 shows the GA input parameters in this analysis.

Table 8.2: UPS hub locations for Case Study 5

No.	Location	SST	SET	Longitude	Latitude
1	Louisville, KY	11PM	5AM	-85.70	38.21
2	Philadelphia, PA	11PM	5AM	-75.25	39.88
3	Columbia, SC	11PM	5AM	-81.12	33.95
4	Dallas, TX	10PM	5AM	-97.03	32.90
5	Ontario, CA	8PM	5AM	-117.45	33.95

Note: All times are local standard times.

Table 8.3: Hub characteristics for Case Study 5

Hub No.	1	2-4
Unit sorting cost, c_e^h (\$/package)	\$0.10	\$0.10
Unit storage cost, c_s^h (\$/package)	\$0.02	\$0.02
Landing capacity (#aircraft/hour)	80	40
Take-off capacity (#aircraft/hour)	100	50

Table 8.4: EPT and LDT for Case Study 5

No.	Time Zone	EPT	LDT
1	EST	8PM	8AM
2	CST	7PM	8AM
3	MST	6PM	8AM
4	PST	5PM	8AM

Note: All times are local standard times.

Table 8.5: Aircraft characteristics for Case Study 5

Aircraft Type No.	1	2
Availability	300	50
Capacity (packages)	16,000	50,000
Max. Flying Range ¹ (mi.)	3,600	5,600
Avg. Cruising Speed (mph)	550	550
Aircraft Loading/Unloading Time (min)	30	30
Operating Cost/mile	\$9	\$24
Take-Off/Landing Cost	\$300	\$600
Ownership Cost/Day/Aircraft	\$16,000	\$44,000

¹ Maximum flying distance at the maximum payload

Table 8.6: GA parameters for Case Study 5

Population Size	10
#Population for grouping crossover, r_1	2
#Population for grouping mutation, r_2	2
#Population for randomly mutate, n	1
#Population for best mutate, m	1
Termination	20 generations w/o improvement

In this study, for investigating the potential saving of interhub flights between all regional hubs and major hubs, we extend the sorting time window to ensure the connectivity of flights between hubs and having enough time to sort packages. For example, the sorting time of the Ontario, CA hub begins early so that, including the flight time, the interhub flight can meet the sort end time at Louisville, KY. In addition, we ensure that all interhub flights arrive at the downstream hubs at least one hour before the sort end time.

In this chapter, all runs are performed on Pentium 4, 3.2 GHz with 2 GB Ram and UNIX Sun Sparc V250. Due to of sharing resources in the UNIX system, all computational times are reported using Pentium 4 runs.

8.2 Computational Performance

To demonstrate the computational performance when varying the network size, the following input characteristics are used in the test:

- To consider only the effect of the network size, we distribute the demand at each service center equally – without considering the gravity model as described in section 8.1. In addition, to have an unconstrained interhub capacity environment, we set $u_i = 150,000$ packages so that all packages can be transported via interhub flights if that optimizes the system cost.

- To compare the single-stage and two-stage operations, a two-hub network is considered, with hubs at Louisville, KY and Columbia, SC.

Figure 8.1 compares the computational performance of the two operations at various network sizes. The computation time is the average time on 5 different runs on Pentium 4, with 3.2 GHz and 2 GB Ram. The results indicate that the run times increase more than linearly with network size. The run times for two-stage operation generally exceed those of single-stage operations by approximately 25-45%.

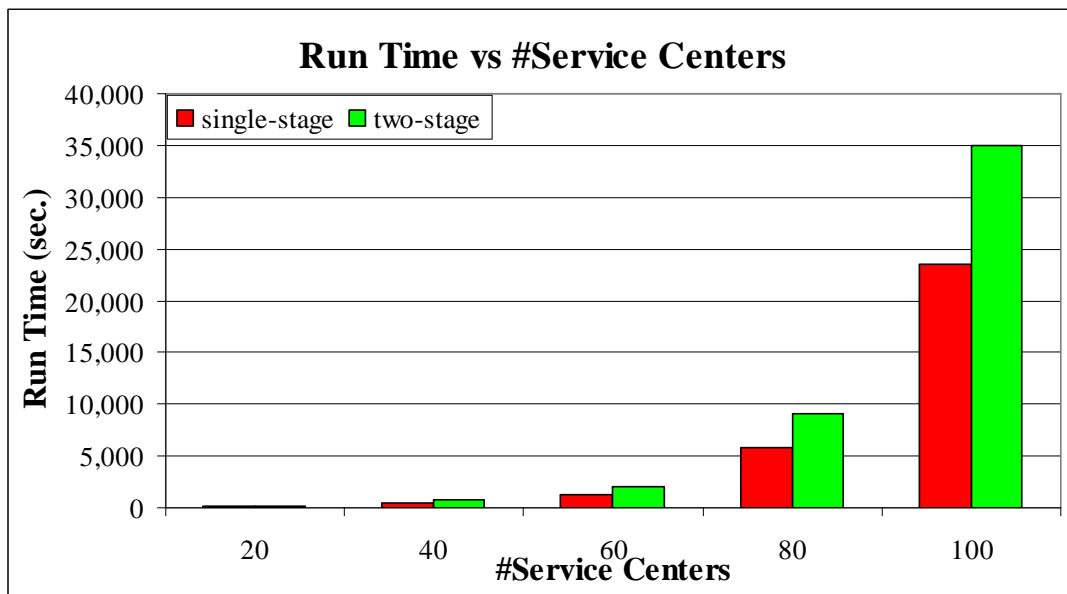


Figure 8.1: Computational performance vs. network size

8.3 Case Study 5: Single Location Two-stage Operation

In this analysis, we determine the optimal distribution network using the top 100 locations from Table 8.1 with 0.8 million total packages. We analyze different interhub routing strategies and vary their interhub capacity for two-stage operations. The optimal solution of each scenario is extracted to compare the cost elements and system characteristics to the single-stage one. Several routing strategies for interhub

flights are tested by varying the location of regional hubs, in which all routes are originated/destined from the main hub location, i.e., at Louisville, KY. The interhub flights' capacities, u_l , are varied to verify the utilization of interhub flight until finding the unconstrained capacity environment, i.e., the load factor of interhub flights is below 100%.

In this section, we focus on determining a *single location* two-stage operation with two pre-selected hubs, in which there are only interhub flights between one specific regional hub and the main hub. The objective is to analyze the effects of two-stage operation for each regional hub location. Later in this chapter, a *multiple location* two-stage operation will be examined.

Tables 8.7 – 8.10 compare the optimal solutions of single-stage operation to two-stage operations by varying interhub routing strategies and its capacities. The analyses first examine a single location two-stage operation from the furthest eastern regional hub to the furthest western hubs respectively, i.e., from the Philadelphia hub to the Ontario hub. For easy reference, we denote the interhub routing between Louisville, KY and Philadelphia, PA as KY-PA, and so on. It is noted that, in each case, the result shown is the best optimal solution found from 10 different replications.

In Tables 8.7 – 8.10, the information is divided into eight blocks. The first block, row 1 – 4, presents the total and detailed cost distribution, including aircraft cost and hub operating cost. The second block, row 5 – 7, presents the system's utilization by means of package-miles, capacity-miles and the resulting load factor. The third block, row 8 – 10, demonstrates another insight into the aircraft utilization

by means of the number of aircraft legs per aircraft (Avg. Legs/Aircraft). The fourth block, row 11 – 13, shows the resulting system slack by post-solution analysis. For comparison with single-stage operation, the interhub slacks are included in the pickup slack. The fifth block (row 14 – 19) and the sixth block (row 20 – 25) present the hubs' designed capacity and their associated utilization. It is noted that the hub utilization is the percentage of capacity usage compared to the maximum designed capacity over time. The last block, row 26 – 27, indicates the average solution time required to solve the GA model until satisfying the termination criteria, i.e., no improvement within 20 generations. In addition, they show the variation in optimal solution among different runs by means of the coefficient of variation.

The detailed slack loss analyses by O/D zones are provided in Tables 8.11 – 8.14 for each interhub routing alternative, while Figures 8.2 – 8.6 demonstrate the resulting optimized network configurations for single-stage and various two-stage operations.

Table 8.7: Scenario analysis: UPS network with 100 SCs, $Q = 0.8M$ packages, and two-stage KY-PA routing

Operational Type	Single-stage	Two-stage: KY-PA					
		$u_I = 50,000$	%Chg	$u_I = 100,000$	%Chg	$u_I = 150,000$	%Chg
Total daily operating cost (TDOC)	\$2,533,590	\$2,594,280	2.4%	\$2,552,960	0.8%	\$2,550,610	0.7%
• Aircraft ownership cost	\$1,168,000	\$1,168,000	0.0%	\$1,152,000	-1.4%	\$1,164,000	-0.3%
• Aircraft operating cost	\$1,344,830	\$1,397,491	3.9%	\$1,364,717	1.5%	\$1,338,603	-0.5%
• Hub operating cost	\$20,760	\$28,789	38.7%	\$36,243	74.6%	\$48,007	131.2%
Load Factor	63%	61%	-2.3%	62%	-1.6%	64%	0.3%
• Package-Miles	1,462	1,465	0.2%	1,454	-0.5%	1,476	1.0%
• Capacity-Miles	2,306	2,399	4.0%	2,353	2.0%	2,318	0.5%
#Legs	256	244	-4.7%	238	-7.0%	232	-9.4%
#Aircraft	62/4	62/4		61/4		59/5	
Avg. Legs/Aircraft Day	3.88	3.70	-4.7%	3.66	-5.6%	3.63	-6.5%
Slack (hours/package)	6.1	2.82	-54%	3.23	-47%	3.37	-45%
• Pickup	5.02	1.72	-66%	2.04	-59%	2.16	-57%
• Delivery	1.08	1.09	1%	1.19	10%	1.21	12%
Hub sorting capacity							
• Louisville, KY	110,459	148,780	35%	167,913	52%	243,263	120%
• Philadelphia, PA	1,800	70,000	3789%	137,789	7555%	207,977	11454%
• Columbia, SC	21,081	12,753	-40%	9,928	-53%	8,438	-60%
• Dallas, TX	0	0	NA	0	NA	0	NA
• Ontario, CA	0	0	NA	0	NA	0	NA
Hub sorting utilization							
• Louisville, KY	100%	81%	-19%	74%	-26%	51%	-49%
• Philadelphia, PA	100%	24%	-76%	24%	-76%	25%	-75%
• Columbia, SC	100%	100%	0%	83%	-17%	82%	-18%
• Dallas, TX	0%	0%	0%	0%	0%	0%	0%
• Ontario, CA	0%	0%	0%	0%	0%	0%	0%
Avg. Run Time (Hrs.)	9.5	11.9	25%	12.3	29%	12	26%
TDOC Coefficient of Variation (%)	1.9%	1.7%	-0.2%	1.1%	-0.8%	1.4%	-0.5%

Table 8.8: Scenario analysis: UPS network with 100 SCs, $Q = 0.8M$ packages, and two-stage KY-SC routing

Operational Type	Single-stage	Two-stage: KY-SC					
		$u_I = 50,000$	%Chg	$u_I = 100,000$	%Chg	$u_I = 150,000$	%Chg
Total daily operating cost (TDOC)	\$2,533,590	\$2,503,010	-1.2%	\$2,472,690	-2.4%	\$2,459,350	-2.9%
• Aircraft ownership cost	\$1,168,000	\$1,144,000	-2.1%	\$1,128,000	-3.4%	\$1,124,000	-3.8%
• Aircraft operating cost	\$1,344,830	\$1,331,655	-1.0%	\$1,311,348	-2.5%	\$1,296,944	-3.6%
• Hub operating cost	\$20,760	\$27,355	31.8%	\$33,342	60.6%	\$38,406	85.0%
Load Factor	63%	65%	1.3%	67%	3.6%	67%	3.6%
• Package-Miles	1,462	1,465	0.2%	1,498	2.5%	1,490	1.9%
• Capacity-Miles	2,306	2,264	-1.8%	2,237	-3.0%	2,224	-3.6%
#Legs	256	264	3.1%	256	0.0%	252	-1.6%
#Aircraft	62/4	66/2		65/2		62/3	
Avg. Legs/Aircraft Day	3.88	3.88	0.1%	3.82	-1.5%	3.88	0.0%
Slack (hours/package)	6.1	3.23	-47%	3.6	-41%	3.31	-46%
• Pickup	5.02	2.17	-57%	2.6	-48%	2.29	-54%
• Delivery	1.08	1.06	-2%	1	-7%	1.02	-6%
Hub sorting capacity							
• Louisville, KY	110,459	125,843	14%	152,740	38%	186,631	69%
• Philadelphia, PA	1,800	8,878	393%	17,878	893%	0	-100%
• Columbia, SC	21,081	75,128	256%	122,248	480%	164,356	680%
• Dallas, TX	0	0	NA	0	NA	0	NA
• Ontario, CA	0	0	NA	0	NA	0	NA
Hub sorting utilization							
• Louisville, KY	100%	93%	-7%	72%	-28%	66%	-34%
• Philadelphia, PA	100%	80%	-20%	100%	0%	0%	-100%
• Columbia, SC	100%	34%	-66%	29%	-71%	31%	-69%
• Dallas, TX	0%	0%	0%	0%	0%	0%	0%
• Ontario, CA	0%	0%	0%	0%	0%	0%	0%
Avg. Run Time (Hrs.)	9.5	10.5	11%	10.9	15%	11.8	24%
TDOC Coefficient of Variation (%)	1.9%	0.8%	-1.1%	1.4%	-0.5%	1.0%	-0.9%

Table 8.9: Scenario analysis: UPS network with 100 SCs, $Q = 0.8M$ packages, and two-stage KY-TX routing

Operational Type	Single-stage	Two-stage: KY-TX					
		$u_I = 50,000$	%Chg	$u_I = 100,000$	%Chg	$u_I = 150,000$	%Chg
Total daily operating cost (TDOC)	\$2,533,590	\$2,603,360	2.8%	\$2,521,690	-0.5%	\$2,468,180	-2.6%
• Aircraft ownership cost	\$1,168,000	\$1,200,000	2.7%	\$1,132,000	-3.1%	\$1,160,000	-0.7%
• Aircraft operating cost	\$1,344,830	\$1,374,622	2.2%	\$1,353,236	0.6%	\$1,260,085	-6.3%
• Hub operating cost	\$20,760	\$28,738	38.4%	\$36,454	75.6%	\$48,095	131.7%
Load Factor	63%	64%	0.8%	66%	2.4%	70%	6.2%
• Package-Miles	1,462	1,500	2.6%	1,506	3.0%	1,489	1.8%
• Capacity-Miles	2,306	2,337	1.3%	2,287	-0.8%	2,140	-7.2%
#Legs	256	262	2.3%	270	5.5%	258	0.8%
#Aircraft	62/4	64/4		68/1		67/2	
Avg. Legs/Aircraft Day	3.88	3.85	-0.7%	3.91	0.9%	3.74	-3.6%
Slack (hours/package)	6.1	3.71	-39%	3.54	-42%	3.95	-35%
• Pickup	5.02	2.72	-46%	2.62	-48%	3.02	-40%
• Delivery	1.08	1	-7%	0.92	-15%	0.93	-14%
Hub sorting capacity							
• Louisville, KY	110,459	115,323	4%	128,571	16%	192,857	75%
• Philadelphia, PA	1,800	7,280	304%	9,653	436%	18,478	927%
• Columbia, SC	21,081	15,566	-26%	13,441	-36%	5,333	-75%
• Dallas, TX	0	79,655	NA	148,577	NA	210,920	NA
• Ontario, CA	0	0	NA	0	NA	0	NA
Hub sorting utilization							
• Louisville, KY	100%	95%	-5%	82%	-18%	53%	-47%
• Philadelphia, PA	100%	100%	0%	100%	0%	100%	0%
• Columbia, SC	100%	100%	0%	100%	0%	84%	-16%
• Dallas, TX	0%	12%	12%	15%	15%	16%	16%
• Ontario, CA	0%	0%	0%	0%	0%	0%	0%
Avg. Run Time (Hrs.)	9.5	10.9	15%	12.4	31%	14.7	55%
TDOC Coefficient of Variation (%)	1.9%	1.5%	-0.4%	1.8%	-0.1%	0.8%	-1.1%

Table 8.10: Scenario analysis: UPS network with 100 SCs, $Q = 0.8M$ packages, and two-stage KY-CA routing

Operational Type	Single-stage	Two-stage: KY-CA					
		$u_I = 50,000$	%Chg	$u_I = 100,000$	%Chg	$u_I = 150,000$	%Chg
Total daily operating cost (TDOC)	\$2,533,590	\$2,504,670	-1.1%	\$2,507,020	-1.0%	\$2,528,050	-0.2%
• Aircraft ownership cost	\$1,168,000	\$1,160,000	-0.7%	\$1,188,000	1.7%	\$1,164,000	-0.3%
• Aircraft operating cost	\$1,344,830	\$1,308,985	-2.7%	\$1,268,646	-5.7%	\$1,300,059	-3.3%
• Hub operating cost	\$20,760	\$35,685	71.9%	\$50,374	142.6%	\$63,991	208.2%
Load Factor	63%	67%	3.3%	68%	4.8%	65%	1.1%
• Package-Miles	1,462	1,482	1.4%	1,485	1.6%	1,471	0.6%
• Capacity-Miles	2,306	2,221	-3.7%	2,177	-5.6%	2,279	-1.2%
#Legs	256	258	0.8%	262	2.3%	242	-5.5%
#Aircraft	62/4	67/2		66/3		59/5	
Avg. Legs/Aircraft Day	3.88	3.74	-3.6%	3.80	-2.1%	3.78	-2.5%
Slack (hours/package)	6.1	3.99	-35%	3.94	-35%	3.81	-38%
• Pickup	5.02	2.94	-41%	2.97	-41%	2.78	-45%
• Delivery	1.08	1.05	-3%	0.97	-10%	1.03	-5%
Hub sorting capacity							
• Louisville, KY	110,459	120,000	9%	122,242	11%	169,599	54%
• Philadelphia, PA	1,800	14,777	721%	7,118	295%	14,476	704%
• Columbia, SC	21,081	5,090	-76%	15,348	-27%	0	-100%
• Dallas, TX	0	0	NA	0	NA	0	NA
• Ontario, CA	0	140,892	NA	285,539	NA	395,843	NA
Hub sorting utilization							
• Louisville, KY	100%	95%	-5%	90%	-10%	70%	-30%
• Philadelphia, PA	100%	100%	0%	100%	0%	100%	0%
• Columbia, SC	100%	83%	-17%	100%	0%	0%	-100%
• Dallas, TX	0%	0%	0%	0%	0%	0%	0%
• Ontario, CA	0%	6%	6%	6%	6%	6%	6%
Avg. Run Time (Hrs.)	9.5	11.4	20%	11.7	23%	11.5	21%
TDOC Coefficient of Variation (%)	1.9%	1.2%	-0.7%	1.6%	-0.3%	1.1%	-0.8%

Table 8.11: Detailed slack analysis for two-stage operation
(KY-PA, $Q = 0.8M$, $u_i = 150,000$)

O/D Zone	EST		CST		MST		PST		Total	
	Slack	%Chg	Slack	%Chg	Slack	%Chg	Slack	%Chg	Slack	%Chg
EST	4.28	-34%	4.78	-32%	4.52	-38%	4.22	-40%	4.41	-35%
CST	3.02	-49%	3.27	-55%	3.28	-54%	3.04	-56%	3.08	-52%
MST	1.60	-68%	1.94	-68%	1.70	-69%	1.61	-72%	1.68	-69%
PST	1.59	-60%	1.94	-60%	1.86	-61%	1.88	-55%	1.71	-59%
Total	3.06	-45%	3.73	-43%	3.70	-45%	3.60	-46%	3.37	-45%

Note: %Chg indicates the percentage change compared to the slack of a single-stage operation

Table 8.12: Detailed slack analysis for two-stage operation
(KY-SC, $Q = 0.8M$, $u_i = 150,000$)

O/D Zone	EST		CST		MST		PST		Total	
	Slack	%Chg	Slack	%Chg	Slack	%Chg	Slack	%Chg	Slack	%Chg
EST	3.97	-39%	4.66	-34%	4.59	-37%	4.38	-38%	4.30	-37%
CST	3.05	-49%	3.83	-48%	3.64	-49%	3.71	-46%	3.35	-48%
MST	1.56	-68%	2.32	-62%	1.96	-64%	2.08	-64%	1.83	-66%
PST	1.12	-72%	1.94	-59%	1.71	-64%	1.43	-66%	1.38	-67%
Total	2.81	-50%	3.77	-42%	3.80	-44%	3.85	-42%	3.31	-46%

Note: %Chg indicates the percentage change compared to the slack of a single-stage operation

Table 8.13: Detailed slack analysis for two-stage operation
(KY-TX, $Q = 0.8M$, $u_i = 150,000$)

O/D Zone	EST		CST		MST		PST		Total	
	Slack	%Chg	Slack	%Chg	Slack	%Chg	Slack	%Chg	Slack	%Chg
EST	4.56	-30%	5.48	-22%	5.43	-25%	4.97	-29%	4.97	-27%
CST	3.75	-37%	4.48	-39%	4.30	-40%	3.91	-43%	3.93	-39%
MST	2.03	-59%	2.50	-59%	1.63	-70%	1.86	-68%	2.10	-61%
PST	2.01	-49%	2.52	-47%	1.98	-58%	2.16	-48%	2.15	-49%
Total	3.50	-37%	4.47	-31%	4.47	-34%	4.31	-36%	3.95	-35%

Note: %Chg indicates the percentage change compared to the slack of a single-stage operation

Table 8.14: Detailed slack analysis for two-stage operation
(KY-CA, $Q = 0.8M$, $u_i = 150,000$)

O/D Zone	EST		CST		MST		PST		Total	
	Slack	%Chg	Slack	%Chg	Slack	%Chg	Slack	%Chg	Slack	%Chg
EST	4.18	-36%	4.83	-31%	4.69	-35%	4.81	-32%	4.55	-33%
CST	3.61	-39%	4.47	-39%	4.30	-40%	4.34	-37%	3.95	-39%
MST	2.09	-58%	3.14	-48%	2.39	-56%	3.18	-45%	2.52	-53%
PST	2.13	-46%	2.70	-43%	2.14	-55%	2.56	-38%	2.31	-45%
Total	3.34	-40%	4.18	-36%	4.10	-39%	4.43	-34%	3.81	-38%

Note: %Chg indicates the percentage change compared to the slack of a single-stage operation



Figure 8.2: Optimized network configuration for single-stage operation,
 $Q = 0.8\text{M}$ packages



Figure 8.3: Optimized network configuration for two-stage operation
 (KY-PA, $Q = 0.8\text{M}$, $u_i = 150,000$)



Figure 8.4: Optimized network configuration for two-stage operation
(KY-SC, $Q = 0.8M$, $u_i = 150,000$)

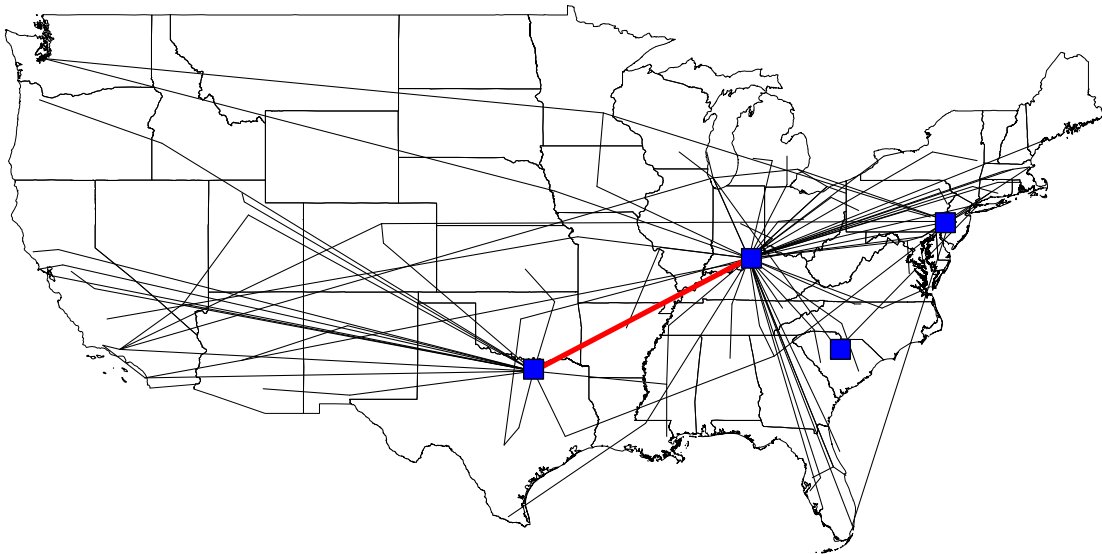


Figure 8.5: Optimized network configuration for two-stage operation
(KY-TX, $Q = 0.8M$, $u_i = 150,000$)

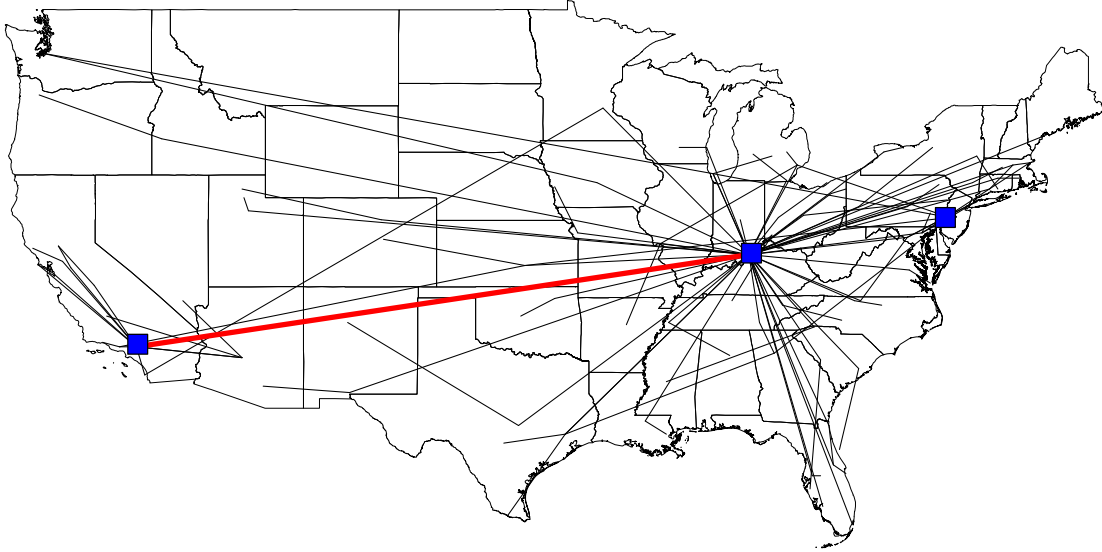


Figure 8.6: Optimized network configuration for two-stage operation
(KY-CA, $Q = 0.8M$, $u_t = 150,000$)

We summarize the findings for each interhub routing by regional hub location as follows:

We summarize the findings for interhub routing alternatives as follows:

1. KY – PA

- a. The two-stage operation performs worse than the single-stage one for all interhub capacities. The total operating cost increases for two reasons. First, because Philadelphia hub is in the same time zone as the main hub, the interhub flight must depart early to meet the sort end time at the downstream hub. As a result, arrival pickup flights at the main hub cannot fully operate two-leg flights, which reduces aircraft utilization – fewer average legs per aircraft. Second, all service centers that can utilize the interhub flights are located east of and quite close to the Philadelphia hub. The

distance saving is insignificant. Therefore, these impacts outweigh the savings from consolidating twice in a two-stage operation.

- b. The reduction in aircraft utilization when operating interhub capacity $u_i \leq 100,000$ reduces load factor compared to the single-stage operation.
- c. The two-stage operation increases the required sorting capacity at both hubs when the interhub flight capacities are increased. When $u_i \geq 100,000$, hub capacity at Philadelphia is almost 80% of the designed hub capacity at the main Louisville hub.
- d. As expected, the hub utilization at the main Louisville hub decreases from 19% to 49% when the interhub capacities are increased. However, the utilization at the Philadelphia hub remains approximately the same.
- e. Operating the proposed system with a regional hub located east of the main hub also reduces the overall system slack by 45%. This reduction is opposite to what we found in the previous chapter due to the dependency on all commodities within the US, instead of just eastern US. From Table 8.11, we find the two-stage operation greatly impacts the slack loss (by 69%) when shipping from the MST zone, while it only reduces the slack when shipping from EST zone by 35%. Surprisingly, we see the slack gain on the delivery routes with a two-stage operation on KY-PA.

2. KY – SC

- a. The two-stage operation provides savings from 1.2% to 2.9% when interhub capacities increase. However, two stages cannot save any more because the load factor of interhub flights is only 81%. A higher interhub capacity, $u_i > 150,000$, will instead increase the total system cost.
- b. The results indicate approximately the same aircraft utilization for single-stage and two-stage operations. Because Columbia is closer than Philadelphia to Louisville, the interhub flight may depart later than the KY-PA flight. This increases opportunities for arrival pickup routes to utilize two-leg flights. In addition, because most service centers connecting to the Columbia hub are quite far from it, there are great distance saving opportunities when applying the two-stage operation. Therefore, two-stage operation is quite desirable in this case. As a result, we see the system load factor increased between 2.1% and 5.7% when varying the interhub capacity.
- c. The effects on both designed hub capacity and hub utilization at the main and regional hubs are found to be the same as for KY-PA. In addition, when allowing higher interhub flows on KY-SC ($u_i = 150,000$), the system does not utilize the hub at Philadelphia.
- d. The system loses slack for both pickup and delivery routes. From Table 8.12, we find shipping from PST incurs the highest slack loss while the lowest slack loss occurs when shipping from EST.

3. KY – TX

- a. The two-stage operation decreases the total operating cost when enough interhub capacity ($u_i \geq 100,000$) is provided. The system achieves the best total operating cost when $u_i = 150,000$, which decreases the capacity-miles by 7.2%.
- b. The proposed system improves load factors for various interhub capacities and incurs higher aircraft utilization. Although Dallas is further from the main hub than Philadelphia, it is in a different time zone. Therefore, an interhub flight may depart fairly late, which provides opportunities for arrival pickup routes to operate two-leg flights.
- c. Due to the difference in time zone between the regional and main hubs, the optimized system loses only 35% of slack.

4. KY – CA

- a. The results indicate that this two-stage system is preferable when operating with a low interhub capacity. Although the regional Ontario hub is the furthest hub from the main Louisville hub and would provide significant savings with a two-stage operation, the KY-CA scenario decreases the total operating cost less than KY-TX. From Figure 8.6, it can be seen that there are not many service centers that can benefit from interhub flights.
- b. A two-stage operation on KY-CA reduces system slack by 38%, which is approximately the same for KY-TX.

- c. For all the cases of interhub capacities, the two-stage operation increases the required sorting capacity at Ontario hub greater than for main Louisville hub.

8.4 Case Study 6: Multiple Location Two-stage Operation

In this section, we examine a multiple hub two-stage operation, with interhub flights on multiple hub pairs. Because each single location two-stage routing improves the total system cost differently according to its own properties as discussed in section 8.3, the hybrid multiple-location two-stage operation could provide significantly savings.

We first analyze the combination in the same system of all four interhub routings from all regional hubs, i.e., KY-PA and KY-SC and KY-TX, and KY-CA. However, the resulting savings are negligible. It is noted that the savings from operating two-stage depend on (1) physical location of service centers compared to the hub and (2) the number of service center nearby the hub. Having all four regional hubs contributing to two-stage and their location distributed over the US incur cost of interhub flights more than the distance savings by two-stage operations.

We reduce the number of interhub routings to only choose the best two locations, as discussed in section 8.3; therefore, we analyze the multiple-location two-stage operation consisting of KY-SC and KY-TX. The results indicate the savings for all different demand levels, from 0.8M – 1.2M, as shown in Table 8.15. It is noted that, in each case, the result shown is the best optimal solution found from 10

different replications. Figure 8.7 shows the optimized network configuration for demand level = 0.8M.

Table 8.15: Scenario analysis: UPS network with 100 SCs and multiple two-stage routings

Operational Type/Demand Levels	$Q = 0.8M$			$Q = 0.9M$		
	Single-Stage	Two-stage	%Chg	Single-Stage	Two-stage	%Chg
Total daily operating cost (TDOC)	\$2,533,590	\$2,427,800	-4.2%	\$2,655,910	\$2,564,730	-3.4%
• Aircraft ownership cost	\$1,168,000	\$1,144,000	-2.1%	\$1,196,000	\$1,156,000	-3.3%
• Aircraft operating cost	\$1,344,830	\$1,242,907	-7.6%	\$1,436,401	\$1,353,517	-5.8%
• Hub operating cost	\$20,760	\$40,893	97.0%	\$23,509	\$55,213	134.9%
Load Factor	63%	70%	6.4%	67%	71%	3.7%
• Package-Miles	1,462	1,467	0.3%	1,656	1,645	-0.7%
• Capacity-Miles	2,306	2,101	-8.9%	2,477	2,332	-5.9%
#Legs	256	262	2.3%	256	262	2.3%
#Aircraft	62/4	66/2		61/5	64/3	
Avg. Legs/Aircraft Day	3.88	3.85	-0.7%	3.88	3.91	0.8%
Slack (hours/package)	6.1	3.4	-44%	5.86	3.23	-45%
• Pickup	5.02	2.42	-52%	4.81	2.31	-52%
• Delivery	1.08	0.98	-9%	1.05	0.92	-12%
Hub sorting capacity						
• Louisville, KY	110,459	163,322	48%	136,666	234,893	72%
• Philadelphia, PA	1,800	7,111	295%	4,912	5,333	9%
• Columbia, SC	21,081	29,578	40%	8,744	34,956	300%
• Dallas, TX	0	147,024	NA	0	218,093	NA
• Ontario, CA	0	0	NA	0	0	NA
Hub sorting utilization						
• Louisville, KY	100%	73%	-27%	100%	55%	-45%
• Philadelphia, PA	100%	100%	0%	100%	100%	0%
• Columbia, SC	100%	29%	-71%	96%	39%	-57%
• Dallas, TX	0%	15%	15%	0%	16%	16%
• Ontario, CA	0%	0%	0%	0%	0%	0%
Avg. Run Time (Hrs.)	9.5	20.2	113%	12.8	19.7	54%
TDOC Coefficient of Variation (%)	1.9%	1.2%	-0.7%	1.9%	2.2%	0.3%

Table 8.15: Scenario Analysis: UPS network with 100 SCs and multiple two-stage routings (Cont.)

Operational Type/Demand Levels	<i>Q</i> = 1.0M			<i>Q</i> = 1.1M		
	Single-Stage	Two-stage	%Chg	Single-Stage	Two-stage	%Chg
Total daily operating cost (TDOC)	\$2,853,780	\$2,736,540	-4.1%	\$3,024,030	\$3,003,220	-0.7%
• Aircraft ownership cost	\$1,320,000	\$1,264,000	-4.2%	\$1,340,000	\$1,340,000	0.0%
• Aircraft operating cost	\$1,507,721	\$1,399,157	-7.2%	\$1,655,628	\$1,580,903	-4.5%
• Hub operating cost	\$26,059	\$73,383	181.6%	\$28,402	\$82,317	189.8%
Load Factor	71%	74%	3.9%	73%	75%	1.6%
• Package-Miles	1,831	1,804	-1.5%	2,081	2,061	-1.0%
• Capacity-Miles	2,593	2,423	-6.6%	2,851	2,764	-3.1%
#Legs	272	272	0.0%	288	290	0.7%
#Aircraft	66/6	68/4		70/5	70/5	
Avg. Legs/Aircraft Day	3.78	3.78	0.0%	3.84	3.87	0.7%
Slack (hours/package)	6.06	3.57	-41%	5.77	3.26	-44%
• Pickup	4.98	2.56	-49%	4.76	2.35	-51%
• Delivery	1.07	1.01	-6%	1	0.91	-9%
Hub sorting capacity						
• Louisville, KY	133,332	337,850	153%	139,220	379,361	172%
• Philadelphia, PA	5,333	5,333	0%	5,844	5,191	-11%
• Columbia, SC	29,287	76,332	161%	38,437	89,511	133%
• Dallas, TX	0	274,265	NA	0	307,023	NA
• Ontario, CA	0	0	NA	0	0	NA
Hub sorting utilization						
• Louisville, KY	100%	43%	-57%	100%	43%	-57%
• Philadelphia, PA	79%	89%	10%	100%	100%	0%
• Columbia, SC	100%	31%	-69%	100%	27%	-73%
• Dallas, TX	0%	17%	17%	0%	16%	16%
• Ontario, CA	0%	0%	0%	0%	0%	0%
Avg. Run Time (Hrs.)	9.5	20.8	119%	11.2	23.2	107%
TDOC Coefficient of Variation (%)	1.6%	1.9%	0.3%	2.0%	1.5%	-0.5%

Table 8.15: Scenario Analysis: UPS network with 100 SCs and multiple two-stage routings (Cont.)

Operational Type/Demand Levels	$Q = 1.2M$		
	Single-Stage	Two-stage	%Chg
Total daily operating cost (TDOC)	\$3,256,150	\$3,145,410	-3.4%
• Aircraft ownership cost	\$1,432,000	\$1,404,000	-2.0%
• Aircraft operating cost	\$1,794,282	\$1,657,744	-7.6%
• Hub operating cost	\$29,868	\$83,666	180.1%
Load Factor	73%	75%	1.9%
• Package-Miles	2,279	2,192	-3.8%
• Capacity-Miles	3,124	2,931	-6.2%
#Legs	306	274	-10.5%
#Aircraft	73/6	63/9	
Avg. Legs/Aircraft Day	3.87	3.81	-1.8%
Slack (hours/package)	5.9	3.54	-40%
• Pickup	4.9	2.57	-48%
• Delivery	1	0.96	-4%
Hub sorting capacity			
• Louisville, KY	141,884	366,191	158%
• Philadelphia, PA	4,320	18,265	323%
• Columbia, SC	54,119	21,333	-61%
• Dallas, TX	0	365,261	NA
• Ontario, CA	0	0	NA
Hub sorting utilization			
• Louisville, KY	100%	46%	-54%
• Philadelphia, PA	100%	100%	0%
• Columbia, SC	100%	25%	-75%
• Dallas, TX	0%	16%	16%
• Ontario, CA	0%	0%	0%
Avg. Run Time (Hrs.)	11.4	24.5	115%
TDOC Coefficient of Variation (%)	2.2%	2.0%	-0.2%

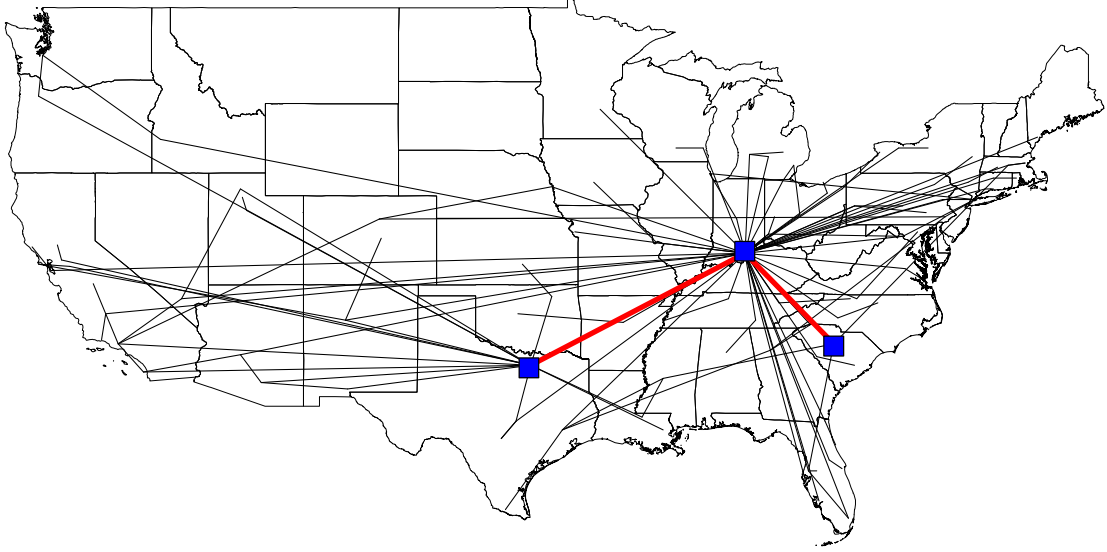


Figure 8.7: Multiple-location two-stage operation, KY-SC & KY-TX, $Q = 0.8M$

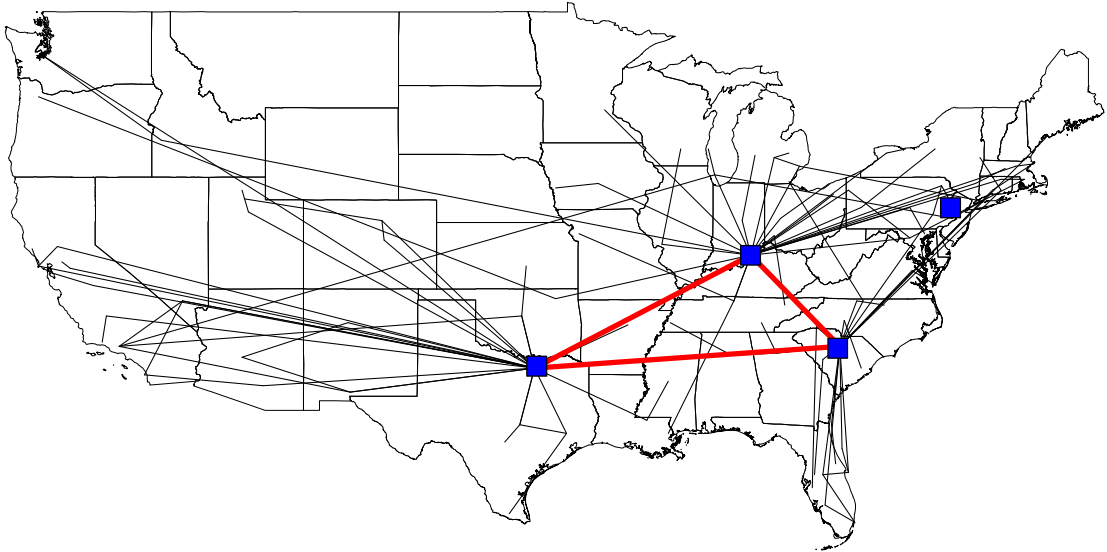


Figure 8.8: Multiple-location two-stage operation, Triangular KY-SC-TX, $Q = 0.8M$

All previous two-stage operations are analyzed under the scenarios where there are two-stage routings between regional hubs and the main hub. It is noted that, our developed GA model is capable to analyze complex systems, such as the triangular of two-stage operation in Figure 8.8. In this case, package flow movement between the regional hubs must also be determined.

8.5 Case Study 7: Effects of Aircraft Mix and Demand Levels

To examine the effects of aircraft mix and demand levels on the performance of the single-stage and two-stage operations, 40 randomly selected service centers in a two-hub network are studied. Two aircraft mix scenarios are analyzed; these have two aircraft types (2A/C) and three aircraft types (3A/C). For the first scenario, the two aircraft types are shown in Table 8.5, while the third aircraft type is added in the second scenario with one-third of the second type capacity. Demand is randomly distributed with the total daily packages ranging from 0.4 to 2.0 millions in 0.4 million increments. In addition, the convex cost for hub sorting capacity is assumed to have a \$0.1/package increment for every 100,000 packages of hub sorting capacity. Three statistics, including cost savings, circuitry factor and average transfers per package, are specifically analyzed here. It is noted that circuitry factor is defined as the ratio of the actual package-miles to the minimum package-miles. The minimum package-miles can be determined from the direct distances between origins and destinations.

The total cost comparison between the single-stage and two-stage operations is shown in Figure 8.9 for different cases of aircraft mix and demand levels. The

savings from the two-stage operation (i.e. the percentage below 100%) occur in both aircraft mix cases when total demand is 0.4 million. At 0.4 million packages, it can be seen that cost savings decrease (i.e. savings are negative) when operating 3A/C compared to 2A/C. However, at 0.8 million packages, operating 3A/C does provide savings. As demand increases further, no savings can be found in any cases.

It can be observed that when operating with 3A/C, the difference in total cost between the single-stage and two-stage operation decreases compared to the cases of 2A/C. To confirm the decrease in the total cost gap between the two systems, 20 problems with randomly generated demands are verified, as shown in Table 8.16.

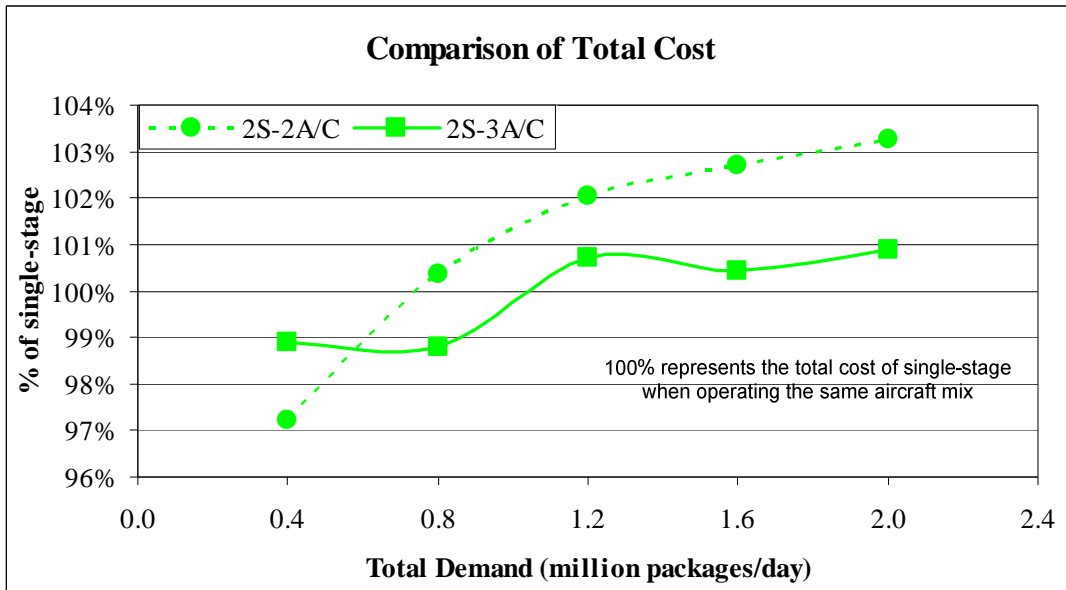


Figure 8.9: Total cost comparisons when varying aircraft mix and demand levels

Table 8.16: Two-stage total cost comparison when varying aircraft mix

Problem Label	%Chg from Single-Stage		Absolute %Chg from Single-Stage	
	2A/C	3A/C	2A/C	3A/C
p01	-4.6% ¹	0.9%	4.6%	0.9%
p02	-3.7%	0.0%	3.7%	0.0%
p03	-2.9%	-0.6%	2.9%	0.6%
p04	-3.8%	-0.2%	3.8%	0.2%
p05	0.8%	2.2%	0.8%	2.2%
p06	-0.5%	-0.2%	0.5%	0.2%
p07	0.8%	0.7%	0.8%	0.7%
p08	-2.8%	0.3%	2.8%	0.3%
p09	1.7%	-0.2%	1.7%	0.2%
p10	0.7%	0.2%	0.7%	0.2%
p11	-7.2%	-0.6%	7.2%	0.6%
p12	-1.5%	1.6%	1.5%	1.6%
p13	-5.5%	1.1%	5.5%	1.1%
p14	1.5%	-1.0%	1.5%	1.0%
p15	0.6%	0.6%	0.6%	0.6%
p16	1.1%	1.1%	1.1%	1.1%
p17	-0.1%	1.9%	0.1%	1.9%
p18	-1.2%	1.3%	1.2%	1.3%
p19	-6.6%	-0.6%	6.6%	0.6%
p20	0.9%	0.8%	0.9%	0.8%
Average	-1.6%	0.5%	2.4%	0.8%

The resulting networks in Figure 8.9 are then extracted to analyze the circuitry factor, as demonstrated in Figure 8.10. In both single-stage and two-stage operations, the circuitry factors decrease when demands increase or more aircraft types are operated. Operating a two-stage system generally increases the circuitry factor compared to a single-stage one. However, at 0.4 million total packages and 2A/C, the two-stage system shows a smaller circuitry factor. That occurs because, in the single-stage system, it is optimal to only utilize one hub instead of both hubs. Therefore, the two-stage operation affects the usage of the second hub by nearby service centers. In addition, as demand increase in the single-stage systems, the gaps of circuitry factor between 2A/C and 3A/C decrease due to less usage of the third aircraft type.

¹ -4.6% indicates the percentage difference in total cost of two-stage operation compared to single-stage one when both systems use the same aircraft mix, i.e., 2A/C in this case.

Figure 8.11 depicts the average transfers per package at various demands and aircraft mixes. The results indicate less usage of two-stage operations (i.e. more directness in package movements) as demand increases. Moreover, with more aircraft types (3A/C), the systems show significant decreases in two-stage flows compared to the 2A/C.

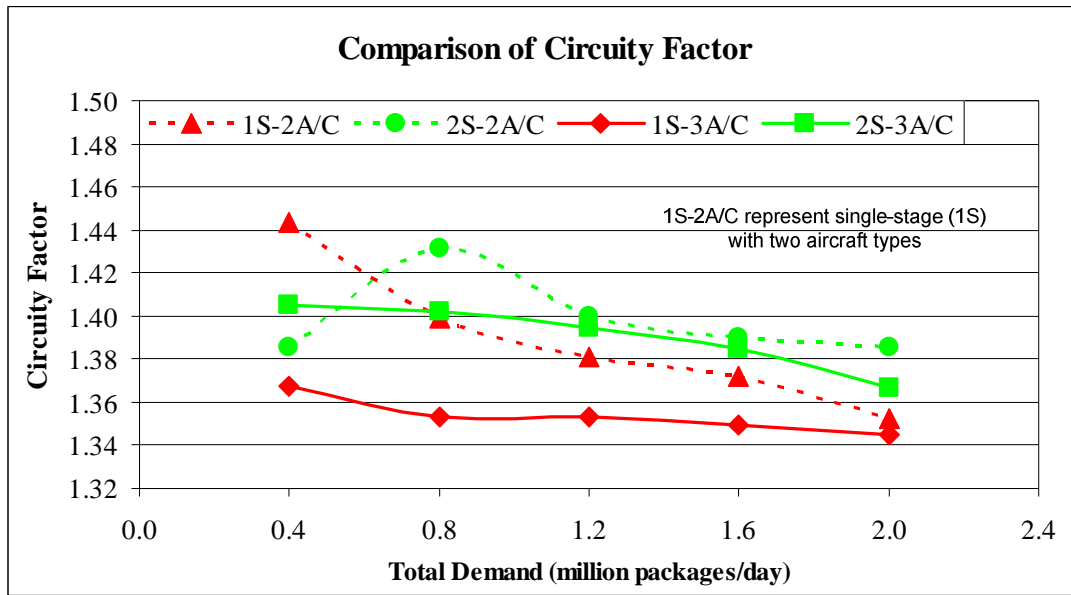


Figure 8.10: Circuity factor at various aircraft mixes and demand levels

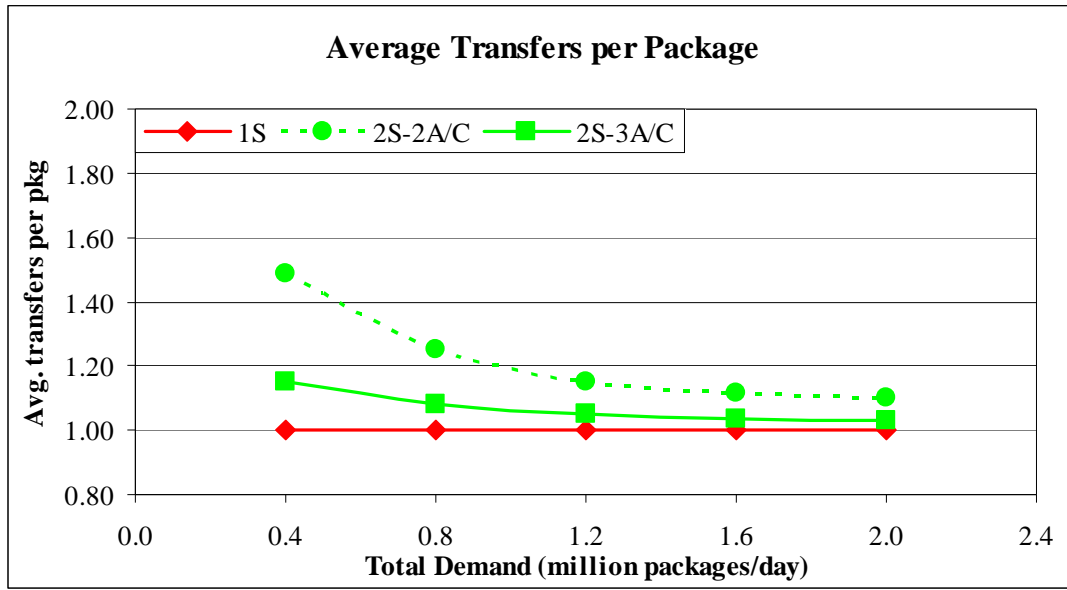


Figure 8.11: Average transfers per package at various aircraft mixes and demand levels

8.6 Case Study 8: Economies of Scale in Aircraft

As concluded, for example in sections 6.5.1 and 7.8.1, when aircraft operating cost increases, cost savings from two-stage operation tend to increase. Because the two-stage operation provides benefits through distance savings and most of the flights are operated with smaller aircraft, greater savings of the two stages compared to the single stage can be obtained when the operating cost of smaller aircraft increases.

Typically, larger aircraft are operated for interhub flights to take advantage of their economies of scale (i.e., the aircraft operating cost per unit capacity that decreases with aircraft size). By directing small aircraft to connect to interhub flight that is operated by larger aircraft, the two-stage system can also provide cost savings when the aircraft operating cost of the interhub flight decreases, as confirmed in Figure 8.12. There, 40 randomly selected service centers are tested over two sets of

randomly generated demands. With no change to the interhub operating cost (0% decrement), two-stage operation provides savings in the first dataset by 2.2% (upper line) while the single-stage outperforms by 1.5% in the second dataset (lower line). However, as the operating cost of interhub flights decreases, the two stages can yield savings in both cases.

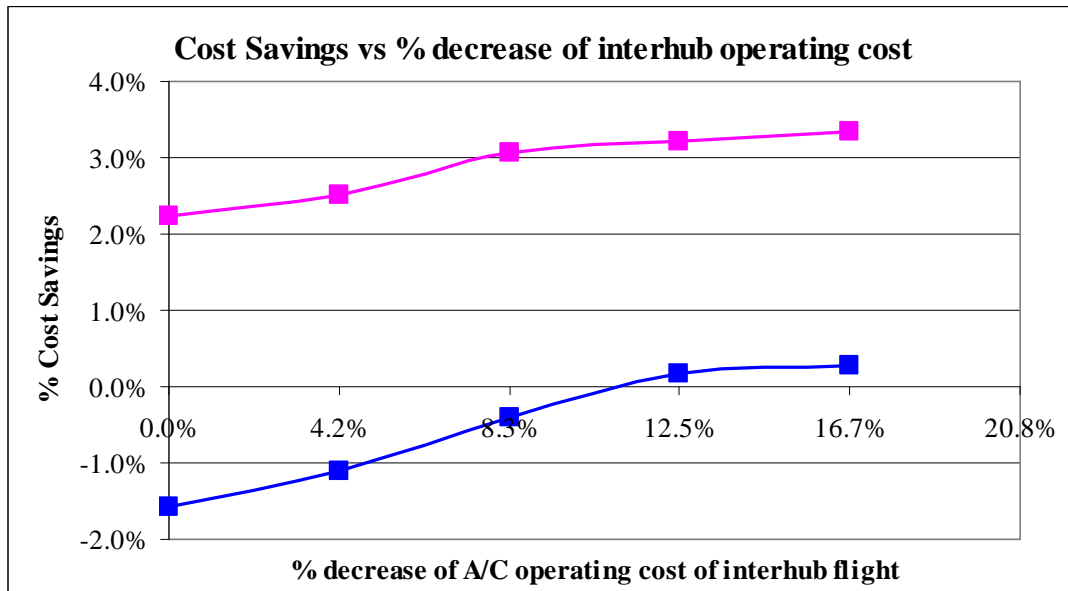


Figure 8.12: Economies of scale on interhub flight

8.7 Summary

This chapter demonstrates the applicability of the developed GA model with acceptable computational times for large problems. The GA model is used to optimize both single-stage and two-stage operations for comparison purposes. The analyses are first conducted for the top 100 metropolitan locations and for various interhub capacities, locations of regional hubs for two-stage operation, and demand levels. The single-location interhub routings are presented first, while later the hybrid

multiple-location cases are analyzed. The results confirm the findings from the small problems. The proposed two-stage operation provides potential savings at low demand levels when operating a single hub pair KY-TX, and high demand levels when operating the two hub pairs KY-TX and KY-SC. However, the two-stage operation results in some negative effects; those are (1) higher required hub sorting capacity, (2) lower hub utilization and (3) loss of system slack. For some cases, such as operating two stages on KY-PA when demand is low, the system performs worse than the single-stage one due to low aircraft utilization.

The effects of aircraft mix and significant demand increase are analyzed for the medium network size, in which total cost savings, circuitry factor and average transfers per package are compared. When demands increase or more aircraft types are used, the circuitry factors and the average transfers per package decrease. In addition, the economies of scale in aircraft operating cost favor the two-stage operation.

Chapter 9

Conclusions and Future Research

This study has mainly investigated the potential cost savings and associated effects of the two-stage operations compared to the single-stage ones for the next-day air network design problem. In Chapter 3, the general concepts of the proposed two-stage operation are discussed in detail. To capture all operational characteristics in the time-space formulation, three network representations, including hub sorting network, aircraft route network and package flow path network, are introduced in Chapter 4. In Chapter 5, the mathematical models for both systems are formulated, while capturing all the operational constraints, including aircraft balancing, aircraft availability, hub landing/take-off capacity, hub sorting process and its sorting/storage capacity. The

exact and heuristic solution approaches, namely the Column Generation and the Genetic Algorithm, are developed in Chapters 6 and 7, respectively. Numerical analyses are conducted for several small test problems. For large problem instances, the Genetic Algorithm approach is applied in Chapter 8.

9.1 Conclusions

This section summarizes the primary contributions of this study in two areas:

Transportation Planning Analysis Contributions:

After analyzing several test problems, including both small and large problems, several findings are reached:

1. The benefits of two-stage operation for the next day air package delivery depend mainly on the demand level relative to the aircraft capacity and scale economies. The proposed system is preferred when demand is low so that more routes can be consolidated, which yields greater distance savings. In some cases, even at high demands, the two-stage operation can be beneficial. For example, if the total demand of a service center is higher than the largest aircraft capacity, the leftover demand ($\sum_{k \in K \cap \{O(k)=i\}} d^k - u^f$ on the pickup side or $\sum_{k \in K \cap \{D(k)=i\}} d^k - u^f$ on the delivery side) can benefit from a two-stage operation.
2. In a distribution network with several regional hubs, each hub can potentially operate two stages depending on its location and surrounding service centers (single location two-stage operation). Moreover, the hybrid multiple location two-stage operation can provide greater savings.

3. In equation 3.2 and Figure 3.2, the expected number of aircraft required is analyzed for a single-stage operation. However, several results indicate that the optimal network uses a master hub located in the east, as discussed in Case C by Hall (1989). The resulting single-stage operation uses fewer aircraft than we have estimated and does not follow equation 3.2. Therefore, there is no indication that the proposed two-stage operation reduces the required number of aircraft.
4. Upon arrival at a hub, if the package sorting order is not based on the packages' destinations, that is, if packages are sorted using FIFO, higher sorting and storage capacities are needed. If we first sort packages that are transferring to the downstream hub, the required hub sorting and storage capacities decrease.
5. Sensitivity analyses indicate the preferability of a two-stage operation when aircraft operating cost increases or hub sorting cost decreases.
6. The *first drawback* of operating the two-stage system is the significant increase in required hub sorting capacity. This is due to the required sorting capacity of (1) arrival packages at the upstream hub to meet the latest departure time of interhub flights and (2) arrival packages at the downstream hub to meet the hub sort end time.
7. Despite an increase in required hub sorting capacity for two-stage operation, this capacity is fully utilized only during some of the hub sorting time window. Therefore, the *second drawback* of the two-stage operation is a significant decrease in hub utilization.

8. In a two-stage operation, arriving aircraft must arrive earlier so that packages can be unloaded, sorted and loaded on interhub flights, which must arrive at the downstream hub before its sort end time. The system slack is reduced in comparison with the single-stage operation. This is the *third drawback*. When operating the two-stage operation on a small network with all service centers physically close or within the same time zone and the regional hub located east of the main hub, the slack loss is minimal. However, the conclusion is not applicable to a larger network. A two-stage operation using the main hub at Louisville, KY and the regional hub at Dallas, TX provides the least slack loss, while routing interhub flights to an eastern regional hub in Philadelphia, PA or Columbia, SC causes the highest slack loss. Moreover, the analysis shows that the loss in slack is approximately invariant with interhub capacity.
9. In some scenarios, such as routing interhub flights between Louisville, KY and Philadelphia, PA, because both hubs located in the same time zone, interhub flights generally depart from the upstream hub early. All arrival pickup flights that must transfer their packages must arrive early too. This indirectly affects aircraft by discouraging two-leg flights and reducing aircraft utilization. This is the *fourth drawback*.
10. When operating more aircraft types, especially with lower aircraft capacities, the single-stage operation is favored. This results in less circuitry and fewer average transfers per package.

Modeling Contributions:

The modeling contributions in this study are summarized as follows:

1. Three major models are developed for air express network design problem with hub sorting. The first model is a single-stage sorting operation, in which packages are sorted only once at a hub before arriving at their destination. Second, a two-stage sorting operation is introduced, where packages are sorted twice at two distinct hubs and delivered to their destinations within a limited time windows. The third model is a mixed-stage sorting operation, which is the combination between the first two models whenever it can benefit the entire system. All models are formulated as mixed integer multicommodity network flow problems, considering aircraft route, package flow path, hub sorting capacity and hub storage size variables.
2. The Column Generation approach is employed to solve the single-stage and two-stage operation, as demonstrated in Chapter 6. Three network representations, which are hub sorting, aircraft route and package flow path representations, are introduced to model the time-space network formulation. However, due to the combinatorial nature of the problems, especially with several side constraints, such as aircraft balancing at service centers and hubs, aircraft availability requirements, hub landing/take-off capacity, the approach is not applicable to a large problem instance.
3. By exploiting the problem structure of air express network design, we develop the solution representations which are then solved using the Genetic Algorithm approach. Our GA representations consist of grouping

representation and aircraft route representation. The first representation aims at finding the optimal partition by means of hub assignment, while the second is used to manipulate the local search according to the pre-specified grouping. Two sets of genetic operators, which are applied specifically to each representation, are developed using the problem characteristics to guide the search. Package flow movements are determined using the Column Generation approach solving over the *capacitated network*, which is the result of GA manipulated representations. These flows are then heavily utilized in guiding the search direction, where probabilistic search is used.

4. With the GA model, the analytical model is developed to determine the required hub sorting and storage capacities. This model works with a FIFO or TFSF (two-stage flow sorted first) sorting process.
5. After obtaining the optimal solution, a post-solution analysis is conducted to analyze the system slack for both single and two-stage operations. Three types of slack are considered; those are pickup, delivery and interhub slacks. The slack can be determined by iteratively shifting the scheduled arrival time (for pickup route) or departure time (for delivery route) without violating the designed hub sorting capacity, hub take-off and landing capacity. The interhub slack is determined from the difference between the earliest and latest arrival time at the downstream hub, that is, without affecting the downstream hub sorting capacity.

9.2 Future Research

Although this study provides several contributions in the transportation planning and modeling fields, especially in the comparison of single-stage and two-stage operations, several additional elements could be considered in future studies.

1. In real practice, packages are loaded and transported in a set of containers. Those containers are then moved by the aircraft. Therefore, the package volumes are constrained by container capacity, and the containers are limited by the aircraft capacity. This “*packages on containers, containers on aircraft*” problem can be cast as a *multi-level mixed integer multicommodity flow problem*.
2. Due to demand variation within each week, in which demand gradually increases from Monday to Wednesday and then decreases through the weekend (see Barnhart and Shen, 2004), *a seven day planning horizon is desirable*. The combination of single-stage and two-stage operation may improve the system cost, such as operating single stages in the middle of the week when demand is high and two stages at the beginning and end of the week when demand is low.
3. The developed models can be further enhanced by considering *direct shipment routing* when the demand between any origin/destination pair is high. Moreover, when the demands are unbalanced, mirroring routes as considered in our model may not be desirable.
4. To better compare the single-stage and two-stage operation, one may consider the *system slack* as one of the cost elements in the objective function.

Appendix A

Abbreviations

AEND	Air express network design
ARN-D	Aircraft route network for delivery routes
ARN-I	Aircraft route network for interhub routes
ARN-P	Aircraft route network for pickup routes
B&B	Branch and bound approach
CG	Column generation approach
EPT	Earliest pickup time at service center
FIFO	First in first out sorting process
GIP	General inventory problem
HSN	Hub sorting network
LDT	Latest delivery time at service center
MCNF	Multicommodity network flow
MIMCF	Mixed integer multicommodity flow
NDP	Network design problem
NH	Air express network design with hub sorting and pricing
PMC	Package movement connectivity
PMN	Package movement network
RMP	Restricted master problem
SET	Sort end time at hub

SNDP	Service network design problem
SST	Sort start time at hub
TFSF	Two-stage flow sorted first

Appendix B

Notation

Sets:

A Set of arcs

$A_{\{ARN-P/D\}}$ Set of arcs on ARN-P/D = $\bigcup_{f \in F} ARN_f^P \cup ARN_f^D$

ARN_f^D Set of arcs and nodes in aircraft delivery route network of fleet type
 $f, f \in F$

ARN_f^I Set of arcs and nodes in aircraft interhub route network of fleet type
 $f, f \in F$

ARN_f^P Set of arcs and nodes in aircraft pickup route network of fleet type
 $f, f \in F$

F Set of aircraft types or facilities

G_h Set of sorting grid time at hub $h, h \in H$

H Set of hubs

$H_{app}(k)$ Set of approachable hubs and associated grid times from commodity
 $k, k \in K$

HSN_h Set of arcs in hub sorting network of hub $h, h \in H$

K Set of commodities

$L_{A(h)}^t$	Set of aircraft routes arriving to hub $h, h \in H$ at grid time $t, t \in G_h \setminus \{SET\}$
$L_{D(h)}^t$	Set of aircraft routes departing from hub $h, h \in H$ at grid time $t, t \in G_h \setminus \{SST\}$
N	Set of nodes
$P_{(t-\Delta t, t)}^{e,h}$	Set of package flow paths that are <i>sorted</i> at hub $h, h \in H$ during grid time $(t - \Delta t, t)$, $t \in G_h$
$P_{(t-\Delta t, t)}^{s,h}$	Set of package flow paths that are <i>stored</i> at hub $h, h \in H$ during grid time $(t - \Delta t, t)$, $t \in G_h$
$P(k)$	Set of package flow paths of commodity $k, k \in K$
R	Set of aircraft routes
R_D^f	Set of aircraft delivery routes using fleet type $f, f \in F$
R_I^f	Set of aircraft interhub routes using fleet type $f, f \in F$
R_P^f	Set of aircraft pickup routes using fleet type $f, f \in F$
S	Set of service centers
$U_h^{(t_a, t_m)}$	Set of all possible package flow paths arriving at grid time $t_a, t_a \in G_h \setminus \{SET\}$ but left to be sorted after grid time $t_m, t_m \in G_h \setminus \{SET\}$
$U_h^{(t_a, t_m)}(x)$	Set of resulting package flow paths in $U_h^{(t_a, t_m)}$

- $V_h^{(t_a, t_m]}$ Set of all possible package flow paths arriving during
 $(t_a, t_m]$, $t_a, t_m \in G_h \setminus \{SET\}$ at hub $h, h \in H$ that are sorted at time t_m
- $V_h^{(t_a, t_m]}(x)$ Set of resulting package flow paths in $V_h^{(t_a, t_m]}$

Data:

- a_h^t Maximum number of aircraft that can land at hub h during the time
 $t - \Delta t$ and t
- b_h^t Maximum number of aircraft that can take-off at hub h during the
time $t - \Delta t$ and t
- c_h^e Cost per unit sorting rate at hub $h, h \in H$
- c_{ij}^k Cost per unit flow of commodity $k, k \in K$ on arc $(i, j), (i, j) \in A$
- c_{ij}^f Cost per unit of installing facility $f, f \in F$ over arc $(i, j), (i, j) \in A$
- c_r^f Cost of flying aircraft route $r, r \in R$ using fleet type $f, f \in F$
- c_h^s Cost of unit storage size at hub $h, h \in H$
- d^k Demand of commodity $k, k \in K$
- $D(k)$ Destination of commodity $k, k \in K$
- $EPT(i)$ Earliest pickup time at service center $i, i \in SC$
- $LDT(i)$ Latest delivery time at service center $i, i \in SC$
- n^f Available number of aircraft fleet type $f, f \in F$
- $O(k)$ Origin of commodity $k, k \in K$

Q	Total demand, $\sum_{k \in K} d^k$
u^f	Aircraft capacity of fleet type $f, f \in F$
u_{ij}^f	Capacity per unit of facility f over the arc $(i, j), (i, j) \in A$

Decision Variables:

e_h	Sorting rate at hub $h, h \in H$
I_h^t	Number of packages in storage waiting to be sorted at hub $h, h \in H$ at grid time $t, t \in G_h \setminus \{SET\}$
I_h^{\max}	Maximum number of packages in storage waiting to be sorted at hub $h, h \in H$ at grid time $t, t \in G_h \setminus \{SET\} = \max_{t \in G_h \setminus \{SET\}} I_h^t = s_h$
s_h	Storage size at hub $h, h \in H$ ($s_h = I_h^{\max}$)
$x_{h(t)}^k$	Number of packages of commodity $k, k \in K$ arriving at hub $h, h \in H$ at grid time $t, t \in G_h \setminus \{SET\}$
x_p^k	Number of packages on path $p, p \in P(k)$ of commodity $k, k \in K$
$X_{\bullet, h(t)}$	Total number of packages arriving at hub $h, h \in H$ at grid time $t, t \in G_h \setminus \{SET\} = \sum_{k \in K} x_{h(t)}^k$
$X_{h(t), \bullet}$	Total number of packages departing from hub $h, h \in H$ at grid time $t, t \in G_h \setminus \{SST\}$

- $X(h_1(t_1) \rightarrow h_2(t_2))$ Total number of packages from hub $h_1, h_1 \in H$
 departing at grid time $t_1, t_1 \in G_{h_1} \setminus \{SST\}$ to hub $h_2, h_2 \in H$ arriving at
 grid time $t_2, t_2 \in G_{h_2} \setminus \{SET\}$
- y_{ij}^f Number of facilities of type f installed over arc (i, j)
- y_r^f Number of flight of fleet type $f, f \in F$ traveling on route $r, r \in R$

Indicators:

- α_a^p 1 if package flow path p includes on arc a , 0 otherwise
- δ_a^{fr} 1 if aircraft route r of fleet type f includes on arc a , 0 otherwise
- β_i^r 1 if aircraft route r starts on service center i , -1 if aircraft route r
 ends at service center i , 0 otherwise
- $\gamma_{k,p}^{e,h}$ 1 if $p \in \{P_{(t_m-\Delta t, t_m)}^{e,h} \cap P(k)\}$, 0 otherwise
- $\gamma_{k,p}^{s,h}$ 1 if $p \in \{P_{(t_m-\Delta t, t_m)}^{s,h} \cap P(k)\}$, 0 otherwise
- $\gamma_{p,k}^{v,h}(t_a, t_m)$ 1 if $x_p^k \in V_h^{(t_a, t_m)}$, 0 otherwise
- $\gamma_{p,k}^{u,h}(t_a, t_m)$ 1 if $x_p^k \in U_h^{(t_a, t_m)}$, 0 otherwise
- $I[V_h^{(t_a, t_m)}(x)]$ 1 if $V_h^{(t_a, t_m)}(x)$ is nonempty set, 0 otherwise
- $I[U_h^{(t_a, t_m)}(x)]$ 1 if $U_h^{(t_a, t_m)}(x)$ is nonempty set, 0 otherwise

Matrices:

- \mathbf{A}_a Constraint matrix for package flow variables in arc constraints (5.12.4)

- \mathbf{A}_e Constraint matrix for package flow variables in hub sorting capacity constraints (5.12.8)
- \mathbf{A}_k Constraint matrix for package flow variables in total package flow constraints (5.12.3)
- \mathbf{A}_s Constraint matrix for package flow variables in hub storage size constraints (5.12.9)
- \mathbf{A}_u Constraint matrix for package flow variables bounded on horizontal arc in HSN constraints (5.12.12)
- \mathbf{A}_v Constraint matrix for package flow variables bounded on vertical arc in HSN constraints (5.12.11)
- \mathbf{B}_a Constraint matrix for aircraft route variables in arc constraints (5.12.4)
- $\mathbf{B}_{h,b}$ Constraint matrix for aircraft route variable in fleet balancing at hub constraints (5.12.6)
- \mathbf{B}_n Constraint matrix for aircraft route variables in fleet availability constraints (5.12.7)
- $\mathbf{B}_{sc,b}$ Constraint matrix for aircraft route variables in fleet balancing at service center (5.12.5)

Vectors

- $\boldsymbol{\pi}^{\mathbf{A}_a}$ Dual price vector for package flow variables in arc constraints (5.12.4)
- $\boldsymbol{\pi}^{\mathbf{A}_e}$ Dual price vector for package flow variables in hub sorting capacity constraints (5.12.8)

- π^{A_k} Dual price vector for package flow variables in total package flow constraints (5.12.3)
- π^{A_s} Dual price vector for package flow variables in hub storage size constraints (5.12.9)
- π^{A_u} Dual price vector for package flow variables bounded on horizontal arc in HSN constraints (5.12.12)
- π^{A_v} Dual price vector for package flow variables bounded on vertical arc in HSN constraints (5.12.11)
- π^{B_a} Dual price vector for aircraft route variables in arc constraints (5.12.4)
- $\pi^{B_{hb}}$ Dual price vector for aircraft route variable in fleet balancing at hub constraints (5.12.6)
- π^{B_n} Dual price vector for aircraft route variables in fleet availability constraints (5.12.7)
- $\pi^{B_{sc,b}}$ Dual price vector for aircraft route variables in fleet balancing at service center (5.12.5)

Others:

- ρ Aircraft load factor

References

Ahuja, R. K., T. L. Magnanti, J. B. Orlin. 1993. Network Flows: Theory, Algorithms and Applications. Prentice Hall, Inc., Englewood Cliffs, New Jersey.

Annual Estimates of the Population of Metropolitan and Micropolitan Statistical Areas: April 1, 2000 to July 1, 2005. *U.S. Census Bureau homepage*, <http://www.census.gov/population/www/estimates/metropop/2005>, accessed March 21, 2007

Armacost, A. P., C. Barnhart, K. A. Ware, A. M. Wilson. 2004. UPS optimizes its air network. *Interfaces* **34(1)** 15-25.

Armacost, A. P., C. Barnhart, K. A. Ware. 2002. Composite variable formulations for express shipment service network design. *Transportation Science* **36(1)** 1-20.

Assad, A. 1978. Multicommodity Networks Flows – A survey. *Networks* **8** 37-91.

Aykin, T. 1995a. Theory and methodology: The hub location and routing problem. *European Journal of Operational Research* **83** 200-219.

Aykin, T. 1995b. Networking policies for hub-and-spoke systems with application to the air transportation system. *Transportation Science* **29(3)** 201-221.

Barnhart, C., C. A. Hane, E. L. Johnson, G. Sigismondi. 1995. A column generation and partition approach for multicommodity flow problems. *Telecommunication System* **3** 239-258.

Barnhart, C., C. Hane, P. Vince. 2000. Using branch-and-price-and-cut to solve origin-destination integer multicommodity flow problems. *Operations Research* **48(2)** 318-236.

Barnhart, C., N. Krishnan, D. Kim, K. Ware. 2002. Network design for express shipment delivery. *Computational Optimization and Applications* **21(3)** 239-262.

Barnhart, C., R. R. Schneur. 1996. Air network design for express shipment service. *Operations Research* **44(6)** 852-863.

Barnhart, C., S. Shen. 2004. Logistic Service Network Design for Time-Critical Delivery. In E. Burke and M. Trick, editors, *Practice and Theory of Automated Timetabling V, Lecture Notes in Computer Science* **3616** 86 – 105, Pittsburg, PA, USA, 2004. Springer.

Bertsimas, D., J. N. Tsitsiklis. 1997. Introduction to Linear Optimization. Athena Scientific, Belmont, Massachusetts.

Crainic, T. G. 2000. Service network design in freight transportation. *European Journal of Operation Research* **122(2)** 272-288.

Crainic, T. G., G. Laporte. 1997. Planning models for freight transportation. *European Journal of Operational Research* **97(3)** 409-438.

Crainic, T. G., J. M. Rousseau. 1986. Multicommodity, multimode freight transportation: A general modeling and algorithmic framework for the service network design problem. *Transportation Research B* **20B(3)** 225 – 242.

Crainic, T. G., M. Gendreau, J. M. Farvolden. 2000. A simplex-based tabu search method for capacitated network design. *INFORMS Journal on Computing* **12(3)** 223-236.

Distance Calculation: How to calculate the distance between two points on the earth. *Meridian World Data homepage*, <http://www.meridianworlddata.com>, accessed December 15, 2006.

Farvolden, J. M., W. B. Powell. 1994. Subgradient methods for the service network design problem. *Transportation Science* **28(3)** 256-272.

Falkenauer, E. 1996. A hybrid grouping genetic algorithm for bin packing. *Journal of Heuristics* **2** 5-30.

FedEx Corporation 2000 Annual Report

FedEx Corporation 2001 Annual Report

FedEx Corporation 2002 Annual Report

FedEx Corporation 2003 Annual Report

FedEx Corporation 2004 Annual Report

Ford, L. R., D. R. Fulkerson. 1958. A suggested computation for maximal multicommodity network flows. *Management Science* **5** 97-101.

Gamvros, I., B. Golden, S. Raghavan, D. Stanojević. 2004. Heuristic Search for Network Design. In H. J. Greenberg, editor, *Tutorials on Emerging Methodologies and Applications in Operations Research* 1:1-45, Denver, CO, USA, 2004. Springer's International Series.

Ghamlouche, I., T. Crainic, M. Gendreau. 2003. Cycle-based neighborhoods for fixed-charge capacitated multicommodity network design. *Operations Research* **51(4)** 655-667.

Grünert, T., H. J. Sebastian. 2000. Planning models for long-haul operations of postal and express shipment companies. *European Journal of Operational Research* **122(2)** 289-309.

Haghani, A. E. 1989. Formulation and solution of combined train routing and makeup, and empty car distribution model. *Transportation Research B* **23B(6)** 431-433.

Hall, R. W. 1987. Comparison of strategies for routing shipments through transportation terminals. *Transportation Research A* **21A(6)**, 421-429.

Hall, R. W. 1989. Configuration of an overnight package air network. *Transportation Research A* **23A(2)** 139-149.

Holmberg, K., D. Yuan. 2003. A multicommodity network-flow problem with side constraints on paths solved by column generation. *INFORMS Journal on Computing* **15(1)** 42-57.

ILOG Cplex 9.0 User's Manual, October 2003

Kennington, J. 1978. A survey of linear cost multicommodity network flows. *Operations Research* **26(2)** 209-236.

Kim, D. 1997. Large Scale Transportation Service Network Design: Models, Algorithms and Applications. PhD dissertation, Massachusetts Institute Technology.

Kim, D., C. Barnhart, K. Ware, G. Reinhardt. 1999. Multimodal express package delivery: A service network design application. *Transportation Science* **33(4)** 391-407.

Kim, D., C. Barnhart. 1999. Transportation service network design: models and algorithms. *Lecture Notes in Economics and Mathematical Systems: Computer-Aided Transit Scheduling*. **471** 259-283.

Kuby, M., R. Gray. 1993. The hub network design problem with stopovers and feeders: The case of Federal Express. *Transportation Research A* **27A(1)** 1-12.

Magnanti, T. L., R. T. Wong. 1984. Network Design and Transportation Planning: Models and Algorithms. *Transportation Science* **18(1)** 1-55.

Michalewicz, Z. 1999. Genetic Algorithms + Data Structure = Evolution Programs, Third Edition, Springer-Verlag, New York.

Minoux, M. 1989. Network synthesis and optimum network design problems: models, solution methods and applications. *Networks* **19(3)** 313-360.

O'Kelly, M. E., D. Bryan., D. Skorin-Kapov, J. Skorin-Kapov. 1996. Hub network design with single and multiple allocation: A computational study. *Location Science* **4(3)** 125-138.

O'Kelly, M. E., D. L. Bryan. 1998. Hub location with flow economies of scale. *Transportation Research B* **32B(8)** 605-616.

Roy, J., L. Delorme. 1989. NETPLAN: A network optimization model for tactical planning in the less-than-truckload motor-carrier industry. *INFOR* **27(1)** 22-35.

Shen, S. 2004. Logistics Service Network Design: Models, Algorithms, and Applications. PhD dissertation, Massachusetts Institute Technology.

Standard & Poor's Stock Report: UPS. *TD Ameritrade homepage*, <https://research.ameritrade.com>, accessed November 26, 2006.

Tomlin, J. A. 1966. A linear programming model for the assignment of traffic. *Proceedings of the 3rd Conference of the Australian Road Research Board* **3** 263-271.

United Parcel Service 2000 Annual Report

United Parcel Service 2001 Annual Report

United Parcel Service 2002 Annual Report

United Parcel Service 2003 Annual Report

United Parcel Service 2004 Annual Report

UPS Express Critical Term and Condition of Contract, July 2007